7

ASSESSMENT OF FUEL PERFORMANCE FROM POST-IRRADIATION EXAMINATION AND SAFETY TESTING

The objective of the PIE and safety testing is to characterize and measure the performance of TRISO fuel after irradiation and during postulated accident conditions. These activities also support the fuel development effort by providing feedback on the performance of kernels, coatings, and compacts. Data from PIE and safety testing in combination with the in-reactor measurements will provide the data necessary to demonstrate compliance with fuel performance requirements and to support the development and validation of computer codes. PIE of UCO TRISO fuel irradiated in AGR-1 is complete, while similar work for AGR-2 is nearing completion.

Key aspects of fuel performance that were investigated were fission product release from particles and compacts, radiation-induced changes in kernel and coating microstructures, and coating failure.[19] Safety tests were performed by heating the fuel compacts in helium at temperatures of 1600, 1700, or 1800°C, with nominal hold times of 300 hours. An additional AGR-1 test was performed involving three compacts heated using a temperature profile resembling the peak temperature trajectory during an HTGR depressurized loss of forced cooling accident. These results are discussed in the following sections.

7.1   Fission Product Release During Irradiation

7.1.1 Methods

Several different experimental measurements are used to assess the extent of fission product release from the fuel particles and compacts. These involve quantifying either the fission product inventory remaining in the fuel specimen, or the inventory that has been released from the specimen. When compared with the predicted inventory generated during irradiation (based on physics calculations), the numbers can indicate a fraction of total inventory retained or released.

---

[19]   In Section 7, coating failures are commonly categorized as either *SiC failure* or *TRISO failure* to differentiate between the two. SiC failure is defined as loss of integrity of the SiC layer with at least one pyrocarbon layer remaining intact, such that fission gases will be retained but fission products such as cesium may be released in significant quantities. TRISO failure is defined as loss of integrity of all three dense coating layers, such that fission gases will be released from the particle. This is also often referred to as an exposed kernel.

The basic measurements that were part of the AGR-1 and AGR-2 PIE are listed below. The methods have been summarized in the *AGR-1 Post Irradiation Examination Final Report* [82], with numerous specific references provided containing additional details on methods and results. Similar methods are being used for the AGR-2 PIE:

- **Fission product inventory on the capsule components outside of the fuel compacts**. This is obtained by gamma counting of certain components, burn-leach of carbonaceous matrix components, and acid leaching of metallic components. The results provide the capsule-average fractional release from the fuel compacts. AGR-1 and AGR-2 results are provided in dedicated reports [83,84].

- **Fission product inventory in the compacts outside of intact SiC**. This includes any inventory residing in the OPyC layer and the compact matrix and is determined by deconsolidation-leach-burn-leach (DLBL) analysis of selected compacts. This inventory represents fission products that were released from the fuel particles but not released from the compact.

- **Gamma counting of individual particles**. This provides the total gamma-emitting fission product inventory in each particle. In most cases, the fractional release of fission products from an individual particle is sufficiently small (for example, <1%) and the uncertainty on the inventory sufficiently large (minimum uncertainty typically in the range of 5%) that no conclusions can be drawn regarding the extent of fission product release using these data. Two notable exceptions include (1) assessing silver release from intact particles and (2) assessing cesium release from particles with failed coatings. In these cases, the release from a particle can be sufficiently large that the approximate fractional release can be estimated by examining the remaining inventory.

- **Gamma counting of individual compacts**. This provides the total gamma-emitting fission product inventory in each compact. This is primarily of use for assessing silver release from a compact, which can be very significant (that is, tens of percent).

All of the release fractions expressed in this report are based on calculated inventories determined from neutronics simulations of the irradiation experiments. Some measurements of whole compact and individual particle inventories have been performed and compared to the calculated values to assess the accuracy of the calculations. This includes gamma spectrometry measurements of total fuel compact inventories for gamma-emitting fission products and gamma counting of individual particles from numerous compacts.

The data for AGR-1 compacts indicate that the measured inventories for certain fission products (including ^{134}Cs, ^{137}Cs, ^{144}Ce, and ^{106}Ru) are in good agreement with the calculated inventories: the measured-to-calculated (M/C) inventory ratios (averaged for all AGR-1 compacts) are between 0.96 and 1.0 for these isotopes. For other isotopes there is evidence of a bias in the calculation as the measured inventories are somewhat less than the calculated inventories; the average M/C ratio is 0.83 for ^{154}Eu and 0.70 for ^{125}Sb for AGR-1 fuel compacts. Similar analysis is being performed on the AGR-2 fuel, including an analysis of ^{90}Sr inventories to compare with the calculated values (^{90}Sr is not detected by gamma spectrometry as it decays with no gamma

ray emission). Nonetheless, calculated values are used exclusively in the results presented here for consistency. For certain isotopes, reliable M/C values may not be available for all specimens analyzed, and the variation in M/C ratio for individual specimens means that no single correction can be applied to account for these differences.

7.1.2 Results

Several aspects of fission product behavior in the AGR-1 fuel are graphically highlighted in Figure 7-1. Two sets of data are presented: red columns represent the range of fission product inventories measured in selected compacts outside of intact SiC [82], expressed as a fraction of the total compact inventory, and blue columns represent the range of fission product inventories measured outside of the fuel compacts in the six capsules [83], expressed as a fraction of the total capsule inventory.

Preliminary data for the AGR-2 UCO fuel compacts [85] and capsules [84] are presented in Figure 7-2. Note that for ^{154}Eu and ^{90}Sr, the data ranges for Capsule 2 are plotted separately because they fall significantly outside the range of values for Capsules 5 and 6, a result of the higher fuel temperature in Capsule 2. For the remaining isotopes, all data are plotted together since the ranges of values overlap.
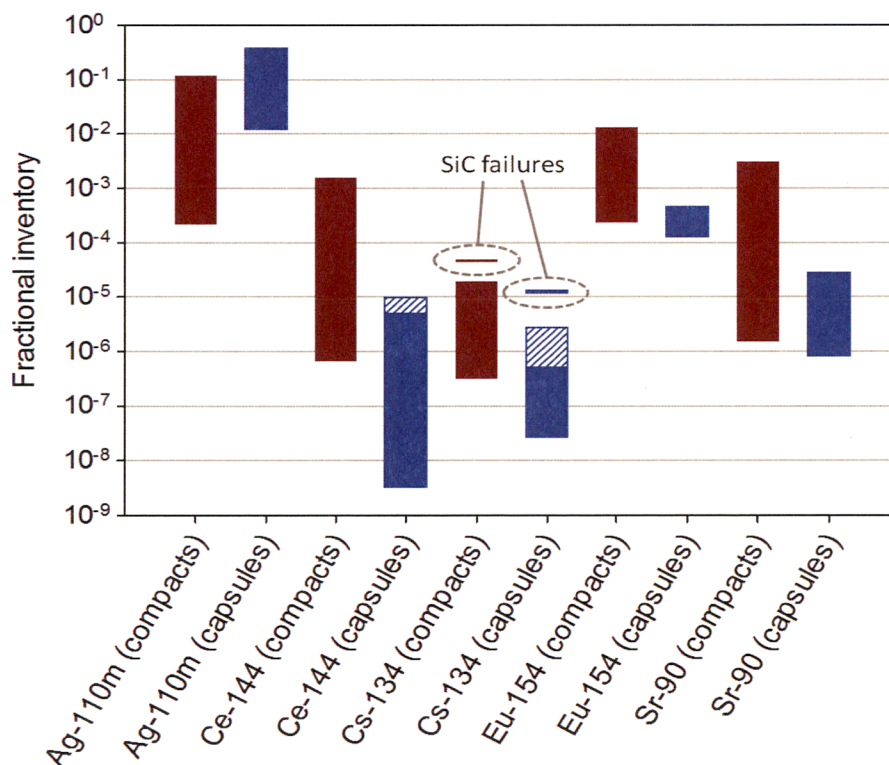

Figure 7-1
Range of AGR-1 fractional fission product inventories found in the matrix of examined compacts (red columns) and on the irradiation capsule components (blue columns). Instances where compacts and capsules contained SiC failures are indicated separately on the plot. Hashed areas indicate that the inventory on some capsule components was below the detection limit of the techniques. Therefore, the sum of contributions from all components represents a conservative upper bound for the total inventory in several of the capsules.
Courtesy of Idaho National Laboratory and used with permission of Battelle Energy Alliance, LLC

Interpretation of the AGR-2 ^{154}Eu data is complicated because almost all components from Capsules 5 and 6 contained no measurable inventory and the techniques used in some cases resulted in relatively high minimum detectable activities. Therefore, the range denoted by the hatched regions were established based on these minimum detectable activities. However, given the similarities in temperature between AGR-1 capsules and AGR-2 Capsules 5 and 6, as well as the generally similar trends in Eu and Sr behavior in the two experiments, it is likely that the actual ^{154}Eu fractional releases from the fuel compacts are in the ~10^{-4} range. The behavior of specific elements presented in Figures 7-1 and 7-2 is discussed further below.
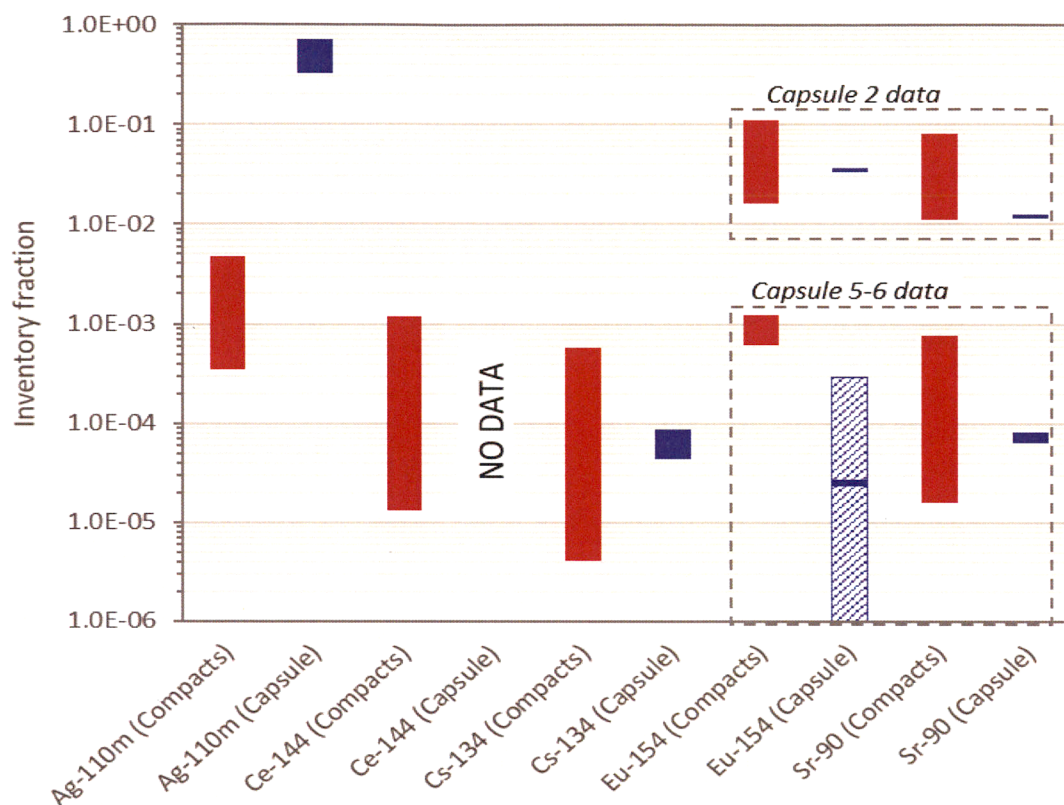

Figure 7-2
Range of AGR-2 fractional fission product inventories found in the matrix of examined compacts (red columns) and on the irradiation capsule components (blue columns). See text for explanation of the multiple data sets for ^{154}Eu and ^{90}Sr.
Courtesy of Idaho National Laboratory and used with permission of Battelle Energy Alliance, LLC

Cesium. As indicated in Figure 7-1, the Cs release from the AGR-1 fuel compacts was very low based on the inventory measured on the capsule components. The PIE of the capsule components and fuel compacts indicated two capsules (Capsules 5 and 6) contained a small number of particles with SiC layer failure (see Section 7.4 for further discussion), and these particles released higher levels of cesium relative to intact particles. As a result, the inventory of cesium in the compact matrix was found to be higher in compacts containing particles with SiC failures. Similarly, cesium release from fuel compacts was higher in capsules where SiC layer failures occurred. This distinction is indicated in Figure 7-1 by the separate data sets labeled "SiC failures."

In compacts containing SiC failures, the ^{134}Cs fractional inventory was approximately 5×10^{-5}, while in compacts containing only intact particles the fractional inventory was $<2 \times 10^{-5}$. In capsules containing SiC failures, the fractional release was approximately 1×10^{-5}, while in capsules with only intact particles the fractional release was $<3 \times 10^{-6}$ (with the highest measured inventory outside of compacts amounting to approximately 5×10^{-7}). At these low levels, the contribution of cesium from the dispersed uranium contamination in the matrix could be a significant portion of the total release from the compacts. These data therefore demonstrate that release from intact particles is extremely small. In addition, the higher peak compact matrix inventory relative to the inventory released from the compacts indicates a significant amount of retention of cesium in the matrix during irradiation.

The cesium inventories for AGR-2 shown in Figure 7-2—both the inventory in the matrix of analyzed compacts and the inventory released from the compacts to the capsule components— are notably higher compared to AGR-1. This is due in part to the higher overall temperatures in AGR-2 and the presence of exposed kernels and/or particles with failed SiC in all three capsules, and exacerbated by elevated incidence of SiC failure driven by proximity to test train components and not related to fuel performance (discussed further in Section 7.4). For this experiment, cesium fractional inventory in the matrix of compacts was found to peak at approximately 6×10^{-4}. Total fractional release of cesium from the compacts in UCO Capsules 5 and 6 (similar temperature to AGR-1 fuel) was 4.4×10^{-5}, while fractional release in Capsule 2 was $\sim 9 \times 10^{-5}$.

Europium and strontium. Both the ^{154}Eu and ^{90}Sr data for AGR-1 in Figure 7-1 exhibit a trend of higher fractional inventory in the matrix of compacts compared to the inventory released from compacts, indicating significant retention in the matrix during irradiation. This trend is evident for AGR-2 as well (Figure 7-2), with the range of values for Capsules 5 and 6 significantly overlapping those from AGR-1. Both experiments exhibit a similar trend in slightly lower Sr release relative to Eu. The AGR-2 Capsule 2 data demonstrate the notably higher inventory of Eu and Sr in the matrix of compacts at the higher irradiation temperature, peaking at around 10^{-1} and 8×10^{-2}, respectively.

Silver. Ag behavior is unique among the elements presented in Figure 7-1 and Figure 7-2 in that the release from the compacts to the capsule components generally exceeded the inventory retained in the matrix. AGR-2 matrix fractional inventory values overlap the range for AGR-1 but exhibit a maximum (5×10^{-3}) which is significantly less than the AGR-1 maximum (1.1×10^{-1}). The fractional release from compacts for the two experiments ranges from 10^{-2} to 7×10^{-1}. The temperature dependence of the Ag release from compacts is demonstrated in Figure 7-3, which presents the total ^{110m}Ag inventory measured outside of fuel compacts in all AGR-1 and AGR-2 capsules as a function of capsule time-average maximum temperature.

At the individual compact level, total Ag release varied considerably, from essentially complete retention to complete release. Figure 7-4 shows the measured ^{110m}Ag inventory in AGR-1 and AGR-2 compacts [73,74] divided by the calculated inventory from physics simulations (defined as the M/C ratio) as a function of time-average maximum compact temperature. Note values in excess of 1.0 result from more ^{110m}Ag measured in the compact than was predicted, which could be due to uncertainty on the measured inventory as well as a low bias on the predicted inventory. Similarly, at the individual particle level, Ag release could range from complete retention to complete release, as demonstrated from particle gamma counting data [82].
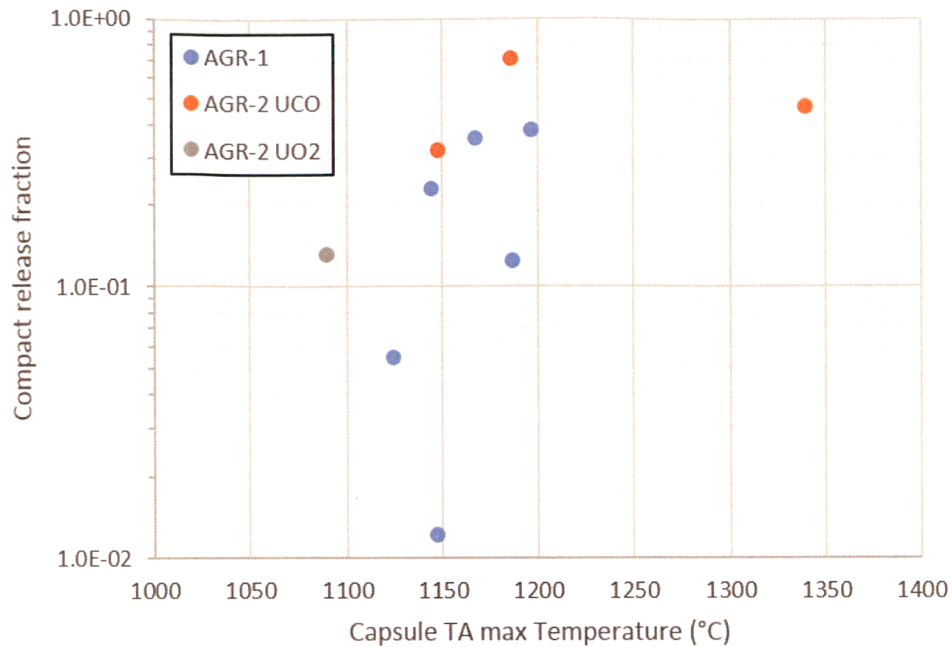
Figure 7-3
AGR-1 and AGR-2 capsule-average compact ^{110m}Ag release based on total inventory measured on capsule components as a function of the capsule time-average maximum temperature
Courtesy of Idaho National Laboratory and used with permission of Battelle Energy Alliance, LLC
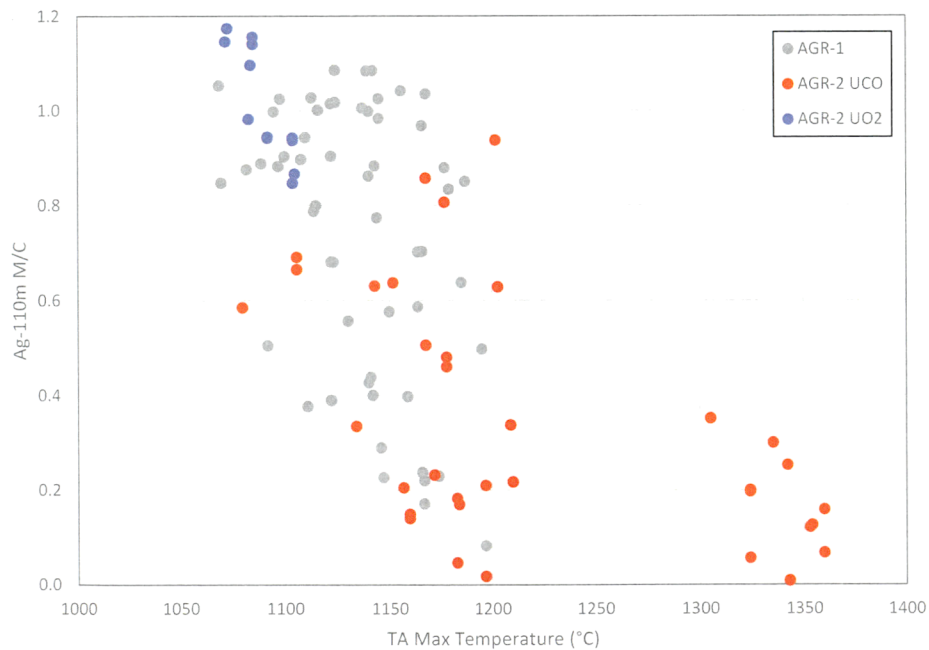

Figure 7-4
Ratio of measured ^{110m}Ag inventory to calculated inventory in AGR-1 and AGR-2 fuel compacts plotted vs. time-average maximum temperature
Courtesy of Idaho National Laboratory and used with permission of Battelle Energy Alliance, LLC

Palladium. The level of Pd found in the compacts outside the SiC was approximately 1% in five AGR-1 compacts for which this element was analyzed in the DLBL solutions. Despite this large amount of Pd in the fuel matrix, no widespread Pd corrosion or attack of SiC has been observed during metallographic examination of the as-irradiated TRISO particles. This was unexpected since Pd attack of SiC at high burnup in TRISO fuel has been postulated as a potential failure mode [68]. As will be described further below, Pd attack appears only to be a cause of SiC layer failure when IPyC layer failure allows localized Pd concentration at the inside of the SiC layer.

7.2   Irradiated Fuel Particle Microstructural Evolution

Extensive microscopic examination of particle cross sections has been performed to understand kernel and coating layer morphology evolution during irradiation. This included cross sections of select as-irradiated AGR-1 and AGR-2 compacts [86,87], as well as loose particles deconsolidated from numerous as-irradiated or safety-tested compacts [82,85]. In addition, a select number of particles were analyzed using x-radiography with 3-D tomographic reconstruction, which has enabled nondestructive examination of the kernel periphery and the coating layers. Common features observed in the irradiated particles include densification of the buffer layer and swelling of the kernel with related formation of gas-filled bubbles, as shown in Figure 7-5. High-burnup kernel migration (the so-called "amoeba effect") has not been observed in any particles, indicating the efficacy of the UCO fuel in limiting the oxygen partial pressure in the fuel and the formation of carbon monoxide.

In the majority of particles, the buffer layer debonded from the IPyC layer, driven by buffer densification and volume shrinkage, and leaving a void between the buffer and IPyC layer. This was observed as either complete (see Figure 7-5a) or partial (see Figure 7-5b) debonding in the polished plane analyzed. Much less common were particles in which the buffer and IPyC layers remained completely bonded in the plane observed (see Figure 7-5c), where the buffer densification resulted in the inner diameter increasing while the kernel swelled to fill the increasing volume. Such particles constituted 4% of approximately 1,000 particles observed in a study of AGR-1 compact cross sections [86], and no such particles were observed in a study of over 500 AGR-2 UCO particles in compact cross sections [87].

While all of the coating layers appeared intact for most particles in the plane examined, fracture of the buffer layer was not uncommon in the AGR-1 and AGR-2 particles. Buffer fracture was often accompanied by expansion of the kernel into the gap formed at the point of fracture (see Figure 7-5d). The percentage of particles with observable buffer fracture was relatively consistent among six AGR-1 compacts examined in cross section, varying 13 to 35% with an average of 23% [86]. The extent of buffer fracture exhibited much greater variation in AGR-2 UCO compacts (compact-average values from 0 to 86% based on examination of particles from seven UCO compacts), and this appeared to be influenced to some degree by irradiation temperature.

Comparing compacts irradiated to a calculated fast fluence of 3×10^{25} n/m^2 $\pm$ 0.12×10^{25}, those irradiated at TAVA temperatures of approximately 1100°C exhibited an observed buffer failure fraction of 86%, while those irradiated at TAVA temperatures >1200°C exhibited buffer failure fractions of 1–2%. This is believed to be due to greater magnitude of thermal creep occurring at

the higher temperatures, which relaxes stresses developed due to buffer densification and shrinkage. Given the relatively high rates of buffer fracture observed in many of the UCO compacts along with the very low SiC and TRISO coating failure fractions, it is clear that buffer fracture does not represent a significant threat to particle integrity.

While particles with buffer and IPyC layer separation and the representative buffer fracture shown in Figure 7-5d were fairly common, there appeared to be no obvious detrimental effects on the outer, dense coating layers that resulted in layer failure, even in cases where the kernel was in direct contact with the IPyC layer. However, if the buffer-IPyC interface remained intact as in Figure 7-5c, fracture of the buffer layer was always accompanied by fracture of the IPyC layer, and often included debonding of the IPyC from the SiC layer (see Figure 7-5e).

Fracture of the buffer layer was not necessary for IPyC fracture to occur. In some particles, partial debonding of the buffer-IPyC layer apparently led to development of sufficient stress in the IPyC layer to cause fracture (see Figure 7-5f), often with resultant debonding between the IPyC and SiC layers and in rare cases, partial fracture of the SiC at the IPyC-SiC interface (as shown in Figure 7-5f) that did not lead directly to SiC failure.

Because partial buffer-IPyC debonding (see Figure 7-5b) was much more common than no debonding (see Figure 7-5c), this type of IPyC fracture was more common than the type shown in Figure 7-5e. IPyC fracture and IPyC-SiC debonding of this nature was found to be an important contributor to SiC layer failure, as discussed in detail in Section 7.4.

A notable difference between the AGR-1 and AGR-2 irradiated particles is the absence of through-layer IPyC fractures observed in random AGR-2 particles examined in compact cross sections [87]. It is postulated this may be due to a less adherent buffer-IPyC interface strength (potentially a result of the longer fluidization time between buffer layer and IPyC layer deposition, which may result in fewer sites on the buffer surface for integration of the IPyC layer), such that the layers more easily detach during irradiation in the AGR-2 fuel. This would also tend to provide less opportunity for SiC layer failure from IPyC-SiC delamination.

7.3 Safety Testing

7.3.1 Isothermal Safety Tests in Dry Helium

Post-irradiation accident simulation heat-up testing ("safety testing") in dry helium has been performed on the AGR-1 and AGR-2 fuel compacts. The majority of these tests have been isothermal tests at a temperature of 1600, 1700, or 1800°C for a nominal duration of 300 hours. Tests have been performed using the Fuel Accident Condition Simulator (FACS) furnace at INL and the Core Conduction Cooldown Test Facility (CCCTF) at ORNL. Fifteen such tests were performed on AGR-1 fuel compacts. AGR-2 safety testing is still in progress, with seven AGR-2 UCO fuel compacts and three AGR-2 UO_2 fuel compacts tested to date.

Safety testing has demonstrated excellent robustness of the AGR UCO TRISO fuel. Figure 7-6 presents 1600°C test results from an AGR-2 UCO compact (AGR-2 5-2-2) that are typical of a significant number of the UCO safety tests [88]. In particular, the compact exhibited very low fractional release of Cs isotopes for the duration of the test, modest release of Eu and Sr isotopes (with the overall release behavior of these two isotopes being relatively similar), and fairly high release of ^{110m}Ag.
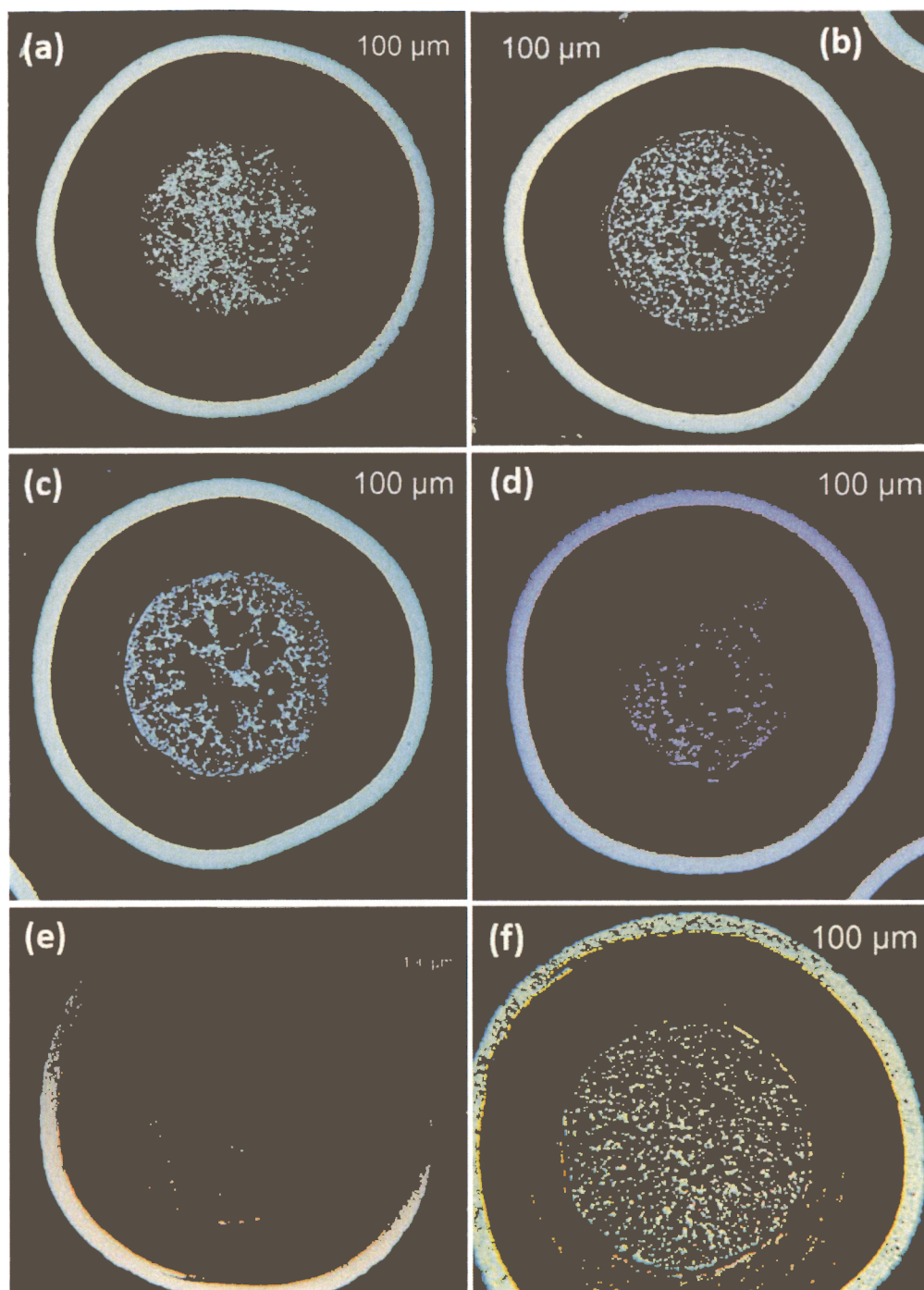
Figure 7-5
Examples of various AGR-1 irradiated particle microstructures
Courtesy of Idaho National Laboratory and used with permission of Battelle Energy Alliance, LLC

Typical of a number of the AGR safety tests to date, no ^{85}Kr was detected in the gas effluent during this test, with the total estimated detection limit corresponding to fractional release in the range of 1×10^{-6} to 5×10^{-6}. Note in most tests, the fractional release of several other isotopes was also quantified, including ^{137}Cs and ^{155}Eu. The discussion below omits these, as the behavior of these elements is better characterized using the isotopes ^{134}Cs and ^{154}Eu. For Cs, the isotope ^{137}Cs tends to be influenced to a greater degree by contamination in shielded hot cells because of its long half life ($t_{1/2}$ = 30 years), with for Eu, the isotope ^{154}Eu has gamma emissions that make detection more favorable than for ^{155}Eu.

Summary plots of ^{134}Cs, ^{110m}Ag, ^{154}Eu, and ^{90}Sr fractional release from all AGR-1 and AGR-2 isothermal safety tests completed to date are shown in Figure 7-7 and Figure 7-8. The x-axis represents elapsed time after reaching the target hold temperature. Releases are expressed as a fraction of the total calculated inventory generated in the compact during irradiation. Test temperature is indicated by the plot colors: 1600°C (blue), 1700°C (green), or 1800°C (red). The inventory fraction corresponding to a single particle is indicated by the dashed horizontal lines on the plots (as labeled on the ^{110m}Ag plots in each figure).

The total number of particles per compact was approximately 4100 for AGR-1, 3180 for AGR-2 UCO, and 1540 for AGR-2 UO$_2$. The AGR-2 UO$_2$ test data are represented by dotted lines and gray-filled symbols in Figure 7-8. The key trends in fractional release behavior based on these data are summarized for specific elements in the discussion below. Krypton fractional release data are not provided in Figure 7-7 and Figure 7-8, as the level of ^{85}Kr released during many of the tests was below detection limits. ^{85}Kr release observations are included in the discussion below.
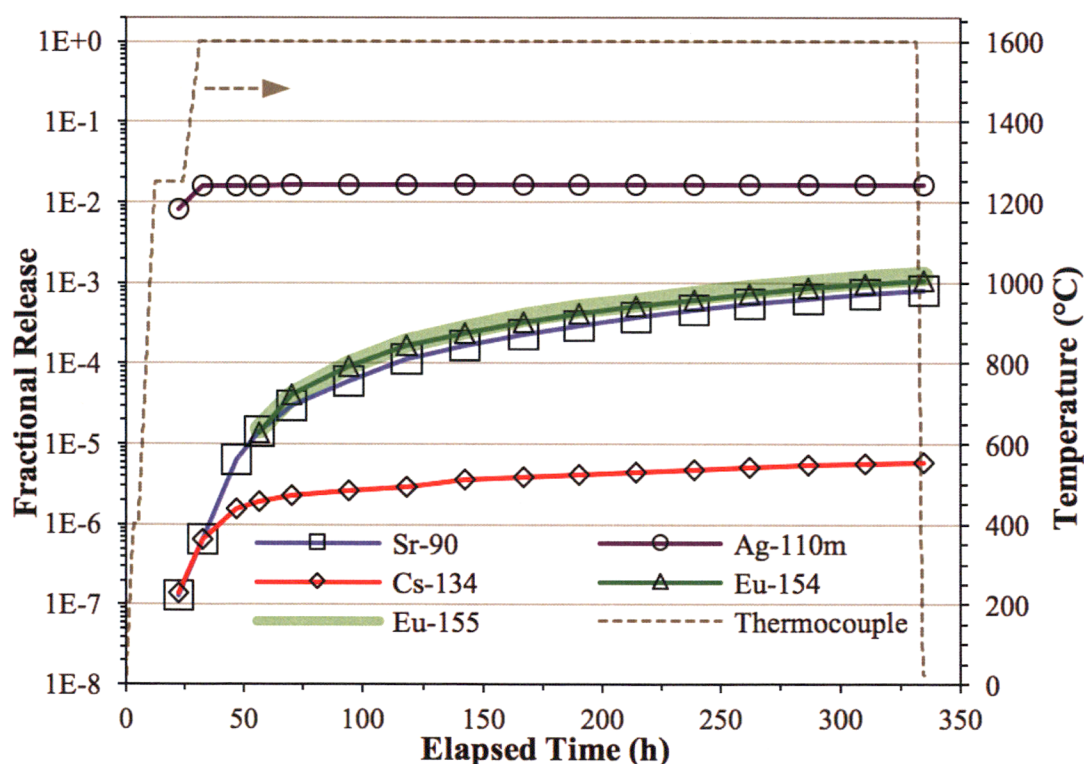
Figure 7-6
Fission product release from heating of AGR-2 compact 5-2-2 at 1600°C
Courtesy of Idaho National Laboratory and used with permission of Battelle Energy Alliance, LLC

Figure 7-7

Fission product releases from AGR-1 compacts during isothermal safety tests. Plot color indicates test temperature: 1600°C (blue), 1700°C (green), or 1800°C (red)

Courtesy of Idaho National Laboratory and used with permission of Battelle Energy Alliance, LLC

Figure 7-8
Fission product releases from AGR-2 compacts during isothermal safety tests. Plot color indicates test temperature: 1600°C (blue), 1700°C (green), or 1800°C (red). UO₂ tests are indicated by dotted lines with gray-filled symbols
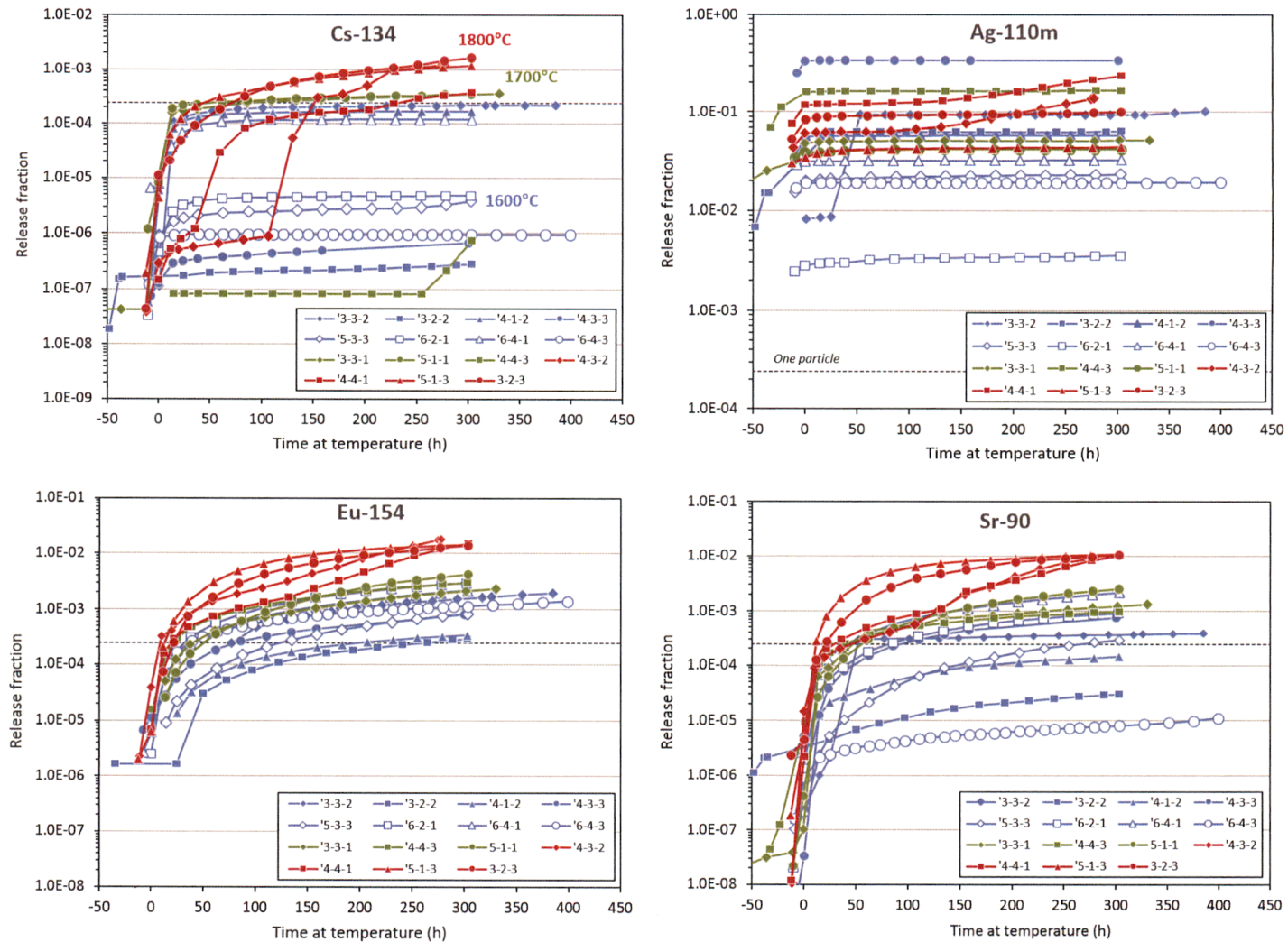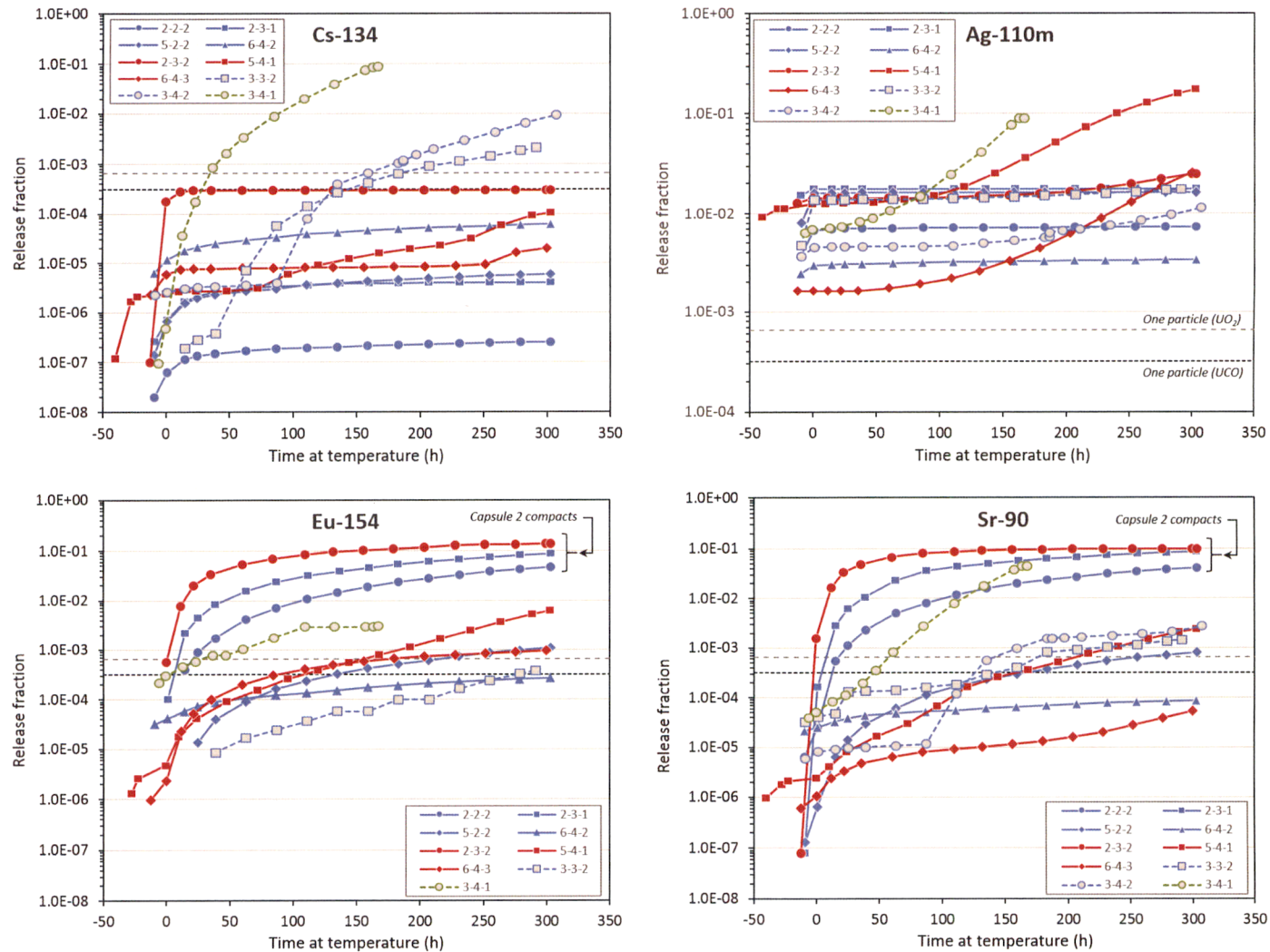*Courtesy of Idaho National Laboratory and used with permission of Battelle Energy Alliance, LLC*

7.3.2 Cesium

The AGR-1 ^{134}Cs release data indicate two distinct sets of release curves, exhibiting end-of-test release $>10^{-4}$ or $<5 \times 10^{-6}$. Extensive PIE following the safety tests has demonstrated all compacts with releases $>1 \times 10^{-4}$ contained one or more particles with a SiC layer that had failed (in some cases these were found to be particles with as-fabricated defective layers) [82,85]. These particles typically retained an intact pyrocarbon layer, such that ^{85}Kr release remained low (the exception was Compact 4-3-2, which experienced two TRISO failures). Recovery and inspection of the particles with SiC failures has helped to understand the failure mechanism, as discussed further in Section 7.4. In the remaining compacts with release $<5 \times 10^{-6}$, no evidence of any coating failures was found.

The results demonstrate cesium release through intact SiC is extremely low; therefore, cesium release from the fuel is dictated largely by the number of particles experiencing SiC layer failure. Peak ^{134}Cs release was approximately 2×10^{-4} after 300 hours at 1600°C and approximately an order of magnitude higher at 1800°C. Note during the safety test of Compact 4-3-2, the ^{134}Cs release remained below 1×10^{-6} for approximately 100 hours before a suspected SiC failure resulted in a significant increase, demonstrating excellent retention by intact SiC even at 1800°C.

Cesium release during the AGR-1 UCO tests (Figure 7-7) was lower compared to AGR-2 (Figure 7-8), primarily reflecting a lower incidence of SiC failure. The highest release at 1600°C was approximately 6×10^{-5} (Compact 6-4-2). While this is roughly an order of magnitude higher than releases from AGR-1 compacts containing only intact particles, it is still ~5x lower than the level of one particle. This observation, along with a lack of evidence of failed particles during post-test destructive examination of the compact, suggest no particles suffered SiC failure.

One of the compacts tested at 1800°C experienced an early TRISO failure (Compact 2-3-2), with ^{134}Cs release reaching 3×10^{-4} by the end of the test (equivalent to a single particle inventory, and the highest ^{134}Cs release observed from all AGR-2 UCO compacts), and a second compact (Compact 5-4-1) experienced a SiC layer failure with ^{134}Cs release reaching 1×10^{-4} at the end of the test. The third compact tested at 1800°C (Compact 6-4-3) experienced no SiC layer failure during the test and ^{134}Cs release was 2×10^{-5} at the end of the test, the lowest for any 1800°C UCO fuel tested to date. Notably, the AGR-2 data do not exhibit the same bifurcated ^{134}Cs release behavior as observed for AGR-1. This is largely a consequence of the lower number of SiC failures (and zero failures at 1600°C), which limited the number of tests with ^{134}Cs $>10^{-4}$ to only Compact 2-3-2 (1800°C).

Recovered AGR-1 and AGR-2 particles that experienced SiC layer failure during safety tests were found to have widely varying levels of Cs retention. Values ranged from extremely low (less than 10%) to relatively high (values as high as approximately 80% were measured). Higher levels of retention are possible, but particles with such high retention would be indistinguishable from particles with intact SiC and could not be isolated during PIE.

A key observation with regard to AGR-2 UO$_2$ ^{134}Cs release during the tests is the obviously higher values compared to UCO. Total release at 1600°C was 2×10^{-3} to 10^{-2}, and nearly 10^{-1} at 1700°C (note the 1700°C test was terminated prior to the originally planned 300-hour duration due to the rapidly increasing release of fission products). Post-test analysis of the compacts revealed a significant number of particles that experienced measurable cesium release.

Analysis of these particles revealed the cause to be reaction of CO(g) with the SiC layer and concomitant degradation of the layer, such that cesium retention was impacted while fission gas remained largely retained in the particles due to an intact OPyC layer. An example is shown in Figure 7-9. The observed corrosion of the SiC layer is similar to that observed in previous tests with UO_2 TRISO particles [89]. It is estimated approximately 400–800 particles in AGR-2 Compact 3-4-1 (1700°C) had a SiC layer with degraded Cs retention [85]. The significantly increased level of SiC failure and Cs release in the UO_2 fuel highlights one of the key advantages of UCO fuel, which results in far less production of CO(g) within the particle. With an average end-of-test release of 5.7×10^{-3} at 1600°C, the UO_2 fuel exhibited over 300x higher ^{134}Cs release compared to the average release from UCO tested under the same conditions (1.8×10^{-5}).

Figure 7-9
Optical (left) and electron (right) micrographs of a region of the SiC layer corroded by CO in an irradiated UO_2 particle heated to 1600°C
Courtesy of Idaho National Laboratory and used with permission of Battelle Energy Alliance, LLC.

7.3.3 Silver

The most common Ag release behavior for UCO at 1600 and 1700°C was rapid early release of a fraction between 3×10^{-3} and 3×10^{-1} followed by little measurable additional release for the remaining duration of the test. This released inventory is roughly comparable to the range of inventories found in the matrix of as-irradiated compacts (Figure 7-1 and Figure 7-2) and is believed to be due to depletion of silver in the compact matrix at the end of irradiation.

A notable behavior during 1800°C safety tests of AGR-1 compacts was an increase in ^{110m}Ag release after approximately 100 hours for Variant 3 (that is, Capsule 4) compacts (see the ^{110m}Ag data for Compacts 4-3-2 and 4-4-1 in Figure 7-7). The Variant 3 fuel was fabricated with a variation in the SiC coating process that resulted in a finer-grain microstructure relative to the Baseline fuel (Sections 5.3.2.2 and 5.3.2.5). A similar increase in ^{110m}Ag release was not observed for the other two compacts heated at 1800°C. These two compacts both had SiC with the larger-grained, Baseline microstructure. All three of the AGR-2 UCO compacts heated at 1800°C exhibited increasing ^{110m}Ag release similar to the similar AGR-1 Variant 3 compacts

(see red data plots in Figure 7-8). The AGR-2 fuel particles were fabricated with SiC layer deposition conditions based on the AGR-1 Variant 3 process, and a similar fine-grained microstructure (Sections 5.3.2.3 and 5.3.2.5). The conclusion is the finer-grain SiC allows Ag diffusion to a greater extent than the larger-grain AGR-1 Baseline microstructure, but the effect is only detectable after ~100 hours at 1800°C.

The AGR-2 UO_2 tests at both 1600°C and 1700°C exhibited an increase in ^{110m}Ag release rate after the initial release observed at the start of the test. The onset of this release occurred earlier in the 1700°C test compared to the 1600°C tests. It is likely this increase is related to the significant number of particles experiencing failure of the SiC layer rather than diffusion through intact SiC, which was fabricated using a similar process as the AGR-2 UCO fuel.

7.3.4 Europium and Strontium

The release behavior for Eu and Sr was typically very similar during the AGR UCO safety tests. AGR-1 data exhibit similar release curves for the two elements and a similar range of total release values at each temperature (with the exception of a greater spread in 1600°C ^{90}Sr data toward lower values, as shown in Figure 7-7). For both elements, the data demonstrate a clear trend of increasing release with increasing temperature. In the 1600 and 1700°C tests, the data exhibit relatively constant release rate throughout the tests, and the final release is within the range of values quantified in the matrix of as-irradiated AGR-1 compacts (Figure 7-1). This suggests the release during these tests was primarily from inventory present in the compact matrix at the end of irradiation that was slowly released at elevated temperature.
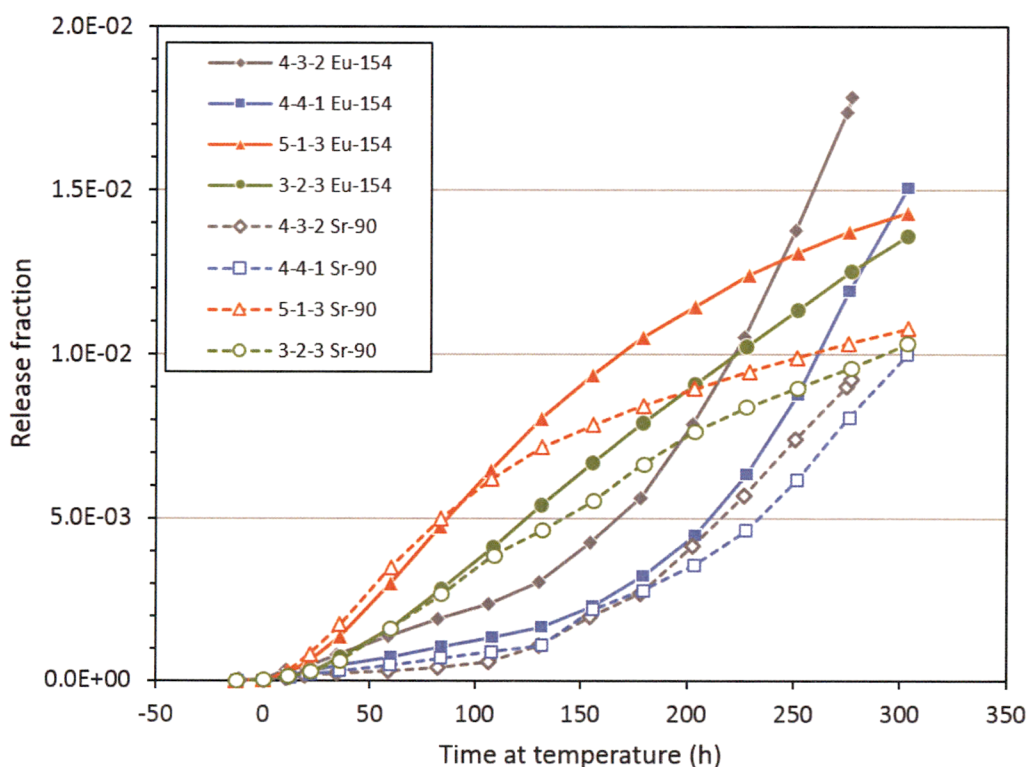

Figure 7-10
^{154}**Eu and** ^{90}**Sr release from AGR-1 compacts heated to 1800°C**
Courtesy of Idaho National Laboratory and used with permission of Battelle Energy Alliance, LLC

The 1800°C tests displayed differing behavior depending on the fuel type. Release from the two AGR-1 Variant 3 compacts (4-3-2 and 4-4-1) exhibited an increase in rate at around 100 hours, similar to that observed for ^{110m}Ag. This suggests the onset of additional release through intact particle coatings. By contrast, the Baseline (3-2-3) and Variant 1 (5-1-3) compacts exhibited a slightly decreasing rate over the same time period. These trends are highlighted in Figure 7-10. The decrease in release rate for the Baseline and Variant 1 compacts may be due to the total ^{154}Eu and ^{90}Sr source in the matrix of these compacts becoming depleted toward the end of the test. Note the final ^{154}Eu and ^{90}Sr release in the 1800°C tests was very near or slightly exceeding the range of values quantified in the matrix of as-irradiated compacts (Figure 7-1).

The AGR-2 Eu and Sr release data in Figure 7-8 are more complex due to (1) the Capsule 2 compacts that were irradiated at significantly higher temperatures compared to other AGR UCO fuel and (2) the UO$_2$ compacts from Capsule 3. The 1600°C ^{154}Eu and ^{90}Sr releases from Capsule 5 and 6 UCO compacts (5-2-2 and 6-4-2)—which had irradiation conditions more closely comparable to AGR-1—were in the same range as the AGR-1 values. However, the 1800°C releases from Capsule 5 and 6 compacts (5-4-1 and 6-4-3) were somewhat lower than the AGR-1 values, particularly in the case of ^{90}Sr; the 5.4×10^{-5} ^{90}Sr fractional release from

Compact 6-4-3 is the lowest value observed at 1800°C in the AGR program to date. Furthermore, only Compact 5-4-1 exhibited the characteristic increase in ^{154}Eu and ^{90}Sr release rate after ~50–100 hours. Compact 6-4-3 exhibited a minor increase in ^{90}Sr release rate near 150–200 hours, and a gradual decrease in ^{154}Eu release rate. Figure 7-11 highlights the 1800°C ^{154}Eu and ^{90}Sr behavior of these two compacts.

The data from AGR-2 Capsule 2 compacts are labeled on the ^{154}Eu and ^{90}Sr plots in Figure 7-8. The end-of-test releases were notably higher compared to other AGR UCO fuel compacts, reaching approximately 10^{-1} at 1800°C, and 4×10^{-2} to 10^{-1} at 1600°C. These high release values during the safety tests are related to the much higher inventory in the matrix of the Capsule 2 compacts, a result of significant diffusion through intact coatings at the relatively high irradiation temperatures. Note these release fractions are near the upper end of the range of values quantified in the matrix of as-irradiated AGR-2 compacts (Figure 7-2).

The AGR-2 UO$_2$ ^{154}Eu and ^{90}Sr releases differed from the UCO behavior. While the final ^{154}Eu fractional release at 1600°C was of a similar magnitude as the UCO values, the ^{90}Sr values were slightly higher and in one instance (Compact 3-4-2) the release experienced noticeable increase at approximately 100 hours, which corresponds to the increase in ^{134}Cs release. The 1700°C ^{154}Eu fractional release from Compact 3-4-1 was approximately 3×10^{-3} at the end of the test, while the ^{90}Sr was over an order of magnitude higher (4.5×10^{-2}). It can be concluded the relatively high number of particles with SiC failure contributed significantly to the Eu and Sr release in the UO$_2$ compacts.
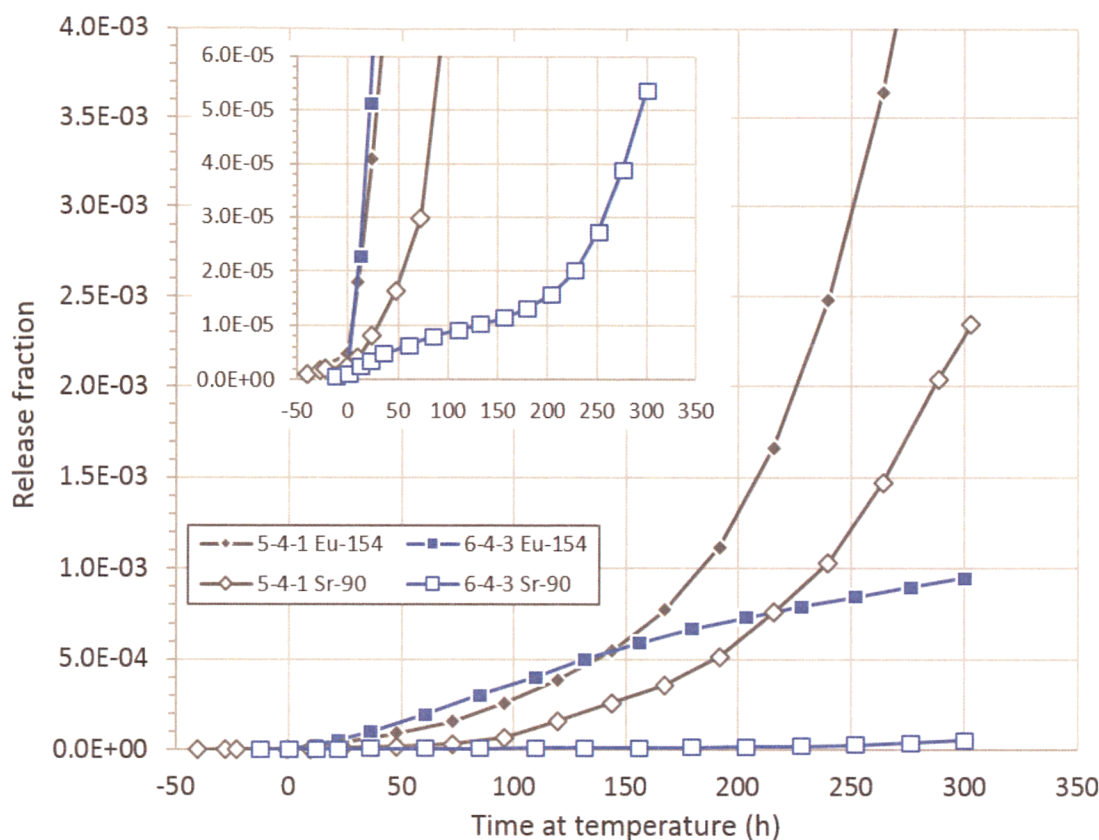
Figure 7-11
^{154}Eu and ^{90}Sr release from AGR-2 Capsule 5 and 6 compacts heated to 1800°C
Courtesy of Idaho National Laboratory and used with permission of Battelle Energy Alliance, LLC

7.3.5 Krypton

Krypton release curves are not presented here, as there was no ^{85}Kr detected in the gas effluent in a significant number of the safety tests. Table 7-1 summarizes the Kr release observations from all AGR-1 safety tests and AGR-2 safety tests completed to date for a nominal heating duration of 300 hours. No TRISO failures have been observed in any 1600 or 1700°C tests for both UCO and UO$_2$ fuel, and two 1800°C tests exhibited one (AGR-2 Compact 2-3-2) or two (AGR-1 Compact 4-3-2) TRISO failures.

7.3.6 Transient Temperature Accident Simulation Tests in Dry Helium

The nominal 300 hours hold at the peak temperature used in the isothermal tests described in the previous section greatly exceeds the duration that fuel will experience peak temperature in a reactor accident. The German UO$_2$ TRISO development program in the 1980s performed several accident tests that involved heating the compacts in dry helium using a time-temperature profile that closely simulated the expected peak fuel temperature trajectory in the reactor core during a depressurized loss of forced cooling accident, based on the HTR-MODUL reactor design [90,91]. Several tests were performed in which the peak temperature reached approximately 1620°C. In two of these tests using spherical fuel elements with burnup of 9-10% FIMA, ^{85}Kr

releases exceeded the level of a single particle, indicating one or more particles experiencing TRISO failure. A separate test using an element with burnup of 9% FIMA (element AVR-91/31) was performed with the temperature curve shifted upwards to obtain a maximum of 1700°C. During this test, ^{85}Kr levels reached approximately 10^{-3}, also indicating several TRISO failures.

Table 7-1
Maximum ^{85}Kr release fractions for AGR UCO and UO$_2$ fuel after ~300 hours at 1600, 1700, and 1800°C

Fuel Type	Temperature	Remarks
UCO	1600°C	$<5 \times 10^{-6}$; undetectable in majority of tests
	1700°C	$<10^{-5}$
	1800°C	$<6 \times 10^{-5}$ in 5 tests with no TRISO failures ~4×10^{-4} in 2 tests where either 1 or 2 TRISO failed
UO$_2$	1600°C	$<2.5 \times 10^{-6}$ (estimated detection level as no ^{85}Kr was measured)
	1700°C	4×10^{-5} after 174 h; increase probably due to diffusion through OPyC in particles with failed SiC layer

The spheres that experienced failures during the tests were at the upper end of normal burnup for UO$_2$ TRISO fuel and the uncertainty in the actual irradiation temperature for fuel spheres in AVR was large (with the possibility irradiation temperatures could significantly exceed the reported values). These factors may have contributed to the elevated particle failure fractions observed. Nonetheless, the results of these tests have raised concerns that variable temperature tests with relatively rapid rise to temperature at the start of the accident phase could result in more particle damage than seen in isothermal tests. To address this concern, the AGR program has repeated the more extreme 1700°C test of fuel element AVR-91/31 using three AGR-1 compacts from Capsule 1 (approximately 12,300 particles) [92].

The average burnup of the compacts was 15% FIMA, the average compact TAVA temperature was 1027°C, and the average compact time-average peak temperature was 1123°C. Results of the heating tests are shown in Figure 7-12. The test involved an isothermal hold at a temperature of 857°C for approximately 70 hours before executing a rapid rise to the peak temperature of 1700°C, followed by a relatively gradual temperature decrease to ~1200°C over the next 270 hours (the temperature profile was based on the previous German test of AVR-91/31).

The results are consistent with the isothermal AGR-1 and AGR-2 UCO tests. ^{110m}Ag fractional release rapidly reached a relatively high level (7×10^{-2}) and did not change appreciably for the remainder of the test. ^{134}Cs, ^{154}Eu, and ^{90}Sr release all increased initially during the rapid temperature rise but little additional release was observed after a total elapsed time of approximately 215 hours (corresponding to a test temperature of ~1500°C).

The final release of these isotopes was lower than observed for the AGR-1 or AGR-2 1600°C isothermal tests, which would be expected based on the shorter duration at high temperatures (total duration at temperatures >1600°C was approximately 70 hours). ^{85}Kr fractional release was low throughout the test, with a final value of 3×10^{-6}. The ^{134}Cs and ^{85}Kr data indicate zero particles with SiC layer failure or complete TRISO layer failure during the test.
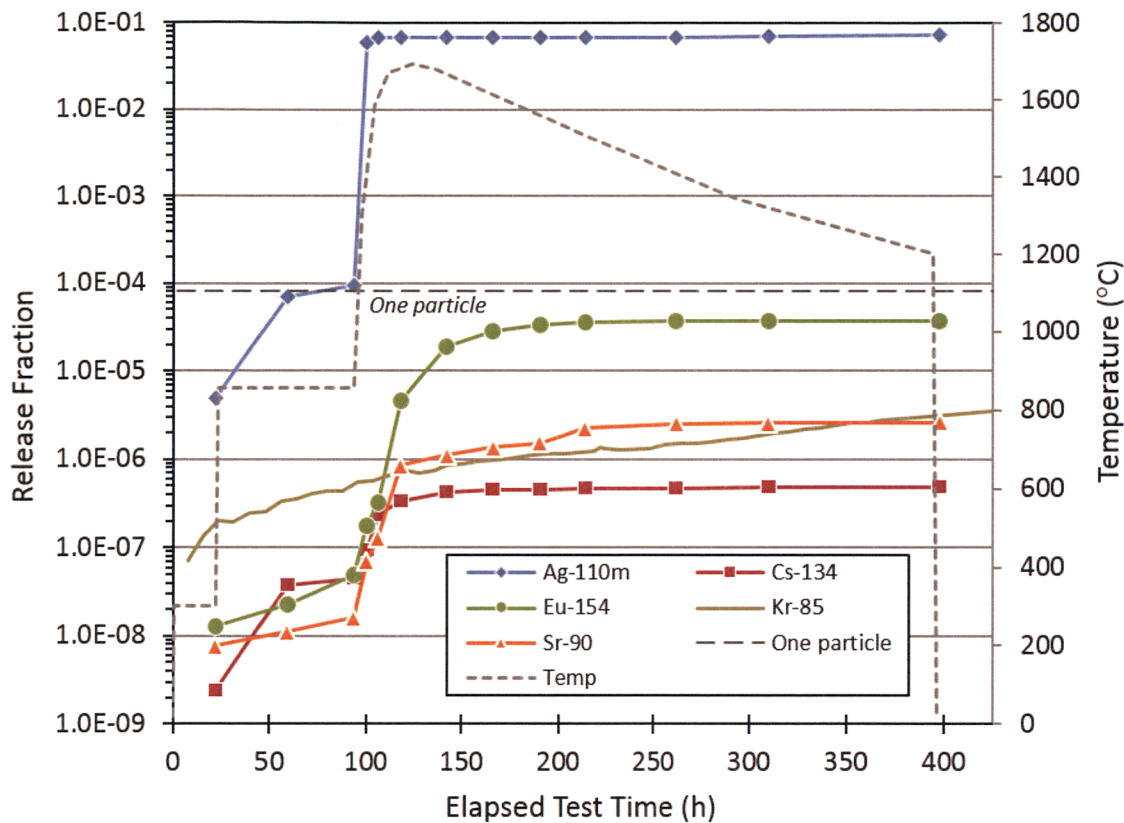
Figure 7-12
Fission product release during an accident simulation test in dry helium using three AGR-1 compacts
Courtesy of Idaho National Laboratory and used with permission of Battelle Energy Alliance, LLC

A similar test is planned using three AGR-2 compacts from Capsule 5 (average burnup of 12.7% FIMA, average compact time-average maximum temperature of 1200°C) to compile additional data and confirm the results from the AGR-1 test.

7.4   SiC Failure Mechanisms

Coating layer failure was relatively rare in the AGR UCO fuel particles, both during irradiation and during safety tests. For the AGR-1 and AGR-2 irradiations combined, TRISO failure occurred in approximately 1 out of every 103,000 particles (with none observed in the AGR-1 irradiation), and no TRISO failures occurred in any of the 1600°C or 1700°C safety tests. Instances of SiC layer failure occurred with higher frequency, but were still relatively rare: approximately one in every 52,000 particles during irradiation and one in every 15,000 particles during 1600°C safety tests (detailed failure statistics are compiled and discussed in Section 7.6). Furthermore, the actual degradation and failure of a SiC layer has been found to occur in a localized region within the particle.

A consequence of the low failure fractions and localized corrosion is that the likelihood of observing the layer failure by random examination of particle cross sections (the method commonly employed during historical PIE of particle fuel) is extremely small. In previous TRISO fuel development and testing efforts, particle failure mechanisms were only observed and understood when the rate was sufficiently high that random observation was likely, often at the percent level or higher. Prior to initiating the AGR-1 PIE, methods were developed to locate particles with failures for further study.

Particles that experienced SiC layer failure during irradiation or during safety tests were identified based on elevated cesium release, and many of these were analyzed in detail both nondestructively, using x-ray imaging with tomographic reconstruction, and by cross-sectioning and microanalysis using a number of analytical characterization methods. The basic approach used for the AGR-1 fuel has been described previously [82] and is being repeated for the AGR-2 fuel [85,93].

For SiC failures during irradiation, the examination process started with gamma-scanning the empty graphite holders to locate regions with elevated cesium activity. The compacts that were adjacent to these regions during irradiation were identified as likely to contain one or more particles that experienced SiC failure in-pile. These as-irradiated compacts, as well as compacts that exhibited Cs release indicative of SiC failure during safety testing, were then deconsolidated to liberate the particles, which were individually gamma counted to quantify the inventory of ^{137}Cs, ^{134}Cs, and ^{144}Ce. Particles that exhibited abnormally low cesium inventory were then collected, and x-ray imaging was used to nondestructively observe the interior particle morphology.

In total, three particles with high cesium release during the AGR-1 irradiation were found in two compacts and examined. (A fourth particle was detected during deconsolidation-leach-burn-leach analysis of another compact but was destroyed in the process; therefore, the particle was not subjected to detailed microstructural analysis). In all of these particles, a similar failure mechanism was implicated. Buffer shrinkage contributed to IPyC fracture due to incomplete debonding at the buffer-IPyC interface.

In one case, arrowhead-like fracture occurred (similar to that shown in Figure 7-5e), while in the other two particles, IPyC fracture was related to stress from the buffer pulling away from the IPyC (similar to Figure 7-5f). The IPyC fracture then exposed the SiC layer to concentrated chemical attack of fission products (notably Pd), which caused degradation through the entire layer (see Figure 7-13).

It is noteworthy significant attack of the SiC layer was never observed in particles without this sort of IPyC fracture, nor in these three particles in areas away from the IPyC fracture. So, while these failures were ultimately caused by Pd attack on SiC, prior fracture of the IPyC layer appears to be a prerequisite for the attack to occur.

Figure 7-13
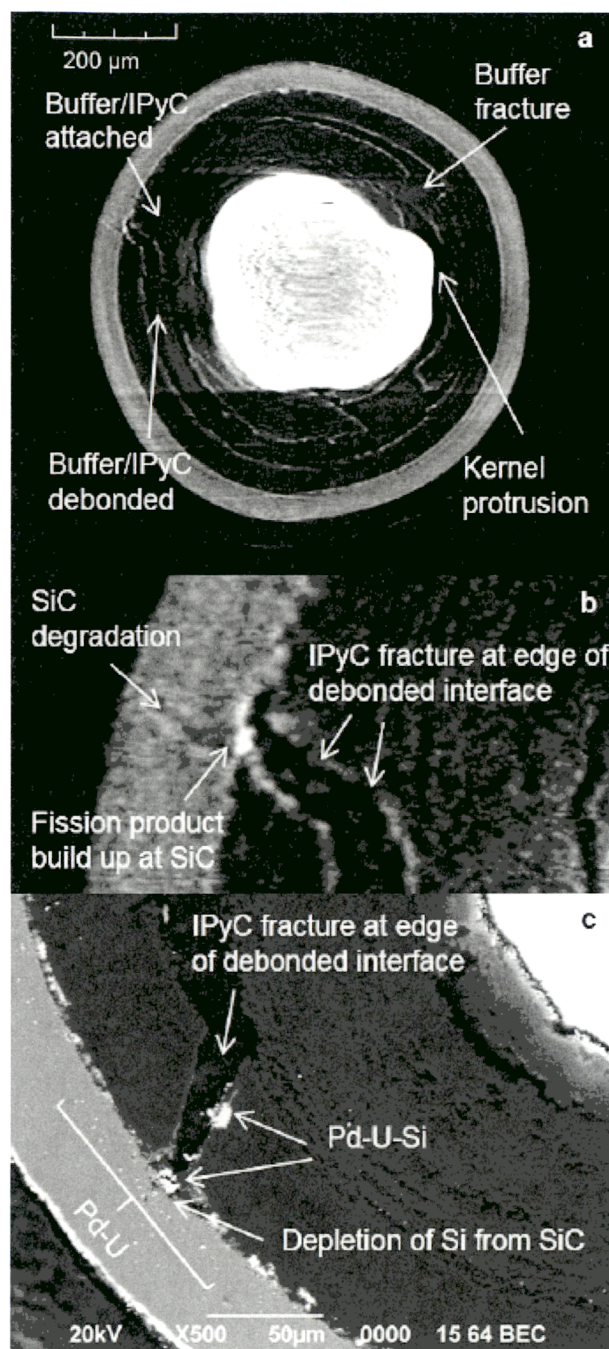**(a) X-ray tomogram showing microstructure in as-irradiated AGR-1 Compact 5-2-3 particle that led to SiC failure and cesium release; (b) x-ray close-up of degraded pathway through SiC; and (c) SEM micrograph of degraded region with EDS identification of Pd and U in the SiC and Si outside the SiC**
Courtesy of Idaho National Laboratory and used with permission of Battelle Energy Alliance, LLC

AGR-1 safety testing produced SiC failures in fractions higher than during irradiation, with the failure fractions increasing with test temperature. At 1600°C, two of the three AGR-1 particles with SiC failures that were identified were examined in detail, and the cause of the SiC failure was determined to be an as-fabricated defect in the SiC layer (the third particle was not recovered for analysis). At 1700 and 1800°C, nearly all of the particles recovered exhibited a similar SiC failure mechanism to the one identified for the as-irradiated particles. However, the elevated temperature increased the severity of the SiC degradation due to enhanced reaction with fission products. Figure 7-14 shows the local corrosion of the SiC layer in an AGR-1 particle from a 1700°C safety test.
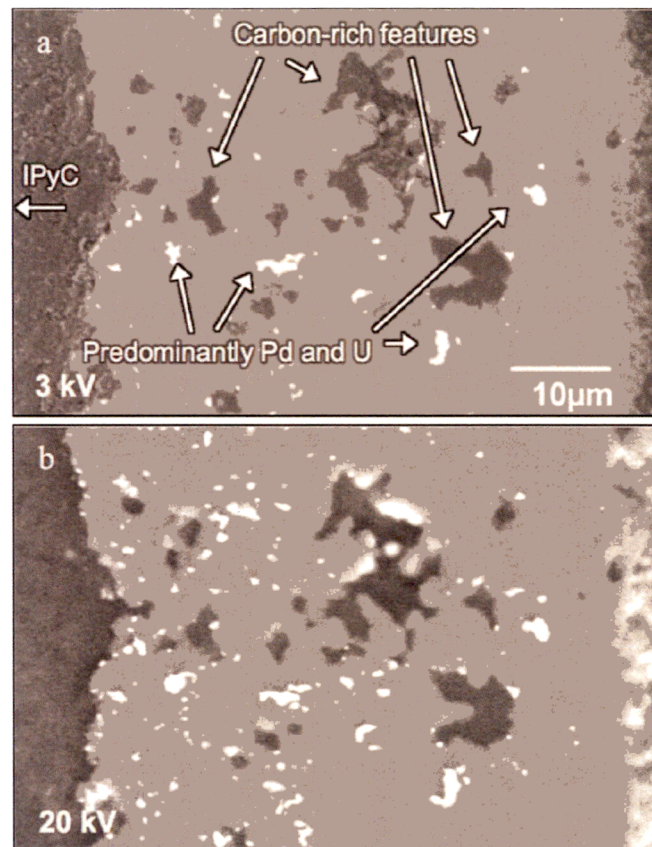
Figure 7-14
Corroded region of the SiC layer of an AGR-1 particle safety tested at 1700°C
Courtesy of Idaho National Laboratory and used with permission of Battelle Energy Alliance, LLC

Examination of SiC failures in AGR-2 particles has been less conclusive, as it appears some particles experiencing SiC failure (both during irradiation and during safety testing) may have been destroyed during the DLBL process, eliminating the opportunity to perform detailed examination. In addition, several particles from AGR-2 Capsule 2 that experienced failed SiC were recovered and examined in detail. Evidence was present of significant degradation of the SiC layer from nickel [93]. The evidence suggests that these particles failed due to interaction with Ni contamination, likely originating from a failed thermocouple in the graphite holder located very close to these compacts during the irradiation as the TCs contain Ni in their

thermoelements. However, some of the AGR-2 particles that have been observed with SiC failure indicate a similar mechanism as described above for the AGR-1 particles.[20]

The dominant SiC failure mechanism described here is significantly different from those currently embedded in fuel performance models.[21] Incorporation of this failure mode into the models is likely to be challenging due to its complex nature (essentially a two-part mechanism, involving thermomechanical behavior of the buffer and IPyC under irradiation, followed by focused chemical attack of the SiC layer) and a lack of some key data (including buffer strength, buffer-IPyC bond strength, fission product partitioning coefficients at the site of the IPyC fracture, and reaction kinetics for the chemical degradation). It is also unclear whether this type of SiC layer failure acts as a precursor to complete TRISO failure (that is, whether eventual failure of the OPyC layer in these particles and related release of fission gas is a likely scenario). While this seems plausible, particles with TRISO failure are sufficiently rare and are not usually recovered intact for further study, such that their specific cause in the AGR UCO particles is not known with certainty in most instances.

7.5   Effect of SiC Microstructure

Notwithstanding differences in grain size, no major differences in fuel performance among the AGR-1 and AGR-2 SiC fuel types were observed in the data. This means primarily that there were no differences in fission product release in-pile or during heating tests at 1600-1700°C, and no differences in TRISO or SiC failure fractions. The only observed difference was an increase in fission product release from particles with fine-grained SiC at a temperature of 1800°C for durations longer than 100 hours. This negligible difference in performance indicates that none of the AGR SiC types were approaching a limiting value in terms of grain size.

7.6   Particle Failure Statistics

The statistics for both SiC layer failure and full TRISO failure for AGR-1 and AGR-2 UCO fuel—both during irradiation and during safety tests—are compiled in Table 7-2 below. The table lists the total number of compacts and particles for each test condition, the number of observed failures of each type based on current best estimate values from irradiation and PIE data, the actual failure fraction (number of failures divided by number of particles tested), and the upper 95% confidence limit on the failure fraction calculated using binomial statistics. Explanation of the AGR-1 data has been provided by Demkowicz et al. [82].

The AGR-2 data are preliminary and are based on PIE and safety testing completed to date. As mentioned in Sections 6.7 and 6.8, exact numbers of particles that experienced failed TRISO during the irradiation could not be reliably determined based on R/B ratios. A conservative

---

[20]   This excludes the particles in AGR-2 Compact 2-2-3 that exhibited obvious evidence of external nickel attack on the SiC layer, which is believed to be due to the combination of a very close proximity to a failed thermocouple in the graphite holder and the relatively high irradiation temperature. See discussion by Hunn et al. for details (Reference 100). These particles are not included in the calculated AGR-2 failure statistics. However, they did contribute to overall Cs release from the fuel compacts in Capsule 2, artificially elevating the reported values.

[21]   Note that the PARFUME code does not consider the possibility of SiC failure with the OPyC remaining intact, as failure of SiC layer automatically results in OPyC failure in the model. Nonetheless, this mode of SiC layer failure (that is, localized Pd attack resulting from IPyC failure and IPyC-SiC debonding) is not considered in the model.

approach was taken in assessing available AGR-2 PIE data in this regard, and is described briefly here.

Particles with exposed kernels in AGR-2 compacts were assessed based on a combination of capsule fission product inventory data (data on fission product—primarily Cs—release from compacts during irradiation), DLBL results (for example, the presence of uranium from dissolved kernels in the pre-burn leach solutions), particle gamma counting and subsequent x-ray analysis of selected particles, and safety testing data (which could indicate exposed kernels in a compact if fission gas release is elevated from the start of the test). This analysis is significantly complicated by several issues, including: (a) particles with failed SiC, but intact OPyC, will release Cs during irradiation along with exposed kernels and therefore the two cannot be distinguished based on Cs release alone; (b) the results of leaching to assess exposed kernels (that is, the uranium content in the leaching solutions) is not always definitive with regard to quantifying the number of kernels leached; (c) kernels that are leached in pre-burn leach solutions could be from particles that had exposed kernels in-pile or to particles that experienced SiC failure in-pile but subsequently experienced OPyC failure during the deconsolidation process; and (d) there is usually no effective means during post-irradiation analysis to distinguish an exposed kernel defect from a particle that experienced TRISO failure in-pile.

In cases where the source of the exposed kernel could not be definitively determined (for example, as-fabricated exposed kernel, in-pile TRISO failure, or TRISO failure during destructive PIE analysis), all suspected exposed kernels were conservatively assessed as in-pile TRISO failure. The result is an estimate of ≤ 4 in-pile AGR-2 TRISO failures (Table 7-2). Given the measured exposed kernel defect fractions for the AGR-2 compacts discussed in Section 6.8, it is possible that one or more of these particles was in fact an as-fabricated defect.

Data for AGR-1 and AGR-2 are listed separately in Table 7-2, and the data are combined for both experiments at the bottom of the table. AGR-2 values may change slightly upon completion of PIE and safety testing. The results of the AGR-1 transient temperature test have not been included in the totals.

The TRISO failure fraction during AGR-1 irradiation for was $\leq 1.1 \times 10^{-5}$ at 95% confidence. The conservative approach for assigning TRISO failure to the AGR-2 capsules during irradiation results in a failure fraction $\leq 8.1 \times 10^{-5}$. Combining the data from both experiments gives a value of $\leq 2.3 \times 10^{-5}$. This is approximately a factor of 9 lower than typical reactor design specifications for allowable in-service TRISO failures under normal operating conditions (2×10^{-4}).

No TRISO failures were observed in any of the 1600°C safety tests. Combining the results gives a total TRISO failure fraction of $\leq 6.6 \times 10^{-5}$ at 95% confidence. This is a factor of 9 lower than typical reactor design specifications for allowable failures during 1600°C accidents (6×10^{-4}). It is also important to note a relatively small percentage of the fuel in the reactor core experiences the peak temperature of 1600°C during an accident, whereas in the AGR safety tests 100% of the particles experienced the target test temperature. In addition, the dwell time of the fuel at peak temperature during an accident is relatively short (for example, the fuel compacts in the AGR-1 transient test shown in Figure 7-12 were within 100°C of peak temperature for 70 h), while the AGR isothermal safety tests have a nominal duration of 300 hours.

The combined AGR-1 and AGR-2 TRISO failure fraction at 1800°C is $\leq 3.0 \times 10^{-4}$ at 95% confidence. While reactor design specifications do not extend to this temperature, given it is significantly beyond

peak core temperatures expected during an accident, it is noteworthy this value is still a factor of 2 below the specification for allowable failures at 1600°C mentioned above.

The combined (AGR-1 + AGR-2) SiC failure fractions are $\leq 3.6 \times 10^{-5}$ during irradiation and $\leq 1.7 \times 10^{-4}$ and $\leq 1.3 \times 10^{-3}$ during safety testing at 1600°C and 1800°C, respectively (all values are the upper limit at 95% confidence). While there are currently no reactor design specifications for SiC layer failure, it is noteworthy the irradiation and 1600°C values are lower than the allowable TRISO failures under these conditions. Another important observation from the safety testing data in this regard is the appreciably lower incidence of SiC layer failure in the AGR-2 fuel; particularly at 1800°C (roughly half the number of particles were tested, but only 13% of the number of AGR-1 SiC failures were observed). It is not known for certain if this may be related to the lower incidence of IPyC failure observed in random particle samples (see discussion in Section 7.2).

Figure 7-15 shows a plot of the total combined (AGR-1 + AGR-2) SiC layer and full TRISO failure fractions for irradiation and for each of the safety test temperatures (note that no combined 1700°C test data are provided, as no 1700°C tests were performed on AGR-2 UCO compacts).
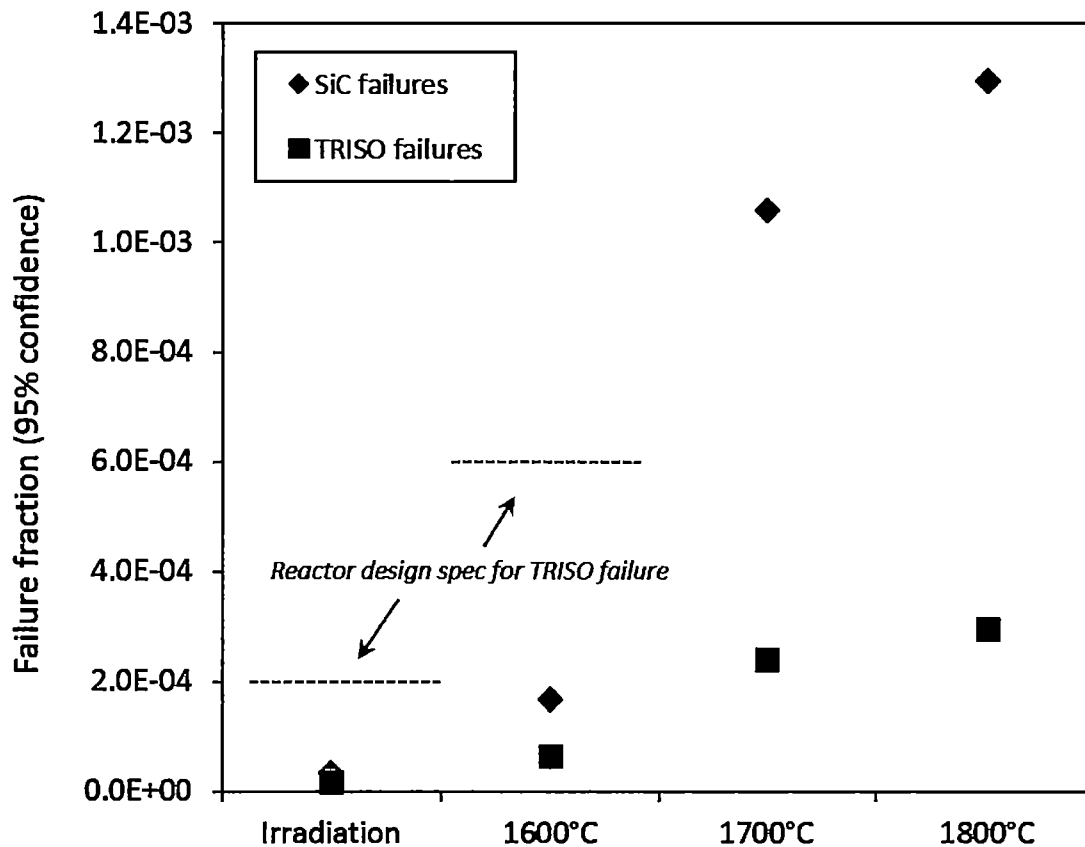

Figure 7-15
SiC layer and full TRISO failure fractions (upper limit at 95% confidence) for combined AGR-1 and AGR-2 UCO results during irradiation and during safety tests
Courtesy of Idaho National Laboratory and used with permission of Battelle Energy Alliance, LLC

No TRISO failures were observed in the AGR-2 UO_2 (Capsule 3) fuel compacts. In spite of the much higher frequency of SiC failure during safety tests relative to UCO, no TRISO failures were observed in the three safety tests completed to date. However, the much smaller number of particles involved in these tests prevents determination of statistically significant failure fractions. Zero observed TRISO failures out of 18,480 particles in the irradiation results in a failure fraction of $\leq 1.7 \times 10^{-4}$ at 95% confidence. The true failure fraction for this population is likely much lower than this, but a significantly greater number of particles need to be tested to confirm this. Zero observed TRISO failures in the 4,630 particles in safety tests results in a failure fraction of $\leq 6.5 \times 10^{-4}$ at 95% confidence.

Calculation of SiC failure fraction during irradiation suffers from the same statistical penalty of low particle numbers, and the value is the same as the TRISO failure fraction since zero failures were observed. During safety testing, there were significantly more SiC failures compared to UCO fuel (as discussed in Section 7.3.1), and quantification of the exact number of particles has not been possible.

Testing of UCO TRISO-coated fuel particles in AGR-1 and AGR-2 constitutes a performance demonstration of these particle designs over a range of normal operating and off-normal accident conditions. Therefore, the testing provides a foundational basis for use of these particle designs in the fuel elements of TRISO-fueled HTR designs (that is, designs with pebble or prismatic fuel and helium or salt coolant).

Aggregate AGR-1 and AGR-2 fission product release data and fuel failure fractions, as summarized in this report, can be used to support licensing of reactors employing UCO TRISO-coated fuel particles that satisfy the parameter envelope defined by measured particle layer properties in Table 5-5 from AGR-1 and AGR-2.

Table 7-2
SiC layer and full TRISO failure statistics for AGR-1 and AGR-2 UCO fuel during irradiation and during safety tests. AGR-2 data are preliminary, pending completion of PIE and safety testing.

Test Conditions	Number of Compacts	Number of Particles	SiC Failures			TRISO Failures		
			Number of Failures	Failure Fraction	95% Conf	Number of Failures	Failure Fraction	95% Conf
AGR-1								
Irradiation	72	298,000	4	1.3×10^{-5}	$\leq3.1\times10^{-5}$	0	0	$\leq1.1\times10^{-6}$
1600°C	8	33,100	3	9.1×10^{-5}	$\leq2.4\times10^{-4}$	0	0	$\leq9.1\times10^{-5}$
1700°C	3	12,400	7	5.6×10^{-4}	$\leq1.1\times10^{-3}$	0	0	$\leq2.5\times10^{-4}$
1800°C	4	16,500	23	1.4×10^{-3}	$\leq2.0\times10^{-3}$	2	1.2×10^{-4}	$\leq3.9\times10^{-4}$
AGR-2								
Irradiation	36	114,336	4	3.5×10^{-6}	$\leq8.1\times10^{-6}$	$\leq4^{a}$	$\leq3.5\times10^{-5}$	$\leq8.1\times10^{-6}$
1600°C	4	12,704	0	0	$\leq2.4\times10^{-4}$	0	0	$\leq2.4\times10^{-4}$
1800°C	3	9,528	1	1.0×10^{-4}	$\leq5.0\times10^{-4}$	1	1.0×10^{-4}	$\leq5.0\times10^{-4}$
AGR-1 + AGR-2								
Irradiation	108	412,336	8	1.9×10^{-5}	$\leq3.6\times10^{-5}$	$\leq4^{a}$	$\leq9.7\times10^{-6}$	$\leq2.3\times10^{-5}$
1600°C	12	45,804	3	6.5×10^{-5}	$\leq1.7\times10^{-4}$	0	0	$\leq6.6\times10^{-5}$
1800°C	7	26,028	24	9.2×10^{-4}	$\leq1.3\times10^{-3}$	3	1.2×10^{-4}	$\leq3.0\times10^{-4}$

[a]This value is the upper bound on the estimated number of in-pile failures. The precise value is not known but is estimated to be between 0 and 4.

8
SUMMARY/CONCLUSIONS

The AGR-1 and AGR-2 data and analyses on UCO TRISO-coated particle fuel performance presented in Sections 5 – 7 of this topical report support the following conclusions:

Conclusion 1:

Testing of UCO TRISO-coated fuel particles in AGR-1 and AGR-2 constitutes a performance demonstration of these particle designs over a range of normal operating and off-normal accident conditions. Therefore, the testing provides a foundational basis for use of these particle designs in the fuel elements of TRISO-fueled HTR designs (that is, designs with pebble or prismatic fuel and helium or salt coolant).

The AGR program has demonstrated excellent irradiation performance of a statistically large population of UCO TRISO fuel particles under conditions of high burnup and high temperature. Compact-average burnup ranged from 7.3 to 19.6% FIMA and fuel compact time-average maximum temperatures ranged from 1069 to 1360°C, fast neutron fluence ranged from 1.94 to $4.3x10^{25}$ neutrons/m^2 (E > 0.18 MeV), and power density ranged from 50 to 92 W/cm^3. Results for irradiation, PIE, and safety testing from two experiments (AGR-1 and AGR-2), with fuel fabricated using a range of process parameters, show consistently robust performance.

Conclusion 2:

The kernels and coatings of the UCO TRISO-coated fuel particles tested in AGR-1 and AGR-2 exhibited property variations and were fabricated under different conditions and at different scales, with remarkably similar excellent irradiation and accident safety performance results. The ranges of those variations in key characteristics of the kernels and coatings are reflected in measured particle layer properties provided in Table 5-5 from AGR-1 and AGR-2. UCO TRISO-coated fuel particles that satisfy the parameter envelope defined by these measured particle layer properties in Table 5-5 can be relied on to provide satisfactory performance.

Beyond the empirical performance data, it is important to note the fissile kernels of the particles in AGR-1 and AGR-2 were of different size and enrichment and the coatings were applied in an uninterrupted manner in coaters of two different sizes (that is, a 2-in. laboratory-scale coater and a 6-in. engineering-scale coater). Further, the coating conditions were varied so different microstructures and properties of the coatings were produced. The behavior with two different UCO kernels confirms the performance of the coatings is the primary factor for achieving good fuel performance such that the kernel is of secondary importance.

In terms of coating characteristics, AGR-1 coated particles were fabricated using a range of coating conditions that produced: (1) different combinations of PyC anisotropy and density, which in some cases were intentionally at the edge of the historic specification range; and (2) different microstructures of the SiC—a larger grain, made with traditional hydrogen and MTS coating gases, and a finer grain, by introducing argon gas as a diluent to improve fluidization

during SiC deposition. Based on the in-pile results available at the time, the AGR program decided the AGR-2 PyC coating would be applied using baseline conditions used in AGR-1 and would use argon dilution during the SiC coating step (similar to Variant 3 in the AGR-1 fuel) for the best fluidization in the 6-in. coater. Coating was carried out using an uninterrupted process for all fuel types, as this was considered important for production of high-quality coatings. Despite these variations in coating conditions, the performance of intact TRISO particles was nominally the same, albeit with slightly higher fission gas release in AGR-2 due to slightly higher uranium contamination of the particle batch fabricated in the larger engineering-scale coater.

These results demonstrate TRISO-coated particles can be made in a variety of coaters under a range of process conditions with some flexibility in coating parameter space in terms of acceptable values of density and anisotropy of the PyC and the microstructure of the SiC to achieve satisfactory irradiation performance.

The values in Table 5-5 are not intended to define a comprehensive envelope of TRISO fuel that is "acceptable." The data characterize the range of properties for particles that performed well during the AGR-1 and AGR-2 irradiations, but do not define the only ranges or combination of ranges that would perform well under these irradiation conditions or under service conditions proposed by fuel fabricators and reactor designers. Ultimately it will be up to an applicant to provide a justification for applying AGR-1 and AGR-2 particle performance results to a TRISO fuel population that deviates from the AGR-1 and AGR-2 fuel properties.

Conclusion 3:

Aggregate AGR-1 and AGR-2 fission product release data and fuel failure fractions, as summarized in this report, can be used to support licensing of reactors employing UCO TRISO-coated fuel particles that satisfy the parameter envelope defined by measured particle layer properties in Table 5-5 from AGR-1 and AGR-2.

Conclusions related to fission product release are limited to those isotopes addressed in Section 6.7, 6.8, 7.1, and 7.3. In-pile release measurements involved short-lived fission gases, while release data obtained during post-irradiation analysis consisted entirely of long-lived isotopes. The fuel failure fractions from AGR-1 and AGR-2 are those summarized in Section 7.6.

The fission gas release measured during AGR-1 was extremely low. About 300,000 TRISO fuel particles were irradiated without a single particle failure, making it the best irradiation performance of a large quantity of TRISO fuel ever achieved in the U.S., and substantially exceeding the German levels of burnup. These results have confirmed the expected superior irradiation performance of UCO at high burnup in that no kernel migration, no evidence of CO attack of SiC, and no indication of severe SiC attack by noble metal or lanthanide fission products has been observed. Zero fuel failures out of 300,000 particles in the AGR-1 irradiation translates into a 95% confidence failure fraction of $<1.1 \times 10^{-5}$, a factor of 18 better than the prismatic reactor design in-service failure fraction requirement of 2×10^{-4}.

The in-pile fission gas release for AGR-2 was higher than AGR-1, partly due to a higher level of HM contamination measured on the fabricated fuel. No particle failures were conclusively identified during irradiation based on fission gas release; however, because of the experimental anomalies associated with the AGR-2 irradiation capsule, the possibility of a small number of failures cannot be precluded.

The preliminary PIE data available indicates that ≤4 particles experienced TRISO failure in the three UCO capsules. Four failures out of a total of 114,000 UCO particles in the experiment corresponds to an actual failure fraction ≤8.1 × 10^{-5} at 95% confidence, which is approximately a factor of 2.5 below the historic MHTGR design specification of 2 × 10^{-4}. Additionally, the high-temperature UCO capsule in AGR-2 showed excellent behavior under irradiation, at a time-average peak temperature of 1360°C, and 10 to 20% of the particles in that capsule were exposed to temperatures in excess of 1400°C for hundreds of days. This early margin test demonstrated the high-temperature capability of these fuel particles.

Aggregate AGR-1 and AGR-2 data yield a TRISO particle failure fraction of ≤2.3 × 10^{-5} at 95% confidence, approximately a factor of 9 below historic MHTGR design specifications.

Cesium fractional release from compacts containing only particles with intact SiC was very low (<3 × 10^{-6} for ^{134}Cs), and as a result, the total Cs release from the fuel compacts is primarily dependent on the extent of SiC layer failure. Total ^{134}Cs fractional release from compacts under normal operating temperatures in both experiments (including all AGR-1 capsules and AGR-2 Capsules 5 and 6) was ≤4.4 × 10^{-5}. Eu and Sr exhibited modest release through intact coatings, although significant retention was observed in the fuel matrix. Inventory in the compact matrix could be as high as ~10^{-2} (^{154}Eu) and 3 × 10^{-3} (^{90}Sr) for fuel irradiated at normal operating temperatures, but fractional release from fuel compacts was ≤4.6 × 10^{-4} (^{154}Eu) and ≤8.2 × 10^{-5} (^{90}Sr).

At higher irradiation temperatures (up to a time-average maximum of 1360°C), Eu and Sr release from compacts is notably higher (approximately 4 × 10^{-3} for ^{154}Eu and 10^{-3} for ^{90}Sr). Silver release was high, consistent with historical observations. No widespread Pd attack or corrosion of SiC was observed despite finding large amounts of Pd outside of the SiC layer.

Safety testing in the 1600 – 1800°C range has demonstrated the robustness of UCO TRISO under depressurized conduction cooldown conditions. No full TRISO particle failures have been observed at 1600 or 1700°C. Fractional release of ^{134}Cs from compacts containing only intact particles at 1600°C was <6 × 10^{-5}. When a SiC layer in a particle failed, some of the Cs from that particle was released.

Releases of Ag, Sr, and Eu at 1600 and 1700°C are attributed to diffusion of these fission products into the fuel matrix during irradiation and subsequent release from the matrix upon high-temperature heating. Overall, the results indicate low incremental release of safety-relevant fission products under accident conditions. These results obtained to date from AGR-2 UCO fuel produced at engineering scale are similar to those from AGR-1 laboratory-scale fuel.

These results demonstrate the UCO TRISO-coated particles that underwent irradiation and subsequent high-temperature heating as part of the AGR-1 and AGR-2 experiments exhibited excellent performance and meet historic design specifications for allowable particle failures with significant margin. The data support the use of LEU UCO TRISO fuel for future high-temperature reactor designs, with specific kernel geometry and enrichment dependent on reactor design and burnup goals, provided overall particle design remains similar to those demonstrated by the AGR program.

The values in Table 5-5 are not intended to define a comprehensive envelope of TRISO fuel that is "acceptable." The data characterize the range of properties for particles that performed well during the AGR-1 and AGR-2 irradiations, but do not define the only ranges or combination of

ranges that would perform well under these irradiation conditions or under service conditions proposed by fuel fabricators and reactor designers. Ultimately it will be up to an applicant to provide a justification for applying AGR-1 and AGR-2 particle performance results to a TRISO fuel population that deviates from the AGR-1 and AGR-2 fuel properties.

9
REFERENCES

1. W. Scheffel and J. Saurwein. *Preliminary Fuel Product Specifications for the Baseline Advanced Gas Reactor Fuel Design.* General Atomics, San Diego, CA: September 2003. 911034, Rev. 0.

2. U.S. Nuclear Regulatory Commission, Office of Nuclear Reactor Regulation. *Office Instruction: Topical Report Process.* LIC-500, Rev. 6. Washington, D.C.: March 2018.

3. P.A. Demkowicz, D.A. Petti, D.W. Marshall, M.R. Holbrook, and W.L. Moe, *Technical Bases for the Performance Demonstration of TRISO-coated UCO Fuel Particles.* Idaho National Laboratory: September 2018. INL/LTD-18-46060, Rev. 0.

4. *NGNP Licensing Plan.* Idaho National Laboratory, Idaho Falls, ID: June 26, 2009. PLN-3202.

5. G.M. Tracy, Director, U.S. Nuclear Regulatory Commission, Office of New Reactors, Letter to Dr. J. Kelly, DOE Deputy Assistant Secretary for Nuclear Technologies, "NGNP – Assessment of Key Licensing Issues," ML14174A734, with Enclosure 1 ("Summary Feedback on Four Key Licensing Issues," ML14174A774) and Enclosure 2 ("Assessment of White Paper Submittals on Fuel Qualification and Mechanistic Source Terms," Rev.1, ML14174A845).

6. U.S. Code of Federal Regulations. *Domestic Licensing of Production and Utilization Facilities.* 10 CFR Part 50. http://ecfr.gpoaccess.gov/cgi/t/text/text-idx?c=ecfr&tpl=/ecfrbrowse/Title10/10cfr50_main_02.tpl

7. U.S. Nuclear Regulatory Commission. *Guidance for Developing Principal Design Criteria for Non-Light-Water Reactors.* RG 1.232. Washington, D.C.: April 2018.

8. R.A. Simon and P.D. Capp, 2002, "Operating experience with the Dragon High Temperature Reactor Experiment", *Proceedings of the Conference on High Temperature Reactors (HTR-2002),* Petten, the Netherlands, April 22-24, 2002. International Atomic Energy Agency, Vienna: 2002.

9. K.I. Kingrey. *Fuel Summary for Peach Bottom Unit 1 High-Temperature Gas-Cooled Reactor Cores 1 and 2,* Idaho National Laboratory, Idaho Falls, ID: April 2003. INEEL/EXT-03-00103.

10. *AVR – Experimental High-Temperature Reactor, 21 Years of Successful Operation for a Future Energy Technology.* VDI-Verlag GmbH, Düsseldorf: June 1990.

11. *A Review of Radionuclide Release from HTGR Cores During Normal Operation*. Electric Power Research Institute, Palo Alto, CA: February 2004. 1009382.

12. *Fuel Performance and Fission Product Behaviour in Gas Cooled Reactors*. International Atomic Energy Agency, Vienna: November 1997. IAEA-TECDOC-978.

13. *Advances in High Temperature Gas Cooled Reactor Fuel Technology*. International Atomic Energy Agency, Vienna: June 2012. IAEA-TECDOC-1674.

14. D. McEachern, R. Noren, and D. Hanson, "Manufacture and irradiation of Fort St. Vrain fuel," *International HTR Fuel Seminar*, Brussels, Belgium, February 2001.

15. D.A. Petti, J.T. Maki, J. Buongiorno, R.R. Hobbins, and G.K. Miller. *Key Differences in the Fabrication, Irradiation and Safety Testing of U.S. and German TRISO-coated Particle Fuel and Their Implications on Fuel Performance*. Idaho National Laboratory, Idaho Falls, ID: April 2002. INEEL/EXT-02-00300.

16. R.R. Hobbins and R.K. McCardell. *Summary of NP-MHTGR Fuel Failure Evaluation*. September 1993. EGG-NPR-10967.

17. *MHTGR TRISO-P Fuel Failure Evaluation Report*. General Atomics, San Diego, CA: October 1993. DOE-HTGR-90390, Rev. 0.

18. G. Bourchardt, B. Hürttlen, and G Pott. *Experiment FRJ2-P24 Bestrahulungsbericht*. Kernforschungsanlage Jülich, Jülich, Germany: August 1982. Interner Bericht KFA-ZBB-1B-19/82.

19. C. Bauer and H. Klöcker. *Elektrolytische Desintegration an 3 Compacts aus dem Experiment FRJ2-P24*. Kernforschungsanlage Jülich, Jülich, Germany: March 17, 1983. Interne Notiz IRW–IN – 8/83.

20. D.T. Goodin. *Accident Condition Performance of High-Temperature Gas-Cooled Reactor Fuels*, GA Technologies, Inc., San Diego, CA: October 1983. GA-A16508.

21. R.E. Bullock, "Fission-product release during postirradiation annealing of several types of coated fuel particles," *Journal of Nuclear Materials*, Vol. 125, pp. 304–319 (1984).

22. B. Myers et al. *Capsule R2-K13: Final Report on Cells 2 and 3*. GA Technologies, Inc., San Diego, CA: September 1985. HTGR-85-08668.

23. *Mechanistic Source Terms White Paper*. Idaho National Laboratory, Idaho Falls, ID: July 2010. INL/EXT-10-17997.

24. D.A. Petti, R.R. Hobbins, P. Lowry and H. Gougar, "Representative source terms and the influence of reactor attributes on functional containment in modular high temperature gas-cooled reactors," *Nuclear Technology*, Vol. 184, pp. 181–197 (2013).

25. F.J. Homan, T.B. Lindemer, E.L. Long, Jr., T.N. Tiegs, and R.L. Beatty, "Stoichiometric effects on performance of high-temperature gas-cooled reactor fuels from the U-C-O system," *Nuclear Technology*, Vol. 35, pp. 428-441 (1977).

26. D. Olander, "Nuclear fuels – Present and future," *Journal of Nuclear Materials*, Vol. 389, pp. 1-22. (2009).

27. E. Proksch, A. Strigl, and H. Nabielek, "Carbon monoxide formation in UO_2 kerneled HTR fuel particles containing oxygen getters," *Journal of Nuclear Materials*. Vol. 139, pp. 83-90 (1986).

28. *NP-MHTGR Material Models of Pyrocarbon and Pyrolytic Silicon Carbide*. Combustion Engineering General Atomics Corporation, San Diego, CA: July 1993. CEGA-002820, Rev. 1.

29. J. Kaae, D. Stevens, and C. Luby, "Prediction of the irradiation performance of coated particle fuels by means of stress-analysis models," *Nuclear Technology*, Vol. 10, p. 44 (1971).

30. H. Walther, "On mathematical models for calculating the mechanical behaviour of coated fuel particles," *Nuclear Engineering and Design*, Vol. 18, No. 1, pp. 11–39 (1972).

31. D.G. Martin, "An analytical method of calculating, to a reasonable accuracy, stresses in the coatings of HTR fuel particles," *Journal of Nuclear Materials*. Vol. 48, No. 1, pp. 35–46 (1973).

32. G.K. Miller, D. A. Petti, D. J. Varacalle, and J. T. Maki, "Statistical approach and benchmarking for modeling of multi-dimensional behavior in TRISO-coated fuel particles," *Journal of. Nuclear Materials,* Vol. 317, pp. 69–82 (2003).

33. G.K. Miller, G. K., D. A. Petti, and J. T. Maki, "Consideration of the effects of partial debonding of the IPyC and particle asphericity on TRISO-coated fuel behavior," *Journal of Nuclear Materials,* Vol. 334, p. 79 (2004).

34. G.K. Miller, G. K., D. A. Petti, J. T. Maki, and D. L. Knudson, "An evaluation of the effects of SiC layer thinning on failure of TRISO-coated fuel particles," *Journal of Nuclear Materials,* Vol. 355, pp. 150–162 (2006).

35. W.F. Skerjanc, J. T. Maki, B. P. Collin, and D. A. Petti, "Evaluation of design parameters for TRISO-coated fuel particles to establish manufacturing critical limits using PARFUME," *Journal of Nuclear Materials*, Vol., 469, pp. 99–104 (2016).

36. J.J. Powers and B.D. Wirth, "A review of TRISO fuel performance models," *Journal of Nuclear Materials*, Vol. 405, pp. 74–82 (2010).

37. W.F. Skerjanc and P.A. Demkowicz. *PARFUME Theory and Model Basis Report*. Idaho National Laboratory, Idaho Falls, ID: September 2018. INL/ EXT-08-14497, Rev. 1.

38. *Technical Program Plan for INL Advanced Reactor Technologies Advanced Gas Reactor Fuel Development and Qualification Program.* Idaho National Laboratory, Idaho Falls, ID: June 2018. PLN-3636, Rev. 7.

39. M. Wagner-Löffler, "Amoeba behavior of UO_2 coated particle fuel," *Nuclear Technology*, Vol. 35, p. 392 (1977).

40. J.W. Ketterer and B. F. Myers. *Capsule HRB-16 Postirradiation Examination Report.* General Atomics, San Diego, CA: September 1985. HTGR-85-053.

41. K. Minato, T. Ogawa, S. Kashimura, K. Fukuda, I. Takahashi, M. Shimizu, and Y. Tayama, "Carbon monoxide - silicon carbide interaction in HTGR fuel particles," *Journal of Materials Science*, Vol. 26, p. 2379 (1991).

42. S. Muñoz. *Fuel Product Specification.* General Atomics, San Diego, CA: May 1994. DOE-HTGR-100209. Rev. 0.

43. *Preliminary AGR Fuel Specification.* Idaho National Laboratory, Idaho Falls, ID: April 2004. EDF-4198, Rev. 1.

44. *Technical Program Plan for the Advanced Gas Reactor Fuel Development and Qualification Program.* Oak Ridge National Laboratory, Oak Ridge, TN: April 2003. ORNL/TM-2002/262.

45. William F. Martin, Chairman, and John Ahearne, Vice Chairman, Nuclear Energy Advisory Committee, Letter to Dr. Steven Chu, Secretary of Energy, Washington, D.C. June 30, 2011.

46. C.M. Barnes. *AGR-1 Fuel Product Specification and Characterization Guidance.* Idaho National Laboratory, Idaho Falls, ID: April 21, 2006. EDF-4380, Rev. 8.

47. C.M. Barnes. *AGR-2 Fuel Specification.* Idaho National Laboratory, Idaho Falls, ID: January 9, 2009. SPC-923, Rev. 3.

48. B&W Nuclear Operations Group, G73AA, "Industrial Fuel Fabrication and Development," Lot G73AA-10-69308, December 2008.

49. BWXT Nuclear Products Division, G73, Industrial Fuel Fabrication and Development, Lot G73D-20-69302, March 2005.

50. BWXT Nuclear Products Division, G73I, Industrial Fuel Fabrication and Development, Lot G73I-14-69307, July 2008.

51. B&W Nuclear Operations Group, G73H, Industrial Fuel Fabrication and Development, Lots: G73H-10-93085B, March 2009.

52. B&W Nuclear Operations Group, G73J, Industrial Fuel Fabrication and Development, Lots: G73J 14-93071A, G73J 14-93073A, G73J 14-93074A, September 2008.

53. J. Einerson. *Statistical Sampling Plan for AGR Fuel Materials*. Idaho National Laboratory, Idaho Falls, ID: February 2006. EDF-4542, Rev. 7.

54. J.D. Hunn and R.A. Lowden. *Data Compilation for AGR-1 Baseline Coated Particle Composite LEU01-46T*. Oak Ridge National Laboratory, Oak Ridge, TN: April 2006. ORNL/TM-2006/019.

55. J.D. Hunn and R.A. Lowden. Data Compilation for AGR-1 Variant 1 Coated Particle Composite LEU01-47T. Oak Ridge National Laboratory, Oak Ridge, TN: April 2006. ORNL/TM-2006/020.

56. J.D. Hunn and R.A. Lowden. Data Compilation for AGR-1 Variant 2 Coated Particle Composite LEU01-48T. Oak Ridge National Laboratory, Oak Ridge, TN: May 2006. ORNL/TM-2006/021.

57. J.D. Hunn and R.A. Lowden. Data Compilation for AGR-1 Variant 3 Coated Particle Composite LEU01-49T. Oak Ridge National Laboratory, Oak Ridge, TN: May 2006. ORNL/TM-2006/022.

58. T.J. Gerczak, J.D. Hunn, R.A. Lowden, and T.R. Allen, "SiC layer microstructure in AGR-1 and AGR-2 TRISO fuel particles and the influence of its variation on the effective diffusion of key fission products," *Journal of Nuclear Materials*, Vol. 480, pp. 257–270 (2016).

59. B. Collin. *AGR-1 Irradiation Test Final As-Run Report*. Idaho National Laboratory, Idaho Falls, ID: January 2015. INL/EXT-10-18097, Rev. 3.

60. *AGR-2 Fuel Compact Pre-Irradiation Characterization Summary Report*. Oak Ridge National Laboratory, Oak Ridge, TN: November 2010. ORNL/TM-2010/226, Rev. 0.

61. B. Collin. *AGR-2 Irradiation Test Final As-Run Report*. Idaho National Laboratory, Idaho Falls, ID: February 2018. INL/EXT-14-32277, Rev. 4,

62. *Advances in High Temperature Gas Cooled Reactor Fuel Technology*. International Atomic Energy Agency, Vienna: December 2012. IAEA-TECDOC-1674.

63. *Statistical Methods Handbook for Advanced Gas Reactor Fuel Materials*. Idaho National Laboratory, Idaho Falls, ID: May 2005. INL/EXT-05-00349, Rev. 0.

64. *Statistical Sampling Plan for AGR-2 Fuel Materials*. Idaho National Laboratory, Idaho Falls, ID: January 2009. PLN-2691, Rev. 4.

65. J.W. McMurray, T.B. Lindemer, N.R. Brown, T.J. Reif, R.N. Morris, and J.D. Hunn, "Determining the minimum required uranium carbide content for HTGR UCO fuel kernels," *Annals of Nuclear Energy*, Vol. 104, pp. 237-242 (2017).

66. D.A. Petti, J. Buongiorno, J.T. Maki, R.R. Hobbins, and G.K. Miller, "Key differences in the fabrication, irradiation and high temperature accident testing of U.S. and German TRISO-coated particle fuel and their implications on fuel performance," *Nuclear Engineering and Design*, Vol. 222, pp. 281–297 (2003).

67. G.S. Chang and M.A. Lillo, *Confirmatory Neutronics Analysis of the AGR-1 Experiment Irradiated in ATR B-10 Position*. Idaho National Laboratory, Idaho Falls, ID: February 13, 2007. EDF-7120, Rev. 1.

68. J.T. Maki, D.A. Petti, D.L. Knudson, and G.K. Miller, "The challenges associated high burnup, high temperature, and accelerated irradiation for TRISO-coated particle fuel," *Journal of Nuclear Materials*, Vol. 371, pp. 270–280 (2007).

69. J.K Hartwell, D.M. Scates, and M.W. Drigert. *Design and Expected Performance of the AGR-1 Fission Product Monitoring System*. Idaho National Laboratory, Idaho Falls, ID: September 2005. INL/EXT-05-00073.

70. *MCNP—A General Monte Carlo N-Particle Transport Code, Version 5—Volumes I and II*. Los Alamos National Laboratory, Los Alamos, NM: April 24, 2003 (Revised 6/30/2004). LA-UR-03-1987 and LA-CP-0245.

71. A.G. Croff, "ORIGEN2: A Versatile Computer Code for Calculating the Nuclide Compositions and Characteristics of Nuclear Materials," *Nuclear Technology*, Vol. 62, pp. 335–352 (1983).

72. J. Sterbentz, J.M. Harp, P.A. Demkowicz, G.L. Hawkes, and G.S. Chang, "Validation of the physics analysis used to characterize the AGR-1 TRISO fuel irradiation test," Paper 15497, *Proceedings of the 2015 International Congress on Advances in Nuclear Power Plants (ICAPP 2015)*, Nice, France, May 3-6, 2015.

73. J.M. Harp. *Analysis of Individual Compact fission Product Inventory and Burnup for the AGR-1 TRISO Experiment Using Gamma Spectrometry*. Idaho National Laboratory, Idaho Falls, ID: May 21, 2014. ECAR 1682, Rev. 3.

74. J.M. Harp, P.A. Demkowicz, and J.D. Stempien. *Fission Product Inventory and Burnup Evaluation for Gamma Spectrometry of the AGR-2 Irradiation*. Idaho National Laboratory, Idaho Falls, ID: September 2016. INL/EXT-16-39777.

75. Harp, J. M., P. A. Demkowicz, P. L. Winston, and J. W. Sterbentz, "An analysis of nuclear fuel burnup in the AGR-1 TRISO fuel experiment using gamma spectrometry, mass spectrometry, and computational simulation techniques," *Nuclear Engineering and Design*, Vol. 278, pp. 395–405 (2014).

76. G.L. Hawkes. *AGR-1 Daily As-Run Thermal Analyses*. Idaho National Laboratory, Idaho Falls, ID: 2014. ECAR-968, Rev. 4.

77. G.L. Hawkes. *AGR-2 As-Run Daily Thermal Analyses*. Idaho National Laboratory, Idaho Falls, ID: 2014. ECAR-2476, Rev. 1.

78. B.T. Pham, J.J. Einerson, G.L. Hawkes, N.J. Lybeck, and D.A. Petti, "Impact of gap size uncertainty on calculated temperature uncertainty for the advanced gas reactor experiments," *Proceedings of the 8th International Topical Meeting on High Temperature Reactor Technology (HTR-2016)*, Las Vegas, Nevada, November 6-10, 2016.

79. B.T. Pham, J.J. Einerson, and G.L. Hawkes. *Uncertainty Quantification of Calculated Temperatures for the AGR-1 Experiment.* Idaho National Laboratory, Idaho Falls, ID: 2013. INL/EXT-12-25169, Rev. 1.

80. B.T. Pham, J.J. Einerson, and G.L. Hawkes. *Uncertainty Quantification of Calculated Temperatures for the U.S. Capsules in the AGR-2 Experiment.* Idaho National Laboratory, Idaho Falls, ID: March 2015. INL/EXT-15-34587.

81. S.B. Grover, D.A. Petti, and J.T. Maki, "Completion of the First NGNP Advanced Gas Reactor Fuel Irradiation Experiment, AGR-1, in the Advanced Test Reactor," *Proceedings of the 5th International Topical Meeting on High Temperature Reactor Technology (HTR 2010)*, Prague, Czech Republic, October 18–20, 2010.

82. P.A. Demkowicz, J.D. Hunn, R.N. Morris, I. van Rooyen, T. Gerczak, J.M. Harp, and S.A. Ploger. *AGR-1 Post Irradiation Examination Final Report.* Idaho National Laboratory, Idaho Falls, ID: 2015. INL/EXT-15-36407.

83. P.A. Demkowicz, J.M. Harp, P.L. Winston, and S.A. Ploger. *Analysis of Fission Products on the AGR-1 Capsule Components.* Idaho National Laboratory, Idaho Falls, ID: 2013. INL/EXT-13-28483.

84. J.D. Stempien and P.A. Demkowicz. *AGR-2 Irradiation Experiment Fission Product Mass Balance.* Idaho National Laboratory, Idaho Falls, ID: May 2019. INL/EXT-19-53559.

85. J.D. Hunn, R.N. Morris, F.C. Montgomery, T.J. Gerczak, D.J. Skitt, C.A. Baldwin, J.A. Dyer, G.W. Helmreich, B.D. Eckhart, Z.M. Burns, P.A. Demkowicz, and J.D. Stempien, "Post-irradiation examination and safety testing of US AGR-2 irradiation test compacts," *Proceedings of the 9th International Topical Meeting on High Temperature Reactor Technology (HTR-2018)*, Warsaw, Poland, October 8-10, 2018.

86. S. Ploger, P. Demkowicz, J. Hunn, and J.S. Kehn, "Microscopic analysis of irradiated AGR-1 coated particle fuel compacts," *Nuclear Engineering and Design*, Vol. 271, pp. 221–230 (2014).

87. F.J. Rice, J.D. Stempien, and P.A. Demkowicz, "Ceramography of irradiated TRISO fuel from the AGR-2 experiment," *Nuclear Engineering and Design*, Vol. 329, pp. 73–81 (2018).

88. R.N. Morris, J.D. Hunn, C.A. Baldwin, F.C. Montgomery, T. Gerczak, and P.A. Demkowicz, "Initial results from safety testing of US AGR-2 irradiation test fuel," *Nuclear Engineering and Design*, Vol. 329, pp. 124–133 (2018).

89. K. Minato, T. Ogawa, S. Kashimura, K. Fukuda, I. Takahashi, M. Shimizu, and Y. Tayama, "Carbon monoxide-silicon carbide interaction in HTGR fuel particles," *Journal of Materials Science*, Vol. 26, pp. 2379–2388 (1991).

90. H. Hantke. *Performance of High Quality HTR LEU Fuel Elements with TRISO Coated Particles*. Forschungszentrum Jülich, Jülich, Germany: 1992. Internal Report HTA-IB-7/92.

91. W. Schenk, D. Pitzer, and H. Knauf. *Simulation der Maximalen MODUL-Störfallaufheizkurve (AVR-GLE 3, 90/20) und deren Extrapolation auf 1700 °C (AVR-GLE 3, 91/31)*. Forschungszentrum Jülich, Jülich, Germany: 1993. Technical Note FZJ-IWE-TN-17/93.

92. J.D. Stempien, P.A. Demkowicz, E.L. Reber, and C.L. Christensen. "High-temperature safety testing of irradiated AGR-1 TRISO fuel," *Proceedings of the 9th International Topical Meeting on High Temperature Reactor Technology (HTR-2018)*, Warsaw, Poland, October 8-10, 2018.

93. J.D. Hunn, C.A. Baldwin, F.C. Montgomery, T.J. Gerczak, R.N. Morris, G.W. Helmreich, P.A. Demkowicz, J.M. Harp, and J.D. Stempien, "Initial examination of fuel compacts and TRISO particles from the US AGR-2 irradiation test," *Nuclear Engineering and Design*, Vol. 329, pp. 89–101 (2018).

A
U.S. REGULATORY BASES

A.1   NRC Regulations

Regulations related to light water reactor (LWR) design are codified primarily in the General Design Criteria (GDC) contained in Appendix A of 10 CFR Part 50 [1]. The U.S. Nuclear Regulatory Commission's (NRC) Regulatory Guide (RG) 1.232 [2] provides guidance for how the GDC in Appendix A may be adapted for non-light-water reactor (non-LWR) designs.

RG 1.232 provides Advanced Reactor Design Criteria (ARDC), which may be used by non-LWR designers and future applicants to develop principal design criteria (PDC) for any non-LWR designs. In addition, RG 1.232 provides guidance for adapting the LWR GDC for modular HTGRs and sodium-cooled fast reactors (SFRs). The design criteria serve as the fundamental criteria for the structures, systems, and components (SSC) that make up a nuclear power plant design, particularly when assessing the performance of their intended safety functions during applicable licensing basis events. RG 1.232 guidance may be used to develop all or part of a design's PDC and users are free to choose among the ARDC, modular HTGR design criteria (MHTGR-DC), or SFR design criteria (SFR-DC) to develop their PDC after considering the underlying safety basis for the criterion and evaluating the RG's rationale for the adaptation.

MHTGR-DC 10, *Reactor Design*, provides guidance related to acceptable system radionuclide releases. Other ARDC that pertain to the reactor core (that is, MHTGR-DC 11, 12, 13, and 27), do not directly pertain to the performance of the tristructural isotropic (TRISO)-coated particle fuel. MHTGR-DC 10, states [2]:

- "The reactor system and associated heat removal, control, and protection systems shall be designed with appropriate margin to ensure that specified acceptable system radionuclide release design limits are not exceeded during any condition of normal operation, including the effects of anticipated operational occurrences."

RG 1.232 includes the following rationale for MHTGR-DC 10 documenting the basis for wording changes from the original LWR GDC [2]:

- "the concept of specified acceptable fuel design limits, which prevent additional fuel failures during anticipated operational occurrences (AOOs), has been replaced with that of the specified acceptable system radionuclide release design limits (SARRDL), which limits the amount of radionuclide inventory that is released by the system under normal and AOO conditions." Design features within the reactor system must ensure the SARRDLs are not exceeded during normal operations and AOOs.

- The TRISO fuel used in the MHTGR design is the primary fission product barrier and is expected to have a very low incremental fission product release during AOOs.

- The SARRDLs will be established so that the most limiting license-basis event does not exceed the siting regulatory dose limits criteria at the exclusion area boundary (EAB) and low-population zone (LPZ), and also so that the 10 CFR 20.1301 annualized dose limits to the public are not exceeded at the EAB for normal operation and AOOs.

- The NRC has not approved the concept of replacing specified acceptable fuel design limits with SARRDLs. The concept of the TRISO fuel being the primary fission product barrier is intertwined with the concept of a functional containment for MHTGR technologies. See the rationale for MHTGR-DC 16 for further information on the Commission's current position.

MHTGR-DC 16, *Containment Design*, provides guidance for a functional containment design, which relies on the use on multiple barriers to control the release or radioactivity. MHTGR-DC 16 states [2]:

- "A reactor functional containment, consisting of multiple barriers internal and/or external to the reactor and its cooling system, shall be provided to control the release of radioactivity to the environment and to ensure that the functional containment design conditions important to safety are not exceeded for as long as postulated accident conditions require."

RG 1.232 includes the following rationale for MHTGR-DC 16 documenting the basis for wording changes from the original LWR GDC, which include [2]:

- "The term "functional containment" is applicable to advanced non-LWRs without a pressure retaining containment structure. A functional containment can be defined as "a barrier, or set of barriers taken together, that effectively limit the physical transport and release of radionuclides to the environment across a full range of normal operating conditions, AOOs, and accident conditions."

- "The NRC staff has brought the issue of functional containment to the Commission, and the Commission has found it generally acceptable"

- "The NRC staff also provided feedback to the DOE on this issue as part of the NGNP project, (*see Appendix to this document*). ... the area on functional containment and fuel development and qualification noted that "...approval of the proposed approach to functional containment for the MHTGR concept, with its emphasis on passive safety features and radionuclide retention within the fuel over a broad spectrum of off -normal conditions, would necessitate that the required fuel particle performance capabilities be demonstrated with a high degree of certainty."

10 CFR Part 52.79 (a)(24) provides guidance on the content for Combined License Applications regarding designs that differ significantly from LWR designs licensed before 1997, or utilize simplified, inherent, passive, or other innovative means to accomplish their safety functions. It references 10 CFR Part 50.43(e) which, in summary, requires a combination of analyses and test programs to demonstrate the performance of safety features and ensure sufficient data exist to assess the analytical tools used for safety analyses.

A.2 NRC Policy Statements

No U.S. Nuclear Regulatory Commission policy statements directly apply to TRISO-coated particle fuel or address testing or monitoring of the fuel, nor does the NRC policy statement on the regulation of advanced nuclear power plants explicitly address nuclear fuel. However, NRC policy issues specific to the MHTGR concept are identified in NRC Commission paper (SECY)-93-092 [3] and in Section 5 of NUREG-1338 [4]. Of the ten issues identified in SECY-93-092, both "Containment Performance" and "Source Term" policy issues are related to TRISO fuel. Their use of a multi-barrier containment configuration and associated mechanistic source terms for accident analyses are based on the performance of the TRISO fuel being both excellent and predictable.

A.2.1 Functional Containment Performance

The current LWR containment leakage requirements are outlined in GDC 16 and Appendix J of 10 CFR Part 50. The containment performance issue involves whether an advanced reactor design should be allowed to employ alternative approaches to the traditional "essentially leak-tight" containment structures used in LWRs to provide for the control of fission-product releases to the environment.

Fundamental to the HTGR and FHR concepts is their emphasis on release prevention by utilizing high-integrity fuel particles, rather than a leak-tight containment barrier to minimize radionuclide releases to the environment. In SECY-03-0047 [5], SECY-04-0103 [6], and SECY-05-006 [7], the NRC approved the use of a standard based on functional containment performance to evaluate the acceptability of the proposed designs, rather than relying on prescriptive containment design criteria. As part of the containment evaluation, the NRC instructed the staff to address the failure of the fuel particles, among other issues.

There is a strong linkage between TRISO particle behavior, functional containment performance, and licensing. Recognizing the importance of this relationship, NRC staff released a draft SECY paper seeking NRC approval of a recommendation that adopts a technology-inclusive, risk-informed, performance-based approach when establishing performance criteria for structures, systems, and components and corresponding programs that limit the release of radioactive materials from non-LWR designs [8]. The staff determined formal Commission direction on functional containment would be beneficial to support development and deployment of advanced reactor technologies seeking to utilize this approach to safety.

The draft SECY was submitted to the Advisory Committee on Reactor Safeguards (ACRS) in early 2018 for review. On May 10, 2018, the ACRS communicated its findings to the Commission and noted the proposed SECY set forth a rational basis for developing functional containment performance criteria. The letter recommended the methodology be further developed for licensing use [9].

On June 27, 2018, the staff indicated its intention to finalize the draft SECY paper and then send it to the Commission for formal approval [10]. SECY-18-0096 entitled, "Functional Containment Performance Criteria for Non-Light Water Reactor Designs,"[11] was approved by the Commission on December 4, 2018.

A.2.2 Source Term

The source term for the MHTGR or FHR technology is defined as the set of quantities of radionuclides released from a reactor building to the environment. This definition is judged appropriate for greater emphasis on fuel retention of radionuclides for events rather than reactor building retention following an event.

In its Staff Requirements Memorandum for SECY-93-092, the Commission approved the staff's recommendation the source terms for non-LWRs be based on a mechanistic analysis, relying on the staff's assurance three conditions are met [3]. One of the conditions was "the performance of the reactor and fuel under normal and off-normal conditions is sufficiently well understood to permit a mechanistic analysis. Sufficient data should exist on the reactor and fuel performance through research, development, and testing programs to provide adequate confidence in the mechanistic approach."

The purpose of this report is to provide the NRC with data on fuel performance through research, development, and testing programs to provide a functional basis for this adequate confidence necessary to support the mechanistic analysis source term approach.

A.3 NRC Guidance/References

A.3.1 NUREG-1338, "Pre-application Safety Evaluation Report for the MHTGR"

In 1989, a draft of a pre-application safety evaluation report (PSER) [12] documented the NRC staff's pre-application review of the MHTGR design and its conclusions. Following DOE submission of additional information for the fuel design in 1991 and 1992 and meetings with the NRC on fuel design and fission-product transport in 1991, a draft of the final PSER was completed in December 1995 [13] and was based upon the draft PSER issued in 1989 and upon a number of reports completed after the draft PSER was issued.

The final PSER draft confirmed the following overall conclusions of the earlier draft with respect to the fuel design, specifically [13]:

- The NRC staff believes that fuel design and quality can be developed to meet the performance objectives proposed by DOE and required by the safety analyses, but notes this conclusion is dependent on the successful outcome of the research program

- The NRC staff notes actual fuel performance in Federal Republic of Germany reactors, together with reported laboratory and in-pile tests, gives promise fuel performance objectives can eventually be demonstrated.

However, NUREG-1338 also states the information provided for the MHTGR up to that time had not demonstrated the necessary design and quality of fuel to meet these performance objectives. It identifies the following information that the NRC needs to reach a determination on the fuel [13]:

- Design thicknesses of fuel particle coatings and the bases for these thicknesses given the proposed fuel failures from manufacturing, normal operation (neutron fluence), and accidents (temperature)

- Quality control of the manufacturing process for the fuel and resulting tolerances on the coatings

- Fuel performance of specific coated particles and coating tolerances demonstrated from irradiation and safety tests

- Expected fuel temperatures throughout the core during accidents and the resulting volume-averaged failed fuel fraction

- Potential dose consequences shown to be within acceptable limits for the predicted volume-averaged failed fuel fraction

NUREG-1338 also includes the following conclusions to be considered in qualifying TRISO-coated particle fuel [13]:

- The statistical question of how many fuel particles are needed in irradiation and safety tests to justify the proposed low failed-fuel fraction within 95% certainty

- The fuel design and containment proposed for the MHTGR, which the NRC staff considers a licensability issue for the MHTGR (licensability issues occur when the design departs significantly from what the NRC has accepted in the past or when changes in the design to resolve a staff concern could fundamentally alter the proposed design.)

- The credible mechanisms for "weak fuel" (fuel that performs acceptably during normal reactor operation, but is subject to failure under more stringent conditions during accidents) to ensure that all mechanisms for fuel failure are recognized and quantitatively accounted for in fuel performance models

The NRC guidance provided in NUREG-1338 indicates successful completion of the Fuel Research and Development (R&D) program must provide a statistically significant demonstration [13]:

- The reference fuel manufacturing processes and quality-control methods ensure the production of fuel meeting specification requirements

- The fuel fabricated using the reference fuel manufacturing processes meets the fuel performance requirements under normal operation and all credible accident conditions

- Validated methods are available to accurately predict fuel performance and fission-product transport.

A.3.2 NUREG-0111, "Evaluation of High Temperature Gas-Cooled Reactor Particle Coating Failure Models and Data"

NUREG-0111[14] addresses highly enriched uranium (HEU) UC_2 TRISO fissile particles with a 200-μm kernel and ThO_2 bistructural isotropic (BISO) fertile particles with a 500-μm kernel for service in a large prismatic HTGR. Major differences in particle design, fabrication specifications, and service conditions relative to the fuel for MHTGRs or FHRs limit the applicability of this report to the current low-enriched uranium (LEU) fuel. Experience with this and other diverse fuel types over the course of TRISO-coated particle fuel development has provided valuable insights into the development and understanding of the LEU UCO TRISO fuel.

A.3.3 NUREG-0800, Standard Review Plan, Section 4.2, "Fuel System Design"

The existing NUREG-0800 Standard Review Plan [15] Section 4.3 for LWRs is technology-specific and deals with fuel performance phenomena that do not apply to HTGR fuel performance. The HTGR design criteria for fuel design limits must be appropriately adapted to reflect the underlying intent in preserving TRISO particle fuel performance and integrity.

Any review of TRISO particle fuel must consider statistically significant measurements that reliably indicate overall fuel system performance. Billions of TRISO fuel particles (each independently functioning as a separate radionuclide containment vessel) are in a HTGR core. These coated fuel particles are embedded in a solid carbonaceous matrix nominally shaped as either a spherical pebble or a compact cylinder. This type of fuel design makes it infeasible for direct damage assessment of individual coated particles after manufacture while loaded in the core. Therefore, a HTGR fuel system design review must encompass the coated particle fuel manufacturing process and rely on appropriate indirect methods of measurement (such as SARRDL) that communicate coated particle fuel failure rates and enable predictions of overall radionuclide barrier performance. Review requirements should focus on:

- Evaluating the quality of TRISO particle fuel during manufacture

- Understanding fuel system performance impacts as a result of normal operation and AOOs

- Characterizing fuel system performance as it relates to reactivity control

- Establishing in-service performance requirements and fission product release requirements for postulated accidents

- Enabling fuel performance and fission product release prediction/modeling under normal operating and postulated accidents with desired statistical certainty

A.3.4 TRISO-Coated Particle Fuel Phenomenon Identification and Ranking Tables

In anticipation of future licensing applications for HTGRs, the NRC commissioned a panel to identify and rank the phenomena associated with TRISO-coated-particle fuel to obtain a better understanding of the significant features of TRISO-coated-particle fuel design, manufacture, and behavior during both normal reactor operation and accidents [16]. Six Phenomena Identification and Ranking Tables (PIRTs) were developed by the panel, including PIRTs on:

- Manufacturing

- Operations

- Depressurized heat-up accident

- Reactivity accident

- Depressurized accident with water ingress

- Depressurization accident with air ingress

In preparing the PIRTs, the panel assumed the plant to be a pebble-bed reactor with UO_2 fuel, except for the reactivity accident PIRT, in which a prismatic reactor was considered instead. The panel also identified and evaluated the importance and knowledge rankings that would be different for prismatic reactor UCO fuel. The PIRTs are documented in NUREG/CR-6844, Vol. 1 [16].

According to NUREG/CR-6844, the NRC will use the PIRT results to:

- Identify key attributes of gas-cooled reactor fuel manufacture that may require regulatory oversight.

- Provide a valuable reference for the review of vendor HTGR fuel qualification plans.

- Provide insights for developing plans for fuel safety margin testing.

- Assist in defining test data needs for the development of fuel performance and fission product transport models.

- Inform decisions regarding the development of the NRC's independent HTGR fuel performance code and fission product transport models.

- Support the development of the NRC's independent models for source term calculations.

- Provide insights for the review of vendor HTGR fuel safety analyses.

A.3.5 Next Generation Nuclear Plant

In 2005, DOE established the Next Generation Nuclear Plant (NGNP) Project at Idaho National Laboratory (INL) to support near-term commercial deployment of a HTGR technology demonstration plant. A key part of the project was the development of a regulatory framework supportive of commercial HTGR deployment. Framework activities were closely coordinated with NRC staff and focused on adapting existing nuclear power plant regulatory requirements to the needs of NGNP licensing. DOE and NRC jointly formulated the approach for this licensing structure and communicated this approach to Congress in 2008.

Under the NGNP project, HTGR licensing precedents and NRC regulations were examined systematically as they relate to the NGNP safety case and associated plant design goals. NRC staff coordinated the scope of this examination and reviewed the results. In 2009, this information was used to develop a strategic implementation plan [17] for establishing the regulatory basis necessary to complete and submit an HTGR license application to NRC. The plan focused on key elements of plant safety design and licensing, and included:

- Developing the basis for establishing a mechanistic radiological source term (based primarily on particle fuel design and available qualification testing results).

- Preventing/mitigating the release of the radiological source terms to the environment, including methods for the structured and comprehensive identification of licensing basis event sequences, along with establishing multiple radionuclide release barriers.

- Developing an updated emergency planning structure that considers collocated industry energy end-users to assure protection of public health and safety in the unlikely event of a radiological release.

- The design and licensing strategy of NGNP centered on radionuclide retention capabilities of TRISO particle fuel. It also relied less on other barriers for limiting offsite releases of radionuclides compared to historical LWR technology. This approach in conjunction with the related HTGR design goals aligns with the NRC's Advanced Reactor Policy Statement [18] regarding pursuit of less complex reactor designs with longer response time constants, passive reactor shutdown, and passive heat removal with limited reliance on operator actions, minimization of severe accident potential, and providing multiple barriers to potential radionuclide releases.

The NGNP project yielded a series of complementary pre-licensing "white papers" that were submitted to NRC staff for formal review and feedback. The review and feedback process included extensive public meeting interactions, conference calls, and written correspondence focused on requests for additional information. Responses were provided to all NRC requests for additional information regarding the Fuel Qualification White Paper.

In early 2012, four licensing framework topics were identified as key focus areas because they represented areas of significant and longstanding regulatory uncertainty for the entire HTGR industry. The four key topical areas targeted for joint examination were:

- HTGR functional containment performance

- Licensing basis event selection

- Source terms

- Emergency planning

Ensuing interactions resulted in NRC staff drafting initial regulatory positions on the four framework topics and submitting them to the NRC's Advisory Committee on Reactor Safeguards (ACRS) for review in early 2013. Staff findings were then updated and released again in July 2014. Major items addressed in the NRC staff position report [19] included:

- The DOE INL AGR program was determined to be reasonably complete within a context of pre-prototype fuel testing. Early fuel test results showed promise in demonstrating much of the desired retention capabilities of the TRISO particle fuel. Outcomes of the regulatory interactions related to the NGNP Fuel Qualification White Paper are documented in Enclosure 2 of the NRC letter to DOE, "NGNP-Assessment of Key Licensing Issues" [19]. Therein, NRC staff generally endorsed the approach to fuel qualification as proposed under the project. The staff identified one area of concern that may require a supplement to the currently planned fuel qualification program. Throughout the interactions, a key question remained regarding the extent to which irradiation testing in water-cooled materials test reactors, such as INL's Advanced Test Reactor (ATR), can provide an adequately prototypical environment for HTGR fuel. A concern existed the neutron spectrum in an HTGR is "harder" than in water-cooled reactors, and the composition of the test capsules irradiated in the program do not result in a prototypical number of plutonium fissions in the test fuel. This, in turn, caused the staff to question whether production of fission products (such as silver and palladium, both of which have higher fission yields from plutonium fission and can affect fuel particle performance) is high enough to ensure an understanding of their effects on fuel performance. Although the NGNP provided analyses information [20, 21] to support a position the proposed fuel irradiation program adequately addresses this

issue, NRC staff concerns remain. The issue could be addressed by conducting a proof test that includes post-irradiation safety testing of fuel from the production-scale fabrication of the initial core of the first reactor. NRC staff has indicated such a proof test would address uncertainties regarding the process of scaling up the fuel fabrication process from laboratory to engineering to production scale. The need for initial core fuel proof testing remains to be addressed by a future applicant.

- General agreement was expressed with the proposed NGNP performance standard concerning HTGR functional containment. The functional containment approach limits radionuclide releases to the environment by emphasizing retention of radionuclides at their source in the fuel rather than allowing significant fuel particle failures and relying upon other external barriers to provide compliance with identified top-level regulatory dose acceptance criteria.

- The licensing basis event identification and categorization process developed and proposed under NGNP included a frequency versus consequence approach for evaluating postulated event sequences against top-level regulatory criteria (primarily offsite dose). Initially, based on public meeting discussions and a draft feedback summary written by NRC staff, this approach appeared to be generally reasonable. Some members of the staff believed a supplement was probably necessary to the proposed set of design basis accidents. This proposed supplement would provide additional deterministically postulated accidents. NGNP personnel felt adding events from outside the proposed event selection process created significant uncertainty for the industry. The concept of a supplement was also subject to challenge by ACRS recommendations. This issue (and other related topics) was not addressed in the July 2014 NRC staff position report. The omission of this topic, as well as the overall licensing basis event identification and categorization process in general, was attributed to staff concerns issuing feedback on the topic at that time might be inconsistent with the concurrent NRC efforts related to post-Fukushima Near-Term Task Force (NTTF) Recommendation 1 and subsequent development of a risk management regulatory framework.

- The proposed mechanistic methodology for defining and evaluating source terms was deemed reasonable by NRC staff.

- The staff was receptive to future emergency planning proposals for a probabilistic risk assessment informed approach in sizing the emergency planning zone. Proposals might include the use of accident dose assessments when determining an appropriate emergency planning zone size. SECY-11-0152 contains a partial response to NGNP white paper proposals [22]. Clarification beyond SECY-11-0152 was not provided due to the need for NRC action on related policy issues. Further staff evaluation of the NGNP emergency planning approach was curtailed pending availability of more site and plant design information.

Certain key issues will require NRC policy determinations. The staff indicated general agreement with the systematic approaches proposed by the NGNP project staff and understood them to provide a reasonably sound basis for developing a license application. There are licensing issues that remain to be addressed by license applicants through direct NRC staff interaction. The status of these licensing activities is summarized in a 2014 INL report [23].

A.4   U.S. HTGR Precedents

A.4.1 Peach Bottom

A construction permit was issued to Philadelphia Electric Company for the Peach Bottom Unit 1 HTGR plant in 1962. This 40-MW(e) plant operated from 1967 to 1974 using BISO-based fuel. Although the fuel type used for this plant is not closely related to TRISO fuel, it was one of the original HTGR plants.

A.4.2 Fort St. Vrain

The Fort St. Vrain (FSV) Nuclear Generating Station was a prismatic fuel HTGR that generated 842 MW(t) to achieve a net output of 330 MW(e). FSV operated from 1974 to 1989. Licensing interactions on FSV were based on HEU TRISO fuel.

A.4.3 Others

During the last 25 years, the NRC has had two occasions to consider LEU TRISO fuel for HTGRs. These include the NRC review of the MHTGR that began in 1985 and resulted in the issuing of NUREG-1338 in 1995. Later in 2001, Exelon initiated pre-application interactions on the Pebble-Bed Modular Reactor (PBMR) design, which resulted in the NRC requesting additional information in June 2002. In late 2002, the NRC issued a closeout letter noticing the closure of the PBMR Project based on Exelon's request. The letter also stated the staff did not perform a detailed technical review of previous documents and was based on a limited screening review to ensure the issues, review status, and views and positions noted within the documents were consistent with the NRC's views and understanding.

A.5   References

1. U.S. Code of Federal Regulations. *Domestic Licensing of Production and Utilization Facilities.*

2. U.S. Nuclear Regulatory Commission. *Guidance for Developing Principal Design Criteria for Non-Light-Water Reactors.* RG 1.232. Washington, D.C.: April 2018.

3. U.S. Nuclear Regulatory Commission. *Issues Pertaining to the Advanced Reactor (PRISM, MHTGR, and PIUS) and CANDU 3 Designs and Their Relationship to Current Regulatory Requirements.* SECY-93-092. Washington, D.C.: July 16, 1993.

4. U.S. Nuclear Regulatory Commission. *Draft Preapplication Safety Evaluation Report for the Modular High-Temperature Gas-Cooled Reactor.* NUREG 1338. Washington, D.C.: March 1989.

5. U.S. Nuclear Regulatory Commission. *Policy Issues Related to Licensing Non-Light-Water Reactor Designs.* SECY-03-0047. Washington, D.C.: March 28, 2003.

6. U.S. Nuclear Regulatory Commission. *Status of Response to the June 26, 2003, Staff Requirements Memorandum on Policy Issues Related to Licensing Non-Light-Water Reactor Designs.* SECY-04-0103, Washington, D.C.: June 23, 2004.

7. U.S. Nuclear Regulatory Commission. *Second Status Paper on the Staff's Proposed Regulatory Structure for New Plant Licensing and Update on Policy Issues Related to New Plant Licensing.* SECY-05-0006, Washington, D.C.: January 7, 2005.

8. U.S. Nuclear Regulatory Commission. *Draft SECY Paper–Functional Containment Performance Criteria for Non-Light Water Reactor Designs.* ADAMS Accession No. ML18031A721, Washington, D.C.: January 30, 2018.

9. U.S. Nuclear Regulatory Commission, Advisory Committee on Reactor Safeguards, Correspondence from M.L. Corradini to K.L. Svinicki, "Draft SECY Paper, Functional Containment Performance Criteria for Non-Light Water Reactor Designs," ADAMS Accession No. ML18108A404, Washington, D.C.: May 10, 2018.

10. U.S. Nuclear Regulatory Commission, Correspondence from V.M. McCree to M.L. Corradini, "Response to the Advisory Committee on Reactor Safeguards' Letter Regarding Draft SECY Paper–Functional Containment Performance Criteria for Non-Light Water Reactor Designs," ADAMS Accession No. ML18156A401, Washington, D.C.: June 27, 2018.

11. U.S Nuclear Regulatory Commission. *Staff Requirements: Functional Containment Performance Criteria for Non-Light-Water Reactors,* SECY-18-0096, Washington, D.C.: December 4, 2018.

12. U.S. Nuclear Regulatory Commission. *Draft Preapplication Safety Evaluation Report for the Modular High-Temperature Gas-Cooled Reactor (MHTGR).* NUREG-1338. Washington, D.C.: March 1989.

13. U.S. Nuclear Regulatory Commission. *Preapplication Safety Evaluation Report for the Modular High-Temperature Gas-Cooled Reactor (MHTGR),*" NUREG-1338. Washington, D.C.: December 1995.

14. U.S. Nuclear Regulatory Commission. *Evaluation of High-Temperature Gas-Cooled Reactor Fuel Particle Coating Failure Models and Data.* NUREG-0111. Washington, D.C.: November 1976.

15. U.S. Nuclear Regulatory Commission. *Standard Review Plan for the Review of Safety Analysis Reports for Nuclear Power Plants: LWR Edition.* NUREG-0800, Rev. 3, Washington, D.C.: March 2007.

16. U.S. Nuclear Regulatory Commission. *TRISO-Coated Particle Fuel Phenomena Identification and Ranking Tables (PIRTs) for Fission Product Transport Due to Manufacturing, Operations, and Accidents.* NUREG/CR-6844, Washington, D.C.: July 2004.

17. *NGNP Licensing Plan.* Idaho National Laboratory, Idaho Falls, ID: June 26, 2009. PLN-3202.

18. U.S. Nuclear Regulatory Commission. *Policy Statement on the Regulation of Advanced Reactors,* Federal Register 73 FR 60612, Washington, D.C.: October 14, 2008.

19. G.M. Tracy, Director, U.S. Nuclear Regulatory Commission, Office of New Reactors, Letter to Dr. J. Kelly, DOE Deputy Assistant Secretary for Nuclear Technologies, "NGNP—Assessment of Key Licensing Issues," ML14174A734, with Enclosure 1 ("Summary Feedback on Four Key Licensing Issues," ML14174A774) and Enclosure 2 ("Assessment of White Paper Submittals on Fuel Qualification and Mechanistic Source Terms," Rev.1, ML14174A845).

20. G. Gibbs, Idaho National Laboratory, letter to U.S. Nuclear Regulatory Commission, September 20, 2010, "Contract Number DE-AC07-05ID14517–Next Generation Nuclear Plant–Response to Questions about the Applicability of the Advanced Gas Reactor Testing Results to Next Generation Nuclear Plant—NRC Project No. 0748," CCN 222202; ML102770386.

21. D. Petti, Idaho National Laboratory, letter to U.S Nuclear Regulatory Commission, September 20, 2013, "Contract Number DE-AC07-05ID14517—Next Generation Nuclear Plant Project Submittal—Additional Information on Selected Fuel Qualification/Mechanistic Source Terms Follow-Up Items—NRC Project No. 0748," CCN 228482; ML12268A031.

22. U.S. Nuclear Regulatory Commission. *Development of an Emergency Planning and Preparedness Framework for Small Modular Reactors*. SECY-11-0152. Washington, D.C.: October 28, 2011.

23. W. Moe. *NRC Licensing Status Summary Report for NGNP*. Idaho National Laboratory, Idaho Falls, ID: November 2014. INL/EXT-13-28205, Revision 1.

B
INTERNATIONAL COATED-PARTICLE DEVELOPMENT EXPERIENCE

B.1 General Experience and Coated Particle Evolution

Coated particles start with a spherical kernel of fissile or fertile material that is surrounded by one or more refractory coatings. By the early 1960s, coated-particle fuel development for carbonaceous matrix-moderated helium-cooled HTGRs was well under way in the United Kingdom in support of the DRAGON research reactor [1], in the U.S. in support of the Peach Bottom Unit 1 prototype power reactor [2], and in Germany in support of the AVR research and power reactor [3]. Coated particle designs for these reactors varied considerably, as illustrated in Figure B-1 (the AVR fuel loadings evolved through many designs in the course of over two decades of plant operation, including the LEU TRISO design discussed in Section 4.2).

Coated-particle fuel development programs have also been conducted in France, Russia, Japan, China, South Africa, and South Korea. The development of coated-particle fuel technology for both the pebble-bed and prismatic designs has drawn from an extensive international background of coated-particle fuel fabrication and testing experience spanning more than 50 years and covering a broad range of parameters as summarized below:

- Kernel characteristics:
    - Diameter – 100 to 800 μm
    - Fissile/fertile materials – uranium, thorium, plutonium (mixed and unmixed)
    - Chemical forms – oxide, carbide, oxycarbide
    - Enrichment – ranging from natural to HEU and plutonium
- Coating characteristics:
    - BISO – variations in buffer and pyrocarbon (PyC) coating thicknesses and properties
    - TRISO – variations in buffer, PyC and SiC (or zirconium carbide) thicknesses and properties
- Fuel forms:
    - Spheres – multiple geometries and fabrication methods
    - Compacts – cylindrical and annular shapes with variations in particle packing fractions and fabrication methods

- Irradiation facilities:

  - Materials Test Reactors – HFR (Netherlands), FRJ 2 DIDO (Germany), IVV-2M (Russia), Siloe (France), R2 (Sweden), BR2 (Belgium), High-Flux Isotope Reactor (HFIR) and ATR (U.S.), with wide variations in neutron energy spectra and degree of irradiation acceleration

  - Research and Demonstration Reactors – DRAGON (United Kingdom), Peach Bottom I (United States), AVR (Germany), FSV (United States), Thorium High Temperature Reactor (THTR) (Germany), HTTR (Japan), and HTR-10 (China)

- Irradiation and testing conditions:

  - Burnup – ranging from below 1% to above 70% fissions per initial metal atom (FIMA)

  - Fast fluence – ranging from below 1×10^{21} to above 10×10^{21} n/cm^2

  - Irradiation temperature – ranging from 600 to 1950°C

  - Accident simulation temperature – ranging from 1400 to 2500°C

This broad range of experience and data has supported the development of a detailed understanding of the parameters and phenomena of importance in the fabrication and performance of coated-particle fuel. Extensive bilateral and multilateral international information exchanges facilitated the incorporation of this broad experience base into the German and other modern coated-particle fuels. A detailed review of U.S. and German experience and the relationship to fuel performance and fuel performance modeling is documented in an Electric Power Research Institute (EPRI) report [4].

The evolution of the German fuel design, arriving at the LEU UO$_2$ TRISO pressed sphere selected as a basis for the pebble-bed reactor concept, is summarized in a section of a report on the AVR [3]. A broader range of international experience, focused mainly on LEU TRISO fuel, was addressed in an International Atomic Energy Agency (IAEA) coordinated research project conducted in the 1990s [5].

A more recent coordinated research project on TRISO-coated particle fuel was conducted in the early 2000s [6]. Two key parts of that project were: (1) an international quality control round robin test campaign for measuring important attributes of TRISO-coated particles; and (2) an international fuel performance benchmarking exercise to compare international codes that model TRISO-coated particle fuel under both normal operation and postulated accident conditions. In considering this experience and data, the international community has converged on common LEU TRISO particle designs, as discussed in Section 4.2, as having very similar coating thicknesses and properties with variations in kernel diameter, enrichment, and composition (UO$_2$ and UCO), depending on specific service conditions and requirements.

B.2   LEU UO₂ Experience in Russia   /

Coated-particle fuel development in Russia was based on a spherical fuel element incorporating UO₂ coated particles similar to a German design, with reactor design enrichments ranging from 6.5 to 21% [5]. Fuel development and testing included both low and high-temperature isotropic pyrocarbon for the dense pyrocarbon[22] layers [7]. In support of these designs, the fuel fabrication, irradiation, and testing program was conducted from 1975 through 1990. As-manufactured particle defect fractions on the order of 10^{-5} were achieved at both laboratory and semi-industrial scale. Russian coated-particle fuel fabrication development is described in several papers in the proceedings of an IAEA meeting on gas-cooled reactor fuel development [8].

The fuel irradiation program was conducted using enrichments higher than the reactor design values, ranging from 21 to 45%. The irradiations covered a wide range of conditions [9]:

- Temperatures: 400 to 1950°C

- Burnup: 1 to 41% FIMA

- Fast fluence: 0.1 to 2.7×10^{25} n/m^{-2}, E >32fJ.

The irradiation temperature and burnup ranges substantially exceeded typical design ranges for coated particles of design similar to the German fuel. Thus, the Russian program produced valuable irradiation data on the ultimate capability of the fuel and fuel behavior at conditions exceeding the nominal operating range. The investigation of the capability of a particle design similar to the German particle yielded the following conclusions [9]:

- Irradiation at 1000°C produced insignificant gaseous fission product release at burnups of 15–20% FIMA

- Irradiation at 1200°C produced depressurization of separate coated particles[23] at burnups of 10–15% FIMA

- Irradiation at 1400°C produced increased gaseous fission product release at burnups of 5–13% FIMA.

The results also indicated particles with low-temperature isotropic PyC layers achieved higher burnups prior to gas release than those with high-temperature isotropic layers.

The Russian program also investigated fuel (both loose particle and sphere forms) response to over-power conditions to explore failure limits. Power pulse experiments of 1 sec duration were carried out at power levels of ~30, 66, and 124 times the nominal maximum power level, with no indications of significant gaseous fission product release. Extended overpower tests at ~10 times the nominal maximum under adiabatic conditions for 5, 10, and 30 seconds showed no

---

[22] At temperatures between 1250 and 1350°C, a low-temperature isotropic coating is produced by chemical vapor deposition. In the range of 1800 to 2100°C, a different type of pyrocarbon, "high-temperature isotropic," is deposited. Both forms were investigated in early coated-particle fuel development, with the low-temperature isotropic form selected for further development.

[23] The phrase, "depressurization of separate coated particles," was taken from the referenced paper. It is interpreted to refer to individual failures of loose particles during irradiation.

indications of damage in the first two cases, but failure of the fuel sphere and a significant fraction of the particles in the last case [8]. These conditions are not achievable in a reactor because of negative temperature reactivity feedback and continued heat removal from the sphere, but the results are relevant to the ultimate capability of the fuel.

B.3   LEU UO₂ Experience in China

The coated-particle fuel program in China was initially established to support the construction and operation of the Institute of Nuclear and newEnergy Technology (INET) HTR-10 reactor. The HTR-10 project was initiated in 1990, following an HTGR conceptual design and feasibility study [10]. Development of fuel fabrication methods was based on the German particle and spherical fuel element design using fuel fabrication equipment obtained from Germany. Fabrication of fuel for the first core of HTR-10 began in December 1999 [11] with the production of 11,700 fuel spheres by September 2000 sufficient to support initial criticality, which was achieved in December 2000 with a core containing a mixture of 16,890 fuel and carbonaceous matrix spheres.[24]

The low power level (10 MWth) combined with the replication of the German fuel design, which enabled the use of the German fuel performance data, supported the demonstration of large margins to fuel service condition limits. The fuel irradiation and testing program was conducted in parallel with the initial operation of HTR-10 [10]. Following initial criticality, a series of tests was completed at a power level of 3.44 MWth, supporting subsequent operation at 10 MWth, which was achieved in January 2003 [12].

The fuel quality, as indicated by the free-uranium content in the fuel spheres, improved by over an order of magnitude during the course of production for the HTR-10 core (a total of 25 batches of spheres). Free-uranium content (as measured by the burn-leach procedure) in the early batches was typically $\sim 10^{-4}$, while the last 15 batches were typically $\sim 10^{-5}$ and lower [11]. To facilitate irradiation and testing of HTR-10 fuel as soon as possible, sphere samples were taken from the first and second batches [13]; thus, the as-manufactured quality of the tested spheres was representative of the lower quality early fuel production.

Irradiation of four fuel spheres taken from early in the first HTR-10 core production, as described above, began in the Russian IVV-2M reactor in July 2000 and was completed in February 2003 [13]. The irradiation rig contained five capsules—capsules 2 through 5 contained fuel spheres, while capsule 1 contained carbonaceous matrix specimens. The irradiations were conducted at $\sim 1000°C$, with short-term increases to $\sim 1200°C$, and to burnups ranging from 95 to 107 GWd/MTHM. In-pile gas release measurements indicated the presence of one or two exposed kernels in two of the irradiated spheres from the beginning, consistent with the as-manufactured free-uranium measurements for early production batches.

---

[24]   The initial core loading for HTR-10 included both fuel and graphite spheres to achieve the desired core volume. As burnup proceeds, the fraction of graphite spheres is decreased to compensate for burnup in the approach to an equilibrium core.

One of the capsules failed during irradiation with loss of gas-release data, and post-irradiation examination (PIE) showed substantial damage to the sphere (in-pile gas-release measurements failed when the capsule failed). Another capsule was subjected to a high-temperature test at the end of the irradiation, resulting in temperatures well beyond the planned conditions (and a significant fraction of exposed kernels as determined in the PIE) when a control thermocouple (TC) failed. In-pile gas-release data indicated no failures occurred during irradiation when conditions remained within specified levels.

An additional irradiation of fuel spheres produced in China for the HTR-10 was conducted in the HFR Petten reactor in an experiment designated HFR-EU1 [14, 15]. The HFR-EU1 experiment included two spheres from China and three from the German program (from AVR 21-2, representative of the highest quality German fuel), with the two fuels placed in separate capsules, each with in-pile gas release measurement capability. A primary objective of the irradiation was to subject the spheres to high burnups (for example, 17% FIMA for Chinese spheres, 20% FIMA for German spheres) to investigate the ultimate capability of the coated-particle design developed in Germany. The experiment was performed in two campaigns from September 2006 to February 2008 and continued from October 2009 to February 2010. The surface temperature of pebble INET 2 during irradiation was approximately 940°C. At the end of irradiation, the experiment had accumulated 16 reactor cycles totaling 445 EFPD.

The calculated burnup was 9.3% FIMA (pebble INET 1) and 11.6% FIMA (pebble INET 2)—both somewhat lower than the originally planned value—and the maximum fast neutron fluence ($E > 0.1$ MeV) was about 4.95×10^{25} n/m^2. The ^{85m}Kr release-rate-to-birth-rate (R/B) ratio for the INET capsule was approximately 8×10^{-8}. Based on the Booth Model [16] and assuming a capsule-average temperature of 900°C, the calculated ^{85m}Kr release fraction from a single coated particle would be 3.26×10^{-3}, and from a single failed particle in the capsule with two INET fuel spheres (~16,600 particles) 1.96×10^{-7}, which is higher than the observed R/B. This indicates no complete particle failure occurred during the irradiation and the measured fission gas release originates from uranium and thorium impurities in the carbonaceous matrix of the pebbles and in the graphite cups used to hold the pebbles in place.

Development of fuel for the High-Temperature Reactor-Pebble-bed Modular (HTR-PM) reactor has been conducted at INET starting around 2004 and is based closely on the development of HTR-10 fuel technology. The manufacturing technology and facilities were enhanced to the industrial scale and a demonstration line was established with the capability to produce 100,000 pebbles per year. The HTR-PM fuel uses the same TRISO-coated particle design as HTR-10, but the uranium loading increased from 5 to 7 g per pebble, corresponding to an increase in particles from 8,000 to 12,000 per pebble. At the same time, the free uranium fraction in the pebbles decreased from 5×10^{-4} to 6×10^{-5}. After establishing the technology, a batch of spheres was fabricated, with several being selected at random for an irradiation qualification test in HFR Petten.

Irradiation testing of five HTR-PM fuel spheres was performed in HFR Petten [17]. The irradiation was designed so the upper four pebbles would reach a burnup higher than 12.3% FIMA with center temperatures of 1050±50°C. The irradiation took 355 full-power irradiation days and was completed in December 2014. Based on neutronics calculations, the total fast fluence levels were between 3.79 and 4.95×10^{25} n/m^2 ($E > 0.1$ MeV). Burn-up estimates are

11.1% FIMA for Pebble 5 and between 12.6 and 13.7% FIMA for the other pebbles. The central temperatures remained within the target boundaries of 1050±50°C. The calculated R/B from a single failed particle (out of 60,000 particles) at 1050°C is 1.1×10^{-7} for ^{85m}Kr. Measured ^{85m}Kr R/B values during the last cycle were between 2.4 and 3.3×10^{-9}, indicating no particle failure.

PIE of the HTR-PM irradiated fuel specimens has been performed at Petten and Karlsruhe separately. The initial PIE at Petten shows the dimensional shrinkage in all five pebbles is between 0.88% and 1.25%, and further PIE has been performed at the European Commission Joint Research Center in Karlsruhe. There, the irradiated fuel pebbles have been exposed to heating tests in pure helium in the KühlFinger-Apparatur (KüFA) facility, which simulates high-temperature accident conditions in the reactor. These final PIE results have not yet been published.

B.4 LEU UO₂ Experience in Japan

The Japanese high-temperature gas reactor program is centered on the HTTR, which has a thermal power of 30 MW and 950°C maximum coolant outlet temperature. The HTTR achieved criticality in November 1998 and has undergone a series of rise-to-power tests [18]. In December 2001, an outlet temperature of 850°C was achieved, and in April 2004, a temperature of 950°C was achieved. As of July 2004, the reactor had operated for 224 effective full-power days (EFPDs). The planned core life cycle is 660 EFPDs [19]. It is planned to couple a high-temperature process-heat application to the HTTR through its intermediate heat exchanger in the future.

The fuel elements are prismatic graphite pin-in-blocks with vertical bore holes containing fuel rods (graphite sleeves) with annular fuel compacts [20]. Each compact contains about 13,000 TRISO-coated fuel particles with a 600-μm-diameter UO₂ kernel, a 60-μm-thick buffer, and 30-μm-thick inner pyrolytic carbon (IPyC), 25-μm-thick SiC, and 45-μm-thick outer pyrolytic carbon (OPyC) layers. Uranium enrichments vary in 12 stages, from 3.4 to 9.9%, and average 6%. The end-of-life core average burnup is designed to be 2.4% FIMA, and the design limit peak burnup is 3.6% FIMA. The fuel quality of the HTTR first core is a heavy-metal (HM) contamination of 2.5×10^{-6}, initial through-coating defects of 2.5×10^{-6}, and initial SiC defects of 8×10^{-5}. The measured R/B ratio of ^{88}Kr at full power, a 950°C outlet temperature, and approximately 200 EFPDs of reactor operation was 1.0×10^{-8}, corresponding to gaseous diffusion from HM contamination and no significant in-reactor fuel particle failures. The high-temperature demonstration was maintained for about 5 days.

HTTR-type fuel was irradiated in the HRB-22 test in the HFIR to burnups in the range of 4.1 to 6.7% FIMA [20, 21]. Online gamma monitoring detected four fuel-particle failures out of 32,200 particles irradiated, or a failure fraction of 1.2×10^{-4}. PIE and safety tests were performed at temperatures ranging from 1600 to 1800°C. In one test at 1600°C, one failed particle was detected out of about 2,800 particles in 219.4 hours. Tests at 1700 and 1800°C revealed large variations in metallic fission-product releases from particle to particle, which could only be explained by the presence or absence of cracks in the SiC layer. A series of irradiations was carried out with HTTR fuels in Oarai Gas Loop-1 in the Japan Materials Testing Reactor. The results of three irradiations with particle numbers of about 65,000 in each experiment indicate through-wall failures were less than 3×10^{-4} at 95% confidence after burnups up to 3.7% FIMA [22].

A modified coated particle design was developed to allow burnups of approximately 10% FIMA in HTTR. Preliminary testing in materials test reactors (MTRs) at ~7 to 9% FIMA indicated good performance, albeit with several particle failures that were postulated to be due to as-fabricated SiC defects based on fuel performance models [23]. This fuel notably involved a change in the specification for kernel diameter (from 600 to ~550 μm), buffer layer thickness (from 60 to 90 μm), and SiC layer thickness (from 25 to 35 μm) compared to the initial HTTR fuel particles. Based on these results, additional modifications in the particle design were implemented with a specified kernel diameter of 500 μm (9.9% ^{235}U enrichment) and buffer thickness of 95 μm [24], such that it closely resembled the standard TRISO particle design from the German program. This fuel was recently irradiated to >9% FIMA in the WWR-K reactor (Kazakhstan). A few exposed kernels were observed based on R/B data, but these were again postulated to be related to particles with as-fabricated SiC defects [25], indicating no in-pile particle failures occurred.

B.5   German High-Quality LEU-UO₂ Pebble-Fuel Experience

Experience with coated particle fuel in Germany began in the early era of particle fuel development, and progressed through varying particle types employed in the AVR. The German LEU UO₂ TRISO fuel design evolved from decades of international coated-particle fuel fabrication, irradiation, and PIE and safety testing experience covering a wide range of particle designs, fuel forms, and irradiation and testing conditions. Numerous international bilateral and multilateral data and analytical methods exchanges (such as those discussed in IAEA-IWGGCR/8 [8] facilitated the effective incorporation of this experience into the definition and development of the German LEU UO₂ TRISO fuel particle and sphere design that began in the late 1970s.

Fuel development in the 1980s demonstrated the high as-manufactured fuel quality and excellent in-pile performance that can be accomplished with LEU UO₂ fuel. Efforts involved refinement of fuel fabrication and quality control capabilities, irradiation testing of fuel spheres both in MTRs and in AVR, and PIE and heating tests to assess performance in-pile and under accident conditions, and have been summarized in several publications [26-28]. The results demonstrated low as-manufactured particle defect fractions and low particle failure fractions during irradiation and during post-irradiation heating tests at postulated accident temperatures.

This effort culminated in the large-scale fabrication campaign of the so-called GLE-4/2 fuel for AVR (16.8% ^{235}U) and the small-scale fabrication of the proof test fuel for the HTR-Modul 200-MWt modular reactor design in 1988 (10.6% ^{235}U), both with very low defective particle fractions (≤2.0 × 10^{-5} and ≤5.3 × 10^{-5}, respectively; representing the upper bound at 95% confidence) [27]. Fuel fabrication efforts ceased in 1988 concurrent with the shutdown of THTR, but irradiation testing in MTRs continued through 1994, finishing with the proof test fuel irradiations (designated HFR-K5 and HFR-K6) in HFR-Petten.

A large body of experimental data obtained by means of an irradiation and PIE program, covering a wide range of operating parameters, supports the German LEU UO₂ TRISO fuel design. This database supports establishment of an operating envelope for this fuel design, covering normal operation as well as transient and accident conditions.

B.5.1 Fabrication

The LEU TRISO fuel types manufactured and tested in Germany are summarized in Table B-1 and Table B-2. Fuel spheres intended for AVR operation were manufactured in large numbers for the purpose of bulk testing in a reactor environment. Fuel spheres manufactured for the German LEU Phase 1 irradiation test program and for the Proof Test for the HTR-Modul were manufactured in smaller numbers.

Table B-1
LEU UO$_2$ TRISO fuels manufactured and tested

Characteristic	Pre-1985 Production			Post-1985 Production	
Year of Manufacture	1981	1981	1983	1985	1988
Designation	GLE 3	LEU Phase I	GLE 4	GLE 4/2	Proof Test Phase 2
Matrix Material	A3-27	A3-27	A3-27	A3-3	A3-3
Irradiation Test Designation	AVR 19	HFR-K3 FRJ2-K13 HFR-P4 SL-P1 FRJ2-P27	AVR 21-1 FRJ2-K15	AVR 21-2	HFR-K5 HFR-K6
Approximate number of fuel spheres manufactured	24,600	100	20,500	14,000	200

The symbols used in the 'Irradiation Test Designation' row have the following meanings:

1. The first 2 to 4 characters describe the reactor in which the test was done:

- AVR = *Arbeitsgemeinschaft Versuchsreaktor* in Jülich, Germany
- HFR = High Flux Reactor in Petten
- FRJ2 = DIDO reactor in Jülich
- SL = Siloe reactor in Grenoble

2. The next group of characters describes the irradiation sample type and test number. In the case of AVR irradiations, the reload number is used (that is, AVR 19), which means that the fuel spheres made up the 19th partial reload of the reactor. In other tests, the letter K designates a full-sized fuel sphere, the letter P designates coated particles in any other form (that is, small spheres, compacts, or coupons) and the number is the test number. Thus, FRJ2-P27 means irradiation test number 27 performed on coated particles in the DIDO reactor in Jülich.

The data indicate the pre-1985 and post-1985 fuel designs are nearly identical, except for enrichment and HM loading in the spheres. Although the enrichment and HM loading varied, the amount of [235]U per sphere was kept at approximately 1 gram.

The delineation between pre-1985 and post-1985 is not based on the fuel design, but rather on two particular improvements in the manufacturing process. Coated particles are "overcoated" with matrix material[25] prior to mixing them with additional matrix material in preparation for pressing of the fuel sphere. For the pre-1985 category, the overcoating of the particles was done manually, whereas for the post-1985 category, overcoating was automated using a specially designed mixer operated by a robot. This change in the overcoating process and the introduction of vibration tables in three stages to remove odd shaped kernels, coated particles, and overcoated particles during particle manufacturing resulted in a significant improvement in the "free uranium" burn-leach test results for completed fuel spheres. The free uranium fraction decreased by about a factor of four from the average of the pre-1985 results to the average of the post-1985 results.

Table B-2
Manufacturing detail for LEU UO₂ TRISO fuel types

Characteristic	Pre-1985 Production			Post-1985 Production	
Designation	GLE 3	LEU Phase I	GLE 4	GLE 4/2	Proof Test Phase 2
Kernel Diameter (μm)	500	497	501	502	508
Kernel Density (g.cm⁻³)	10.80	10.81	10.85	10.87	10.72
Coating Thickness (μm)					
Buffer Layer	93	94	92	92	102
Inner PyC Layer	38	41	38	40	39
SiC Layer	35	36	33	35	36
Outer PyC Layer	40	40	41	40	38
Coating Density (g.cm⁻³)					
Buffer Layer	1.01	1.00	1.01	1.1	1.02
Inner PyC Layer	1.86	~1.9	1.9	1.9	1.92
SiC Layer	3.19	3.20	3.20	3.2	3.20
Outer PyC Layer	1.89	1.88	1.88	1.9	1.92
Fuel Sphere Loading					
Heavy Metal (g/FS)	10	10	6	6	9.4
Uranium-235 (g/FS)	1	1	1	1	1
Enrichment (% U-235)	9.82	9.82	16.76	16.76	10.6
Coated Particle per FS	16400	16400	9560	9560	14580
Free-Uranium Fraction (×10⁻⁶)	50.7	35	43.2	7.8	13.5

---

[25] The matrix material consists of a mixture of natural and synthetic graphite powders and a resin binder.

Forty GLE 4/2 spheres and 10 Proof Test spheres, containing 528,200 coated particles, were subjected to the burn-leach test[26]. Test results indicated the free uranium in these 528,200 particles was equivalent to the uranium in six coated particles. Therefore, the sample mean defect fraction is 1.1×10^{-5} and the expected defect fraction (50% confidence that population fraction is no higher) due to manufacturing is 1.3×10^{-5}, with a 95% confidence maximum defect fraction of 2.2×10^{-5}. Note the substantial majority of the fuel irradiation and testing data summarized in this section was produced from the GLE 3 and LEU Phase 1 (that is, pre-1985 production) fuels.

Details of the German LEU UO_2 TRISO fuel fabrication processes for kernels, coated particles, and spherical fuel elements are beyond the scope of this report. Numerous sources provide additional information as an introduction to the subject, including IAEA TECDOC-978 [5] and Kania et al. 2015 [29].

B.5.2 Irradiation and Accident Safety Testing

The German fuel irradiation experience includes both bulk fuel testing in the AVR and carefully controlled and monitored irradiations in MTRs in Germany, the Netherlands, and France. Results of this test program have been summarized in other publications (an excellent starting point is Kania et al. 2013 [27], and an analysis of the data with a focus on as-manufactured defects and in-pile particle failures has been presented previously in Section 3.3 and associated appendix of the NGNP Fuel Qualification White Paper [30]. Key results, observations, and conclusions from the German program with regard to fuel performance are summarized in this section.

A summary of in-pile fuel conditions (burnup, fast fluence, and temperature) for the irradiation results discussed in this section is shown in Figures B-1 and B-2. The AVR fast fluence values were determined by a correlation with burnup and individually adjusted to reflect the expected ±10% variation based on different trajectories taken by individual spheres. Also included in Figure B-3 is an example operating envelope developed related to the NGNP pebble-bed design [30]. The aggregate envelope of the existing data on German LEU UO_2 TRISO fuel substantially exceeds this envelope in terms of burnup and fast fluence. The MTR data include known temperature histories and extremes in burnup and fluence and time at temperatures well beyond the expected service conditions of pebble-bed fuel. These data also provide insights that support interpretation of the AVR irradiation data, such as particles with exposed kernels present from the beginning of the irradiations.

---

[26] Since the manufacturing process change that delineates the two categories significantly impacts the determination of the free-uranium fraction, only the burn-leach test results from the post-1985 category were used in the calculation of the expected "coated-particle defect fraction" due to manufacturing defects.
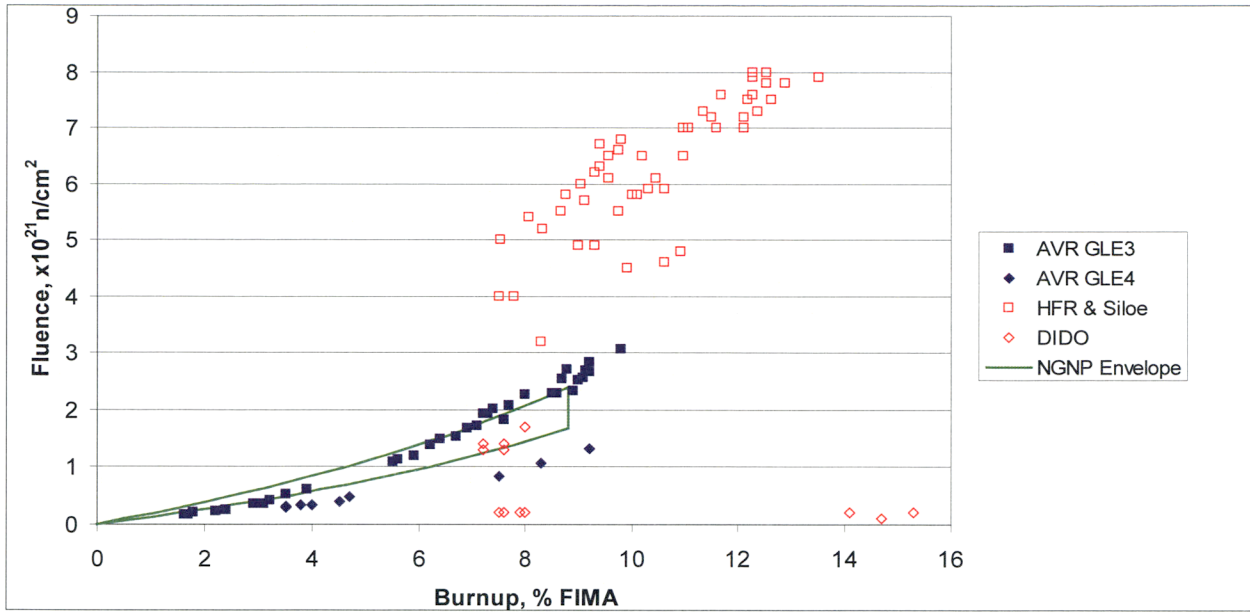
Figure B-1
German LEU TRISO irradiation conditions, AVR and MTRs. The NGNP pebble-bed performance envelope is included for comparison [30]
Courtesy of Idaho National Laboratory and used with permission of Battelle Energy Alliance, LLC
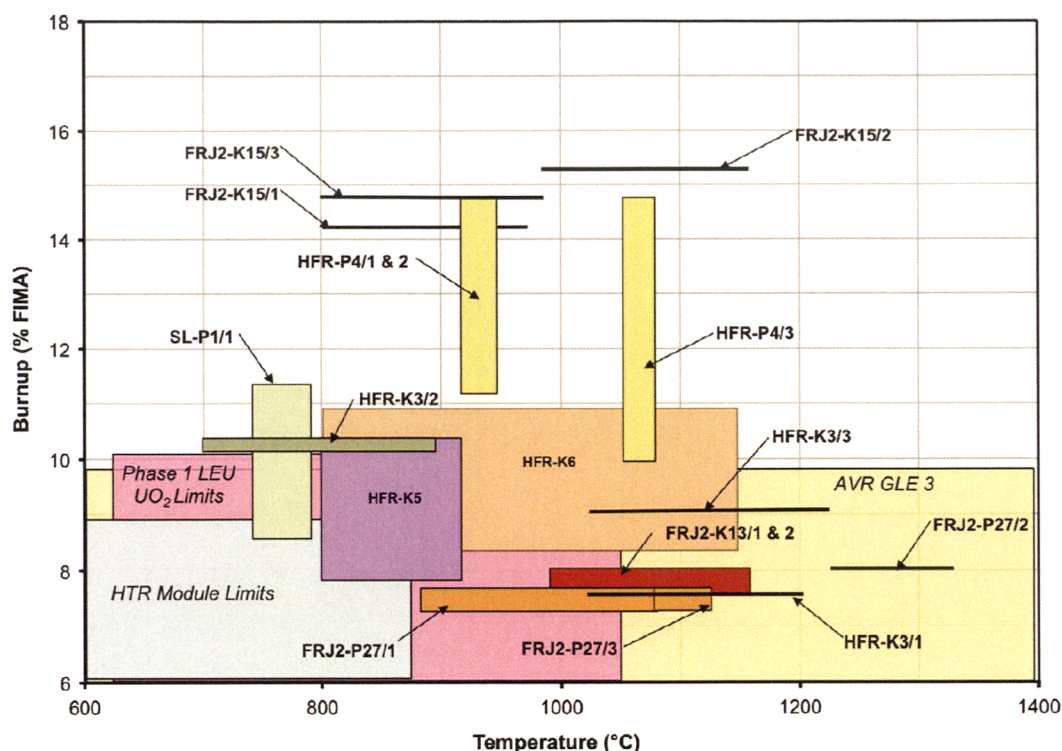
Figure B-2
Fuel burnup and mean operating temperature for German LEU UO2 TRISO particles in accelerated irradiation tests conducted in European MTRs and in AVR prior to 2000
Reprinted from Journal of Nuclear Materials, ©2003, with permission of Elsevier[27]

The two final proof test irradiations (HFR-K5 and HFR-K6) involved eight spheres at temperatures between 800 and 1140°C and peak burnup of about 11% FIMA with low fission gas release indicating no particle failure (^{85m}Kr R/B ratios $\leq 9.0 \times 10^{-7}$), giving a calculated particle failure fraction of $\leq 2.6 \times 10^{-5}$ (upper bound at 95% confidence). Taken as a whole, German irradiation testing of 60-mm-diameter spherical fuel elements in MTRs (totaling approximately 277,000 particles and including Phase 1, GLE 3, and Proof Test fuel) resulted in no particle failures, which corresponds to a particle failure fraction of $\leq 1.1 \times 10^{-5}$ at 95% confidence. Additional analysis, which includes data on exposed kernels in AVR spheres derived from post-irradiation heating test data in addition to the results from MTR irradiations indicates no failures out of approximately 477,000 particles.

---

[27] Reprinted from Kania et al., "Testing of HTR UO2 TRISO fuels in AVR and in material test reactors," *J. Nucl. Mater.*, Vol. 441, 2013, pp. 545-562, Copyright 2003, with permission from Elsevier.

German fuel elements (including both standard spherical fuel elements as well as smaller cylindrical compacts containing ~1,600 particles in a central spherical fueled zone and indicated by the "P" nomenclature in the irradiation test designation in with burnup ≤11% FIMA also exhibited no failures during 1600°C isothermal accident tests in dry helium (based on ^{85}Kr release fractions ≤2 × 10^{-6})[28], and cesium release fractions were below ≤1 × 10^{-4}, indicating intact, retentive SiC layers.

However, at reported burnups ≥14% FIMA[29] or temperatures ≥1700°C during post-irradiation heating tests, particle failures began to manifest as higher ^{85}Kr releases. Cesium release also increased at the higher temperatures, with release fractions reaching ~10^{-2} to 10^{-1} from fuel spheres at 1800°C (burnup <11% FIMA) and >10^{-1} for fuel compacts (burnup 12% FIMA) [31]. Based on these results, it has been asserted, if the fuel is pushed to a burnup of ~15% FIMA, accident temperatures should be limited to 1600°C, but for fuel with peak burnup of 11% FIMA the allowable accident temperature limit may be higher than 1600°C [27]. Additional post-irradiation heating under oxidizing conditions, performed on a more limited scale, demonstrated additional particle failure can occur after prolonged exposure (several hundred hours) in air above 1300°C, and 800°C exposure to steam can result in increased release of fission gas from exposed kernels.

Additional irradiation testing of German TRISO fuel was performed from 2004 to 2010 in HFR Petten using previously manufactured fuel spheres of the GLE-4/2 type and sponsored by the European Commission, with the intent of demonstrating the UO$_2$ fuel performance at temperatures and burnup beyond the conventional fuel performance envelope for modular pebble-bed HTGRs [32-34]. Burnups achieved in these irradiations were approximately 11% and 14% FIMA in the EU1bis and EU1 irradiations, respectively (both falling somewhat short of the originally targeted values) [35], and some PIE results from the EU1bis experiment have been reported [36].

While the AVR spheres in the EU1 irradiation (sphere surface temperatures reported to be 950°C) exhibited relatively low fission gas R/B ratios indicating no failed particles [33], the higher-temperature EU1bis irradiation (sphere center temperatures were reportedly maintained at 1250°C [37][30]) had ^{85m}Kr R/B of 4 × 10^{-6}, indicating some particle failure occurred [34].

---

28   Note that more recent heating tests on proof test spheres from the HFR-K5 and -K6 spheres has resulted in somewhat higher ^{85}Kr release fractions, although still falling below 1 × 10^{-5}, indicating no particle failures (O. Seeger et al., *Nucl. Eng. Des.* Vol. 306, 2016, pp.59-69; D. Freis, *Accident Simulations and Post-Irradiation Investigations on Spherical Fuel Elements for High Temperature Reactors,* 2010 Doctoral dissertation, NRC translation 3806)

29   Several methods were used to empirically measure the burnup of the fuel compacts; the reported values are the highest among the various methods, indicating the possibility that burnup could be overestimated by ~10–20% (W. Schenk et al., *Performance of HTR Fuel Samples under High-Irradiation and Accident Simulation Conditions, with Emphasis on Test Capsules HFR-P4 and SL-P1*, Juel-3373, Research Center Jülich, 1994).

30   Early in the irradiation, an operating error resulted in inadvertent introduction of pure neon, resulting in temperatures well above the target values. Post-irradiation thermal modeling of operation with pure neon indicated a temperature at the outer graphite shroud radius of 1350°C, which could result in sphere centerline temperatures approaching 1600°C for an extended period (S. de Groot, K. Bakker, A.I. van Heek, M.A. Fütterer, Modelling of the HFR-EU1BIS experiment and thermomechanical evaluation, Nucl. Eng. Des. 238 (2008) 3114-3120).
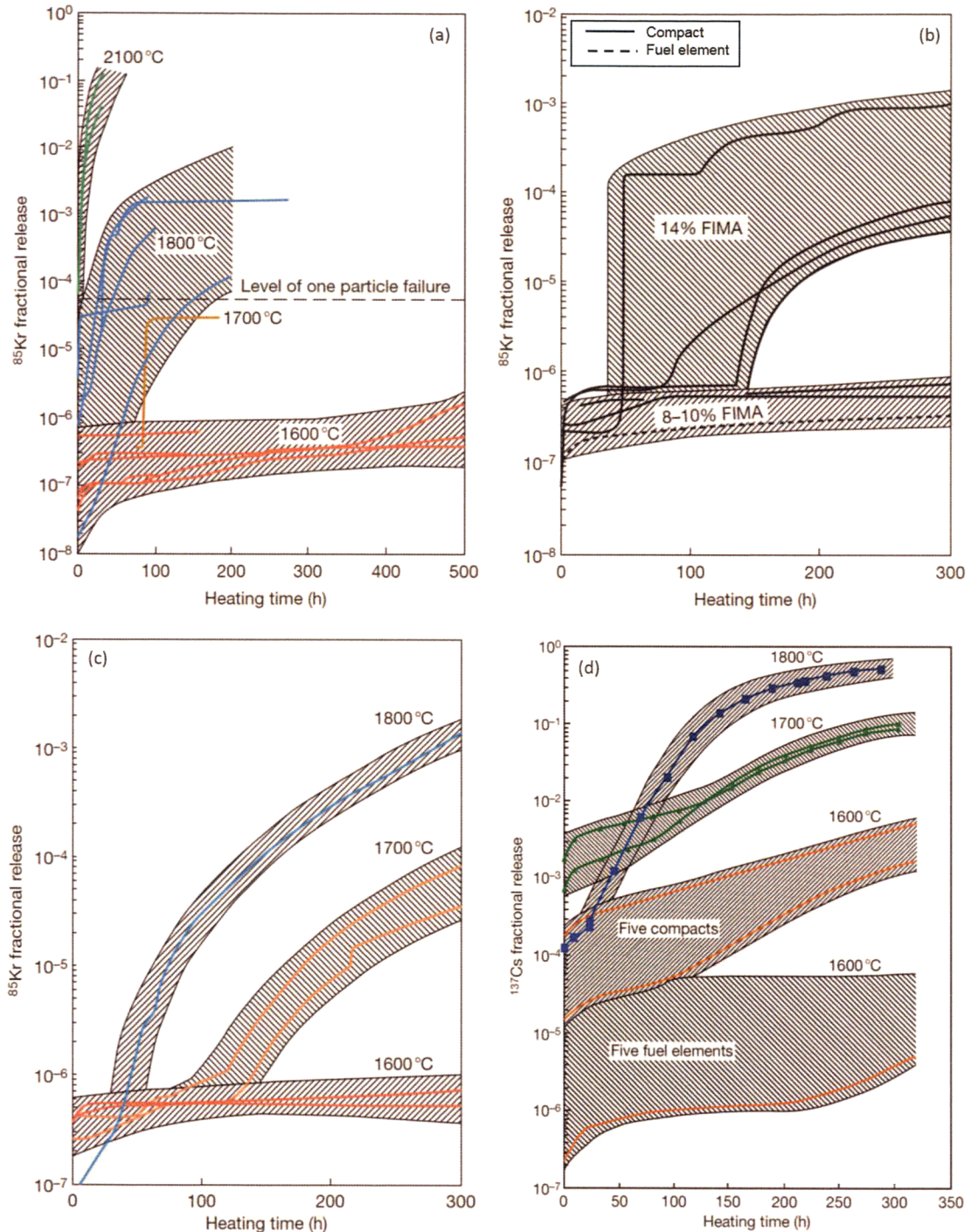
Figure B-3

Summaries of 85Kr and 137Cs release during German accident safety tests in helium. Note: 85Kr release results are for (a) spherical fuel elements at 1600–2100°C, (b) spherical fuel elements and cylindrical compacts with burnup 8–14% FIMA at 1600°C, (c) cylindrical compacts with burnup 10–12% FIMA at 1600-1800°C. (d) 137Cs release results for spherical fuel elements (1600°C) and cylindrical compacts (1600–1800°C)

Courtesy of Idaho National Laboratory and used with permission of Battelle Energy Alliance, LLC

Post-irradiation heating of several spheres from these irradiations resulted in low release of ^{85}Kr, indicating no full TRISO coating failures. However, ^{134}Cs fractional release at 1600°C reached 1–2.5 × 10^{-3} for EU1bis spheres[31] and 6 × 10^{-4} for an EU1 sphere, [38-40] all of which are significantly higher than observed in historic tests of German LEU UO$_2$ TRISO fuel at similar temperatures, which indicates release through the SiC layer of the particles. This indicates the onset of degradation and/or layer failure. It appears these irradiation tests may have challenged an upper limit for acceptable performance for LEU UO$_2$ fuel.

In a compilation of German irradiation and safety testing data, Kania et al. [27] have summarized the performance of spherical fuel elements during 1600°C isothermal heating tests and transient-temperature tests, which simulate the time-varying peak fuel temperature in the reactor during a depressurized loss of coolant flow accident with a maximum temperature of 1620°C. This includes spheres irradiated in AVR as well as fuel from proof test irradiations and the more recent EU irradiations. Based on five observed failures[32] out of 287,480 particles tested, the reported upper bound for the failure fraction at 95% confidence is ≤3.7 × 10^{-5}.

B.6   References

1. R.A. Simon and P.D. Capp, 2002, "Operating experience with the Dragon high temperature reactor experiment," *Proceedings of the Conference on High Temperature Reactors (HTR-2002)*, Petten, the Netherlands, April 22-24, 2002. International Atomic Energy Agency, Vienna: 2002.

2. K.I. Kingrey. *Fuel Summary for Peach Bottom Unit 1 High-Temperature Gas Cooled Reactor Cores 1 and 2.* Idaho National Laboratory, Idaho Falls, ID: April 2003. INEEL/EXT-03-00103.

3. *AVR – Experimental High-Temperature Reactor, 21 Years of Successful Operation for a Future Energy Technology.* VDI-Verlag GmbH, Düsseldorf: June 1990.

4. *A Review of Radionuclide Release from HTGR Cores During Normal Operation.* Electric Power Research Institute, Palo Alto, CA: February 2004. 1009382.

5. *Fuel Performance and Fission Product Behaviour in Gas Cooled Reactors.* International Atomic Energy Agency, Vienna: November 1997. IAEA-TECDOC-978.

6. *Advances in High Temperature Gas Cooled Reactor Fuel Technology.* International Atomic Energy Agency, Vienna: June 2012. IAEA-TECDOC-1674.

---

[31] Subsequent analysis of the testing system by Seeger et al., indicates that the temperature of some of the EU1bis tests was most likely lower than originally reported by approximately 100°C (O. Seeger, "Evaluation of fission product releases obtained from Küfa safety tests in light of the setup's accuracy," *Proceedings of the 8th International Topical Meeting on High Temperature Reactor Technology (HTR 2016)*, , Las Vegas, Nevada, November 6-10, 2016.)

[32] Note that all five failures included in the statistics occurred during transient-temperature tests in which the furnace temperature mimicked the peak fuel temperature during a depressurized loss of forced cooling accident, and were performed using spheres irradiated in AVR. Fuel-performance models would predict that the isothermal testing at ≥1600°C should be more challenging for the fuel. It is possible that these AVR spheres experienced exceptionally high temperatures during irradiation, resulting in elevated failure during post-irradiation heating and biasing the results.

7. G. Gibbs, Idaho National Laboratory, letter to U.S. Nuclear Regulatory Commission, September 20, 2010, "Contract Number DE-AC07-05ID14517—Next Generation Nuclear Plant — Response to Questions about the Applicability of the Advanced Gas Reactor Testy Results to Next Generation Nuclear Plant —NRC Project No. 0748," CCN 222202; ML102770386.

8. *Specialists' Meeting on Gas-Cooled Reactor Fuel Development and Spent Fuel Treatment.* International Atomic Energy Agency, Vienna: October 1983. IAEA-IWGGCR/8.

9. A. Chernikov and A. Deryugin. "Irradiation tests of HTGR Fuel under normal and accident conditions," *OECD Proceedings: The First Information Exchange Meeting on Survey on Basic Studies in the Field of High Temperature Engineering.* Paris, France, September 27-29, 1999. Organization for Economic Cooperation and Development, Paris: 2000.

10. D. Zhong and Z. Qin, "Overview of the 10 MW High Temperature Gas-Cooled Reactor Test Module," *Proceedings of the Seminar on HTGR Application and Development.* Beijing, China, March 19-21, 2001.

11. C. Tang et al., "Fabrication of the first loading fuel of 10 MW High Temperature Gas Cooled Reactor-Test Module (HTR-10)," *Proceedings of the Seminar on HTGR Application and Development,* Beijing, China, March 19-21, 2001.

12. X. Jing X., and Y. Yang, "Physical designs and calculations for the first full power operation of the 10 MW High Temperature Gas-Cooled Reactor – Test Module (HTR-10)," *Proceedings of the 2nd International Topical Meeting on High Temperature Reactor Technology (HTR-2004),* Beijing, China, September 22-24, 2004.

13. C. Tang, X. Fu, J. Zhu, K.N. Koshceev, A.V. Kozlov, O.G. Karlov, Y.G. Degaltsev, and V.I. Vasiliev., "The behavior of HTR-10 fuel under irradiation," *Proceedings of the 2nd International Topical Meeting on High Temperature Reactor Technology (HTR-2004),* Beijing, China, September 22-24, 2004.

14. Marmier, A., et al., 2008, "Preliminary results of the HFR-EU1 fuel irradiation of INET and AVR pebbles in the HFR Petten," *Proceedings of the 4th International Topical Meeting on High Temperature Reactor Technology (HTR-2008),* Washington, D.C., September 28-October 1, 2008.

15. C. Tang, X. Fu, J. Zhu, H. Zhao, and Y. Tang, "Comparison of two irradiation testing results of HTR-10 fuel spheres," *Nuclear Engineering and Design,* Vol. 251, pp. 453–458 (2012).

16. A.H. Booth. *A Method of Calculating Fission Gas Release from UO2 Fuel and Its Implication to the X-2-f Loop Test.* Atomic Energy of Canada Limited, Chalk River, Ontario, Canada: September 1957. Report AECL 496,

17. S. Knol, S. de Groot, R.V. Salama, J. Best, K. Bakker, I. Bobeldijk, J.R. Westlake, M.A. Fütterer, M. Laurie, C. Tang, R. Liu, B. Liu, and H. Zhao, "HTR-PM fuel pebble irradiation qualification in the high flux reactor in Petten," *Nuclear Engineering and Design,* Vol. 329, pp. 82–88 (2018).

18. S. Fujikawa, H. Hayashi, T. Nakazawa, K. Kawasaki, T. Iyoku, S. Nakagawa and N. Sakabas, "Achievement of reactor-outlet coolant temperature of 950°C in HTTR," *Journal of Nuclear Science and Technology,* Vol. 41, p. 1245 (2004).

19. K. Verfondern, J. Sumita, S. Ueta, and K. Sawa. *Modeling of Fuel Performance and Fission Product Release Behavior during HTTR Normal Operation (A Comparison of the FZJ and JAERI Modeling Approach)*. Japan Atomic Energy Research Institute, Tokai-Mura, Japan: March, 2001. JAERI-Research 2000-067.

20. K. Minato, K. Sawa, K. Fukuda, C.A. Baldwin, W.A. Gabbard, O.F. Kimball, C.M., et al., *HRB-22 Capsule Irradiation Test for HTGR Fuel (JAERI/USDOE Collaborative Irradiation Test*, Japan Atomic Energy Research Institute, Tokai-Mura, Japan: March 1998. JAERI-Research 98-021.

21. K. Minato, K. Sawa, T. Koya, T. Tomita, A. Ishikawa, C.A. Baldwin, W.A. Gabbard, C.M. Malone, F.C. Montgomery, B.F. Myers, and N.H. Packan, "Fission product release behavior of individual coated fuel particles for high-temperature gas-cooled reactors," *Nuclear Technology*, Vol. 131, p. 36 (2000).

22. K. Hayashi, K. Sawa, T. Kitajima, T. Shiratori, H. Kikuchi, K. Fukuda, T. Itoh, H. Waragai. *Irradiation Experiments of the 13th–15th OGL-1 Fuel Assemblies*, Japan Atomic Energy Research Institute, Tokai-Mura, Japan: January 2000. JAERI-Research 2000-001.

23. K. Sawa and T. Tobita, "Investigation of irradiation behavior of SiC-coated fuel particle at extended burnup," *Nuclear Technology*, 142, pp. 250–259 (2003).

24. S. Ueta, J. Aihara, K. Sawa, A. Yasuda, M. Honda, N. Furihata, "Development of high temperature gas-cooled reactor (HTGR) fuel in Japan," *Progress in Nuclear Energy,* Vol. 53, pp. 788–793 (2011).

25. S. Ueta, J. Aihara, A. Shaimerdenov, D. Dyussambayev, S. Gizatulin, P. Chakrov, and N. Sakaba, "Irradiation test and post irradiation examination of the high burnup HTGR fuel," Paper 18491, *Proceedings of the 8th International Topical Meeting on High Temperature Reactor Technology (HTR 2016)*, Las Vegas, Nevada, November 6–10, 2016.

26. H. Nickel, H. Nabielek, G. Pott, and A.W. Mehner, "Long time experience with the development of HTR fuel elements in Germany," *Nuclear Engineering and Design*, Vol. 217, pp. 141–151 (2002).

27. M.J. Kania, H. Nabielek, K. Verfondern, and H.-J. Allelein, "Testing of HTR UO_2 TRISO fuels in AVR and in material test reactors," *Journal of Nuclear Materials*, Vol. 441, pp. 545–562 (2013).

28. A.W. Mehner, W. Heit, K. Röllig, H. Ragoss, and H. Müller, "Spherical fuel elements for advanced HTR manufacture and qualification by irradiation testing," *Journal of Nuclear Materials*, Vol. 171, pp. 9–18 (1990).

29. M.J. Kania, H. Nabielek, and H. Nickel, "Coated particle fuels for high-temperature reactors," in *Materials Science and Technology*. Wiley-VCH Verlag GmbH & Co., 2015.

30. *NGNP Fuel Qualification White Paper*. Idaho National Laboratory, Idaho Falls, ID: July 2010. INL/EXT-10-18610.

31. W. Schenk, G. Pott, and H. Nabielek, "Fuel accident performance testing for small HTRs," *Journal of Nuclear Materials*, Vol. 171, pp. 19–30 (1990).

32. M.A. Futterer, G. Berg, A. Marmier, E. Toscano, D. Freis, K. Bakker, and S. de Groot, "Results of AVR fuel pebble irradiation at increased temperature and burn-up in the HFR Petten," *Nuclear Engineering and Design*, Vol. 238 2008, pp. 2877–2885.

33. M. Laurie, A. Marmier, G. Berg, J.-M. Lapetite, M.A. Fütterer, and C. Tang, "Results of the HFR-EU1 fuel irradiation of INET and AVR pebbles in the HFR Petten," *Nuclear Engineering and Design*, Vol. 251, pp. 117–123 (2012).

34. K. Verfondern, A. Xhonneuxa, H. Nabielek, and H.-J. Allelein, "Computational analysis of modern HTGR fuel performance and fission product release during the HFR-EU1 irradiation experiment," *Nuclear Engineering and Design,* Vol. 273, 2014, pp. 85–97.

35. M. Phélip, "European programme on HTR fuel technology," Paper B06, *Proceedings of the 2nd International Topical Meeting on High Temperature Reactor Technology (HTR 2004)*, Beijing, China, September 22-24, 2004.

36. M. Barrachin, R. Dubourg, S. de Groot, M.P. Kissane, and K. Bakker, "Fission-product behavior in irradiated TRISO-coated particles: Results of the HFR-EU1bis experiment and their interpretation," *Journal of Nuclear Material*, Vol. 415, pp. 104–116 (2011).

37. S. de Groot, K. Bakker, A.I. van Heek, and M.A. Futterer, "Modelling of the HFR-EU1BIS experiment and thermomechanical evaluation," *Nuclear Engineering and Design,* Vol. 238, pp. 3114–3120 (2008).

38. O. Seeger, M. Laurie, A. El Abjani, J. Ejton, D. Boudaud, D. Freis, P. Carbol, V.V. Rondinella, M. Fütterer, and H.-J. Allelein, "KüFA safety testing of HTR fuel pebbles irradiated in the High Flux Reactor in Petten," *Nuclear Engineering and Design*, Vol. 306, pp. 59–69 (2016).

39. D. Freis, P.D.W. Bottomley, A.I. Kellerbauer, V.V. Rondinella, and P. Van Uffelen, "Accident testing of high-temperature reactor fuel elements from the HFR-EU1bis irradiation," *Nuclear Engineering and Design*, Vol. 241, pp. 2813–2821 (2011).

40. O. Seeger, K. Knebel, W. de Weerd, P. Carbol, P.D.W. Bottomley, V.V. Rondinella, and H.-J. Allelein, "Simulated accident testing of a fuel element from the HFR-EU1bis irradiation campaign," *Nuclear Engineering and Design*, Vol. 271, pp. 171–179 (2014).

41. D.A. Petti, P.A. Demkowicz, J.T. Maki, and R.R. Hobbins, "TRISO-coated particle fuel performance," in R.J.M. Konings(ed.): *Comprehensive Nuclear Materials*. Elsevier, Amsterdam, Vol. 3, pp. 151-213 (2012).

C

INFORMATION FROM THE AGR-1 AND AGR-2 FUEL SPECIFICATIONS

C.1 TRISO Fuel Particle Properties

The following tables present the AGR-1 and AGR-2 fuel specifications for TRISO coating layer properties and particle aspect ratios. AGR-1 specifications were extracted from Table 5.2 of EDF-4380, "AGR-1 Fuel Product Specification and Characterization Guidance," Rev. 8 [1] and the AGR-2 specifications were extracted from Table 5 of SPC-923, "AGR-2 Fuel Specification, Rev.3 [2].

Table C-1
AGR-1 Layer Property and Aspect Ratio Specifications

Coated Particle Property	Mean [a]	Critical Region	Fraction in Critical Region
Buffer thickness (μm)	100 ± 15	≤ 55	≤ 0.01
IPyC thickness (μm)	40 ± 4	≤ 30	≤ 0.01
		≥ 56	≤ 0.01
SiC thickness (μm)	35 ± 3	≤ 25	≤ 0.01
OPyC thickness (μm)	40 ± 4	≤ 20	≤ 0.01
Buffer bulk density (g/cm^3)	1.03 ± 0.15	not specified	not specified
IPyC density (g/cm^3)	1.90 ± 0.05	≤ 1.80	≤ 0.01
		≥ 2.00	≤ 0.01
SiC density (g/cm^3)	≥ 3.19	≤ 3.17	≤ 0.01
OPyC density (g/cm^3)	1.90 ± 0.05	≤ 1.80	≤ 0.01
		≥ 2.00	≤ 0.01
IPyC anisotropy (BAF$_0$) [b]	≤ 1.035	≥ 1.06	≤ 0.01
OPyC anisotropy (BAF$_0$) [b]	≤ 1.035	≥ 1.06	≤ 0.01
Aspect Ratio (faceting) [c]	not specified	≥ 1.14	≤ 0.01

a. Specified composite mean values and fraction in critical regions determined at the 95% confidence level. The ± values represent an allowable range for the mean value and are not standard deviations of the mean.

b. BAF$_0$ is to be measured on loose TRISO particles before compacting.

c. Aspect ratio is defined as the ratio of maximum to minimum diameters of the OPyC layer.

Table C-2
AGR-2 Layer Property and Aspect Ratio Specifications

Coated Particle Property	Mean [a]	Critical Region	Fraction in Critical Region
Buffer thickness (μm)	100 ± 15	≤ 58	≤ 0.01
IPyC thickness (μm)	40 ± 4	≤ 30 ≥ 52	≤ 0.01 ≤ 0.01
SiC thickness (μm)	35 ± 3	≤ 23	≤ 0.01
OPyC thickness (μm)	40 ± 4	≤ 20	≤ 0.01
Buffer bulk density (g/cm^3)	1.05 ± 0.10	Not specified	Not specified
IPyC density (g/cm^3)	1.90 ± 0.05	≤ 1.80 ≥ 2.00	≤ 0.01 ≤ 0.01
SiC density (g/cm^3)	≥ 3.19	≤ 3.17	≤ 0.01
OPyC density (g/cm^3)	1.90 ± 0.05	≤ 1.80 ≥ 2.00	≤ 0.01 ≤ 0.01
IPyC anisotropy (BAF$_o$) [b]	≤ 1.045	≥ 1.06	≤ 0.01
OPyC anisotropy (BAF$_o$) [b]	≤ 1.035	≥ 1.06	≤ 0.01
Aspect Ratio (faceting) [c]	Not specified	≥ 1.14	≤ 0.01

a. Specified composite mean values and fraction in critical regions determined at the 95% confidence level. The $\pm$ values represent an allowable range for the mean value and are not standard deviations of the mean.

b. BAF$_o$ is to be measured on loose TRISO particles before compacting.

c. Aspect ratio is defined as the ratio of maximum to minimum diameters of the coated particle as measured for SiC-coated particles after removal of the OPyC layer.

C.2 References

1. C.M. Barnes. *AGR-1 Fuel Product Specification and Characterization Guidance*. Idaho National Laboratory, Idaho Falls, ID: April 21, 2006. EDF-4380, Rev. 8.

2. C.M. Barnes. *AGR-2 Fuel Specification*. Idaho National Laboratory, Idaho Falls, ID: January 9, 2009. SPPC-923, Rev. 3.

D
LICENSING CORRESPONDENCE

This appendix contains the licensing correspondence associated with the topical report, as listed below.

1. Requests for Additional Information (RAIs) 1 through 4 provided by e-mail dated January 2, 2020.

2. Responses to RAIs 1 through 4 provided by letter dated February 26, 2020.

3. RAI 5 provided initially by e-mail dated November 25, 2019.

4. Response to RAI 5 provided by letter dated March 9, 2020.

D.1 RAIs 1 through 4 Provided by E-mail Dated January 2, 2020

Good Morning,

By letter dated May 31, 2019, the Electric Power Research Institute (EPRI) submitted for U.S. Nuclear Regulatory Commission (NRC) staff review, "Uranium Oxycarbide (UCO) Tristructural Isotropic (TRISO) Coated Particle Fuel Performance, Topical Report EPRI-AR-1" (Agencywide Documents Access and Management System (ADAMS) Accession No. ML19155A173). The NRC staff is reviewing the submittal to enable the staff to reach a conclusion on the safety of the UCO TRISO particle fuel performance.

The NRC staff has identified that additional information is needed to continue the review. The staff's request for additional information (RAI) is contained in the attachment to this email.

These RAIs were discussed during a public meeting on December 9, 2019. To support the review schedule, you are requested to respond within 30 days of the date of this email.

If you have any questions or comments, please contact me at 301-415-5481.

Sincerely,
Jordan

Jordan Hoellman
Project Manager
Advanced Reactor Policy Branch (UARP)
Division of Advanced Reactors and Non-Power
  Production and Utilization Facilities (DANU)
Office of Nuclear Reactor Regulation (NRR)
U S Nuclear Regulatory Commission
office OWFN 02-C06
phone (301) 415-5481
email Jordan.Hoellman2@nrc.gov

Request for Additional Information (RAI)

Uranium Oxycarbide (UCO) Tristructural

Isotropic (TRISO) Coated Particle Fuel Performance Topical Report

Issue Date: January 2, 2020
Applicant: Electric Power Research Institute
Docket No: 99902021

By letter dated May 31, 2019, the Electric Power Research Institute (EPRI) submitted for U S Nuclear Regulatory Commission (NRC) staff review, "Uranium Oxycarbide (UCO) Tristructural Isotropic (TRISO) Coated Particle Fuel Performance, Topical Report EPRI-AR-1" (Agencywide Documents Access and Management System (ADAMS) Accession No. ML19155A173). This topical report provides a baseline set of data in order to establish a foundation for TRISO fuel performance, based on testing performed as part of the U.S. Department of Energy (DOE) Advanced Gas Reactor (AGR) Fuel Development and Qualification Program. During the course of the technical review, NRC staff has identified areas where additional information and detail are needed to make a safety finding.

This topical report does not have a specific regulatory requirement associated with it because how the TRISO fuel meets regulations will depend on the plant design and other systems, structures and components (SSCs) credited in the overall safety of the design. No matter the design, however, 10 CFR 50.34(a)(3)(i) requires in part that an applicant for a construction permit to build a power reactor provide principal design criteria (PDC) for the facility. Similar regulatory requirements exist for design certification, combined license, and standard design approvals (10 CFR 52.47(a)(3)(i), 10 CFR 52.79(a)(4)(i), and 10 CFR 52.137(a)(3)(i), respectively) The PDC establish requirements for SSCs, and based on historical practice, designs with TRISO fuel have used a safety strategy focused on the radionuclide retention capabilities of the TRISO particles.

General Design Criterion (GDC) 10, "Reactor design", requires that the reactor core and associated coolant, control, and protection systems shall be designed with appropriate margin to assure that specified acceptable fuel design limits are not exceeded during any condition of normal operation, including the effects of anticipated operational occurrences. Although GDC 10 applies only to light water reactor (LWR) designs, the staff expects non-LWR designs to have a similar GDC. Examples of substitute GDC can be found in Regulatory Guide (RG) 1.232 "Guidance for Developing Principal Design Criteria for Non-Light-Water Reactors", which provides guidance for developing PDC for non-LWR designs Establishing fuel design limits and ensuring these limits are not exceeded represent a fundamental underpinning of the safety assessment of a nuclear power plant required by 10 CFR 50.34(a)(1). This topical report forms the basis for establishing the design limits for TRISO fuel.

10 CFR 50.34(a)(1)(ii)(C) requires an applicant describe the extent to which the reactor incorporates unique, unusual or enhanced safety features having a significant bearing on the probability or consequences of accidental release of radioactive materials. TRISO fuel presents a unique safety case in a "functional containment" approach for reducing the release of

- 1 -

radioactive materials, and the mechanisms by which TRISO fuel restricts the release of radioactive materials are described in this topical report. Such an approach could also impact any PDC proposed for containment.

RAI 1

Conclusion 1 of the topical report (TR) states that "testing of UCO TRISO-coated fuel particles in AGR-1 and AGR-2 constitutes a performance demonstration of these particle designs over a range of normal operating and off-normal accident conditions." Discussions under the conclusion reference a compact-averaged burnup of 7.3-19.6% fissions per initial metal atom (FIMA) and time averaged maximum temperatures of 1069-1360°C. Are there other relevant performance parameters that bound the data set, such as those referenced in Figure 4-6 (packing fraction, fluence, power density)? Based on the discussion in the report, it appears some of these parameters could influence particle performance, but these values are not provided as bounds for the "range of normal operating and off-normal accident conditions". Provide context for what constitutes a "range of normal operating and off-normal accident conditions" (e.g. reference a table), or provide a justification for why burnup and time averaged temperature are sufficient.

RAI 2

Conclusion 2 of the TR states "UCO TRISO-coated fuel particles that satisfy the parameter envelope defined by these measured particle layer properties in Table 5-5 can be relied on to provide satisfactory performance." While Table 5-5 provides a list of physical parameters for fuel specifications, it does not appear to directly cover all of the parameters that govern the specifications that constitute the parameter envelope applicable to the tested AGR fuel. Some elements in particular that the report highlights as important but that are not directly referred to in Table 5-5 include kernel-to-buffer ratio for the fuel particle (and potentially its associated size), columnar grain structure of the SiC, and carbon content of the UCO. It is not clear to the staff how these limits are applicable to the conclusions in the report. Provide a justification for how these parameters are implicitly captured in Table 5-5, supplement the report to include these parameters as limits for TR applicability, or provide justification for why these elements are not important.

Further, the report references the importance of an uninterrupted coating process in the manufacturing of the fuel. Do the parameters in Table 5-5 adequately restrict fuel particle specifications such that this process does not need to be explicitly required? If not, provide a justification, consider restricting the applicability of the TR to fuel manufactured using a similar process, or add a proxy measurable parameter to Table 5-5 that does provide assurance that an uninterrupted coating process has been followed.

RAI 3

The TR states that "fuel particles tested in AGR-1 and AGR-2 exhibited property variations...with remarkably similar excellent irradiation and accident safety performance

- 2 -

results. The ranges of those variations in key characteristics of the kernels and coatings are reflected in measured particle layer properties provided in Table 5-5 from AGR-1 and AGR-2." Table 5-5 provides a set of characteristics for both tested fuel and specified ranges for "acceptable" fuel, both for mean values and extremes. In some cases, the specification range is larger than the tested fuel range, sometimes substantially. Based on the provided data, there is a clear basis for use of the measured values in Table 5-5, but the basis for the specified range and especially the Maximum Allowable Fraction Beyond the Critical Limit(s) is not clear. Additionally, the table references the AGR-1 and -2 dataset separately in some cases. Provide a table with a clear requested range for each property for approval to be referenced in the conclusions. Further, provide a basis for useage of the values in this table for ranges beyond the tested ranges, paying particular attention to Maximum Allowable Fraction Beyond the Critical Limit(s), where the allowed particles may be substantially "worse" than those tested.

RAI 4

TR conclusion 3 states "fission product release data and fuel failure fractions, as summarized in this report, can be used for licensing of reactors employing UCO TRISO-coated fuel particles that satisfy the parameter envelope defined by measured particle layer properties in Table 5-5." The phrases "as summarized in this report" and "can be used for licensing of reactors" lack specificity, though the subsequent discussion is relatively clear.

(a) Consider revising to more specifically reference the data presented, and narrow the scope of the request "can be used for licensing of reactors" to something more appropriate for the TR.

(b) Conclusion number 3 further states that the aggregate AGR-1 and AGR-2 fission product release data and fuel failure fractions can be used for licensing of reactors employing UCO TRISO-coated fuel particles that satisfy the parameter envelope detailed in the topical report. The staff notes that while the topical report supports fission gas release rates for most isotopes, it does not cover short-lived isotopes which decayed away before the particles discussed in EPRI-AR-1(NP) could be characterized. Therefore, the data set does not cover all of the fission gas release data necessary for licensing. Provide justification to support the statements in conclusion number 3 or limit the conclusion to the isotopes covered by the topical report

- 3 -

EPRI | ELECTRIC POWER RESEARCH INSTITUTE   Responses to RAIs for Topical Report EPRI-AR-1(NP)

2020-001_____EPRI Advanced Reactor Strategic Program (EPRI-AR)

February 26, 2020

Document Control Desk
U. S. Nuclear Regulatory Commission
11555 Rockville Pike
Rockville, MD 20852

Docket No. 99902021

Attention: Jordan Hoellman, NRO/DAR/ARPB

Subject: Responses to Requests for Additional Information (RAIs) on Topical Report EPRI-AR-1(NP), "Uranium Oxycarbide (UCO) Tristructural Isotropic (TRISO) Coated Particle Fuel Performance"

Please find enclosed the Electric Power Research Institute (EPRI) responses to U. S. Nuclear Regulatory Commission (NRC) requests for additional information (RAIs) related to its review of Topical Report EPRI-AR-1(NP). EPRI submitted Topical Report EPRI-AR-1(NP) "Uranium Oxycarbide (UCO) Tristructural Isotropic (TRISO) Coated Particle Fuel Performance" to the NRC for review on May 31, 2019. The NRC notified EPRI that it had accepted the topical report for review, by letter dated August 5, 2019. On October 8 and 9, 2019 the NRC conducted a regulatory audit of the topical report at the Idaho National Laboratory (INL) Offices and documented the results of the audit in an audit report dated November 19, 2019. EPRI, INL and the NRC met on December 9, 2019 for technical discussions related to the topical report, and the NRC provided formal RAIs on January 2, 2020 (ML20009E065).

For each RAI on Topical Report EPRI-AR-1 (NP), Enclosure 1 provides the official response and a summary of planned changes to the topical report pursuant to that response. Enclosure 2 provides all planned changes to the topical report, in detail and in an integrated fashion.

If you have questions about this submittal, please contact EPRI project manager Cristian Marciulescu by phone at 704-595-2401, or by email at cmarciulescu@epri.com.

Sincerely,

Helen Cothron

Helen Cothron
EPRI Advanced Nuclear Technology Program Manager

Together . . Shaping the Future of Electricity

EPRI-AR-2020-001   Responses to RAIs for Topical Report EPRI-AR-1(NP)
2020-001_____EPRI Advanced Reactor Strategic Program (EPRI-AR)

February 26, 2020
Page 2

Enclosure:
1) Responses to EPRI-AR-1(NP) RAIs Dated January 2, 2020
2) Planned Changes to EPRI-AR-1(NP) Resulting from RAIs Dated January 2, 2020

c: A. Cubbage, NRO/DAR/ARPB
    J. Monninger, NRO/DAR
    John Segala, NRO/DAR/ARPB
    A. Sowder, EPRI
    C. Marciulescu, EPRI
    S. Nesbit, LMNT Consulting
    P. Demkowicz, INL
    J. Kinsey, INL

Enclosure 1

**Responses to EPRI-AR-1(NP) Requests for Additional
Information (RAIs) Dated January 2, 2020**

Each RAI is discussed separately below. Each RAI is repeated, followed by a response. Planned changes resulting from the RAIs are summarized at the end of the response and are provided in detail in Enclosure 2.

RAI 1

Conclusion 1 of the topical report (TR) states that "testing of UCO TRISO-coated fuel particles in AGR-1 and AGR-2 constitutes a performance demonstration of these particle designs over a range of normal operating and off-normal accident conditions." Discussions under the conclusion reference a compact-averaged burnup of 7.3-19.6% fissions per initial metal atom (FIMA) and time averaged maximum temperatures of 1069-1360°C. Are there other relevant performance parameters that bound the data set, such as those referenced in Figure 4-6 (packing fraction, fluence, power density)? Based on the discussion in the report, it appears some of these parameters could influence particle performance, but these values are not provided as bounds for the "range of normal operating and off-normal accident conditions". Provide context for what constitutes a "range of normal operating and off-normal accident conditions" (e.g. reference a table), or provide a justification for why burnup and time averaged temperature are sufficient.

Response

There are additional relevant performance parameters associated with the data. The key parameters for tristructural isotropic (TRISO) fuel performance are burnup, temperature, fast neutron fluence, and power. The ranges of values have been summarized in Table 1 and Figure 1 below. Additional details on these parameters for the two irradiation experiments were provided in Section 6 of the report, including time-dependent variation throughout the irradiation.

The ranges provided here are based on volume averaged values for individual compacts, with the exception of time averaged temperature and particle power. Temperature and power are time averaged over the course of the irradiation. Burnup and fast fluence ranges are based on end-of-life values. Two different sets of parameter ranges have been provided: one data set for all Advanced Gas Reactor (AGR)-1 capsules and AGR-2 Capsules 5 and 6, and a separate data set for AGR-2 Capsule 2. This approach has been taken because the AGR-2 Capsule 5 and 6 values predominantly fall within the range for the AGR-1 capsules; the exception is the slightly lower minimum burnup for AGR-2 (7.3% FIMA) compared to AGR-1 (11.1% FIMA). AGR-2 Capsule 2

was Irradiated at a significantly higher peak temperature relative to the other capsules, so this population of fuel compacts is considered separately.

Power is provided in two different units in the table. The first represents power density over the entire compact (W/cm^3) and the second is the power per particle (mW/particle). The AGR-1 and AGR-2 particles had kernels with different diameters (350 μm and 427 μm, respectively) so the power per particle values are given for each of these experiments separately in columns 2 and 3 (see footnotes a and b).

Table 1. Range of values for key irradiation parameters for AGR-1 and AGR-2 fuel.

Property	AGR-1 + AGR2 Capsules 5 and 6		AGR-2 Capsule 2	
	Max	Min	Max	Min
Burnup (% FIMA)	19.6	7.3	13.2	10.8
Fast fluence (n/m^2 x 10^{-25}; E > 0.18 MeV)	4.30	1.94	3.47	2.88
Time-average temperature (°C)	1210	800	1360	1034
Time-avg compact power density (W/cm^3)	90	50	92	74
Time-avg particle power (mW/particle)	66[a]/86[b]	37[a]/48[b]	88	71

   a. *AGR-1 values*
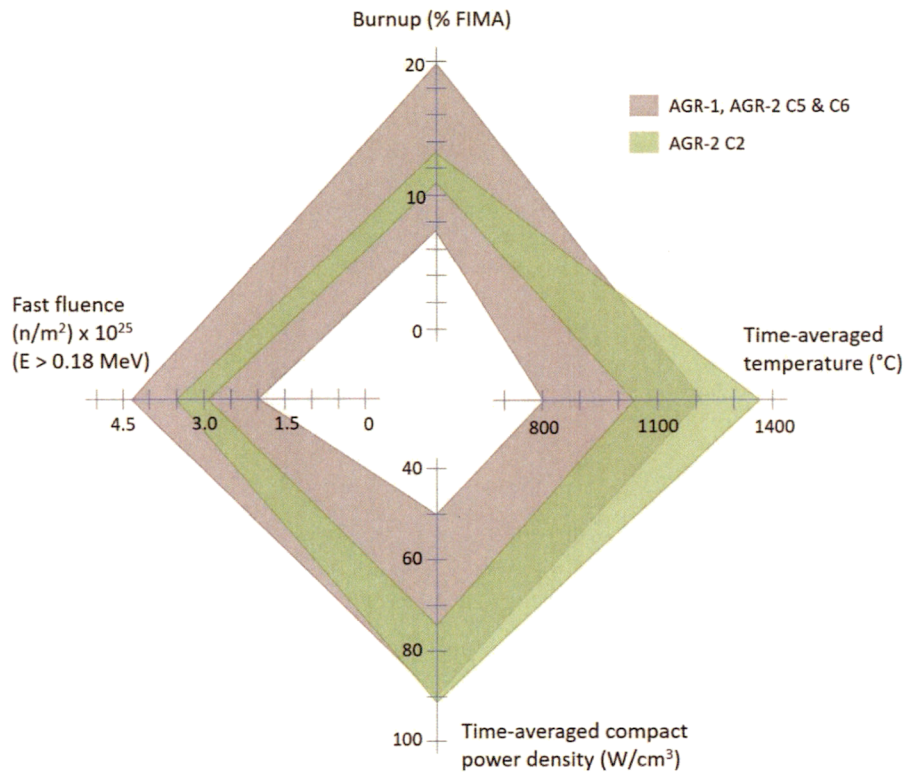   b. *AGR-2 Capsules 5 and 6 values*

D-12

Figure 1. Radar plot of the ranges for key irradiation parameters for AGR-1 and AGR-2 fuel.

The safety test data presented in the report are for heating in dry helium at temperatures of 1600-1800°C for durations as long as 400 hours. These data generally bound the ranges of conditions typical of past modular high temperature gas reactor designs. Future license applicants will need to justify the applicability of the data to their specific designs.

Planned Changes to EPRI-AR-1(NP):

Material from the above response, including Table 1 and Figure 1, will be added to Section 6.6 (Broader Comparisons of Key Service Conditions). In addition, the supporting discussion under Conclusion 1 in Section 8 (Summary/Conclusions) will be modified.

RAI 2

Conclusion 2 of the TR states "UCO TRISO-coated fuel particles that satisfy the parameter envelope defined by these measured particle layer properties in Table 5-5 can be relied on to provide satisfactory performance." While Table 5-5 provides a list of physical parameters for fuel specifications, it does not appear to directly cover all of the parameters that govern the specifications that constitute the parameter envelope applicable to the tested AGR fuel. Some elements in particular that the report highlights as important but that are not directly referred to in Table 5-5 include kernel-to-buffer ratio for the fuel particle (and potentially its associated size), columnar grain structure of the SiC, and carbon content of the UCO. It is not clear to the staff how these limits are applicable to the conclusions in the report. Provide a justification for how these parameters are implicitly captured in Table 5-5, supplement the report to include these parameters as limits for TR applicability, or provide justification for why these elements are not important.

Further, the report references the importance of an uninterrupted coating process in the manufacturing of the fuel. Do the parameters in Table 5-5 adequately restrict fuel particle specifications such that this process does not need to be explicitly required? If not, provide a justification, consider restricting the applicability of the TR to fuel manufactured using a similar process, or add a proxy measurable parameter to Table 5-5 that does provide assurance that an uninterrupted coating process has been followed.

Response

A response is provided for each of the following topics:

1. Kernel-to-buffer volume ratio
2. SiC microstructure
3. UCO kernel stoichiometry
4. Uninterrupted coating process

1. Kernel-to-buffer volume ratio

Section 4.2.6 of the topical report discusses certain aspects of particle design. The stress in the SiC layer is stated to be proportional to the volume of kernel (V_k) and buffer (V_b), the inner radius (r_{SiC}) and thickness (t_{SiC}) of the SiC layer, and the intended peak burnup (B). Equation 4-1 is provided as follows:

$$\sigma \propto \frac{B \cdot V_k}{V_b} \cdot \frac{r_{SiC}}{t_{SiC}}$$

This is a more useful metric of stress in the SiC layer than the simple kernel/buffer volume ratio, because burnup and other particle geometry parameters are also important factors. Values for

this tensile stress metric for various TRISO particle designs are provided in Table 4-2 in the report based on nominal particle dimensions, showing that historic particle design has sought to maintain a value similar to that of the German reference UO_2 TRISO particle.

Using the as-fabricated fuel characterization data, bounding values for the stress metric σ in Eq. 4-1 were calculated to demonstrate the particle-to-particle variability in the AGR-1 and AGR-2 fuels. The distribution of σ for particles with the greatest burnup achieved by each particle type was calculated using Monte Carlo simulation, based on sample means and standard deviations of kernel diameter and layer thicknesses of each particle type. In simulation, the distribution of the quantity of interest is estimated by generating normal random deviates for each of the uncertain terms involved in its calculation and calculating the resultant stress metric for each set of those values. Using Monte Carlo simulation to calculate the distribution of the stress metric avoids many of the difficulties involved in its mathematical calculation, such as determination of the expected values of cubed random variables and the effect of non-zero covariance between the volume of the kernel, volume of the buffer and radius of the SiC shell. Even where the shell thicknesses are independent, terms involving products or ratios of their sums are not independent, and those covariances are naturally incorporated in the Monte Carlo approach.

In the stress metric, the four fundamental geometric terms are the kernel radius, buffer thickness, IPyC thickness, and SiC thickness. Each of these quantities is assumed to have a normal distribution with mean and standard deviation estimated from sampling data (Table 2). The outer boundary of the buffer shell is calculated from a radius that is the sum of the kernel radius and buffer thickness, with the kernel volume subtracted from that volume. Likewise, the radius of the inner boundary of the SiC shell (r_{SiC}) is the sum of the kernel radius, buffer thickness and IPyC thickness. The greatest burnup associated with each fuel type was taken as a known constant.

Random deviates were generated independently for each of the four measures. One million random variates for each layer measure, for each fuel variant, were created and the necessary radii for volume calculations determined from the sums of the appropriate resulting radius/thickness values. Histograms of the simulated stress metric demonstrate right skewness in the distributions, with heavier tails on the higher end, and Chi-square goodness of fit tests reject at 5% significance that the data reflect a normal distribution. The 1st, 50th, and 99th percentiles of the simulated stress metric distribution, for compacts with highest burnup for each fuel type, are provided in Table 3. Realizations of the calculated stress metric display different means and dispersion in histograms (Figure 2) for each fuel type. Vertical lines on the histogram represent the means of the distributions.

Table 2. Means and standard deviations (SDs) for particle properties of fuel types considered in the Monte Carlo simulation of the stress metric, σ. Burnup and number of particles represented the compact of each fuel type with highest measured burnup. Particles numbers are the expected number of particles in each compact.

Fuel Type	Kernel radius (μm)		Buffer thickness (μm)		IPyC thickness (μm)		SiC thickness (μm)		Burnup (%FIMA)	Particle number
	Mean	SD	Mean	SD	Mean	SD	Mean	SD		
AGR-1 Baseline	174.9	4.5	103.5	8.2	39.4	2.3	35.3	1.3	19.56	4154
AGR-1 Variant 1	174.9	4.5	102.5	7.1	40.5	2.4	35.7	1.2	18.22	4145
AGR-1 Variant 2	174.9	4.5	102.9	7.3	40.1	2.8	35.0	1.0	19.12	4095
AGR-1 Variant 3	174.9	4.5	104.2	7.8	38.8	2.1	35.9	2.1	19.43	4132
AGR-2	213.4	4.4	98.9	8.4	40.4	2.5	35.2	1.2	13.15	3176

AGR-1 source documents:
a. ORNL/TM-2006/019 Data Compilation for AGR-1 Baseline Coated Particle Composite LEU01-46T, Revision 1, April 2006
b. ORNL/TM-2006/020 Data Compilation for AGR-1 Variant 1 Coated Particle Composite LEU01-47T, Revision 1, April 2006
c. ORNL/TM-2006/021 Data Compilation for AGR-1 Variant 2 Coated Particle Composite LEU01-48T, Revision 1, May 2006
d. ORNL/TM-2006/022 Data Compilation for AGR-1 Variant 3 Coated Particle Composite LEU01-49T, Revision 0, May 2009
e. AGR-1 Irradiation Test Final As-run Report, INL/EXT-10-19097 Revision 3, January 2015.
AGR-2 source documents:
f. B&W Nuclear Operations Group, G73I, Industrial Fuel Fabrication and Development, Lot G73I-14-69307, Book 1
g. B&W Nuclear Operations Group, G73J, Industrial Fuel Fabrication and Development, Lots: G73J-14-93071A, G73J-14-93073A, G73J-14-93074A
h. JMOCUP As-Run Daily Depletion Calculation for the AGR-2 Experiment in ATR B-12 Position, ECAR-2066 Revision 2, Project No 23841, effective 04/25/2014.

Table 3. Mean and percentiles of the stress metric calculated from the Monte Carlo simulation. Minimum, median and max are the 1%, 50%, 99% percentile values of the generated stress metric values.

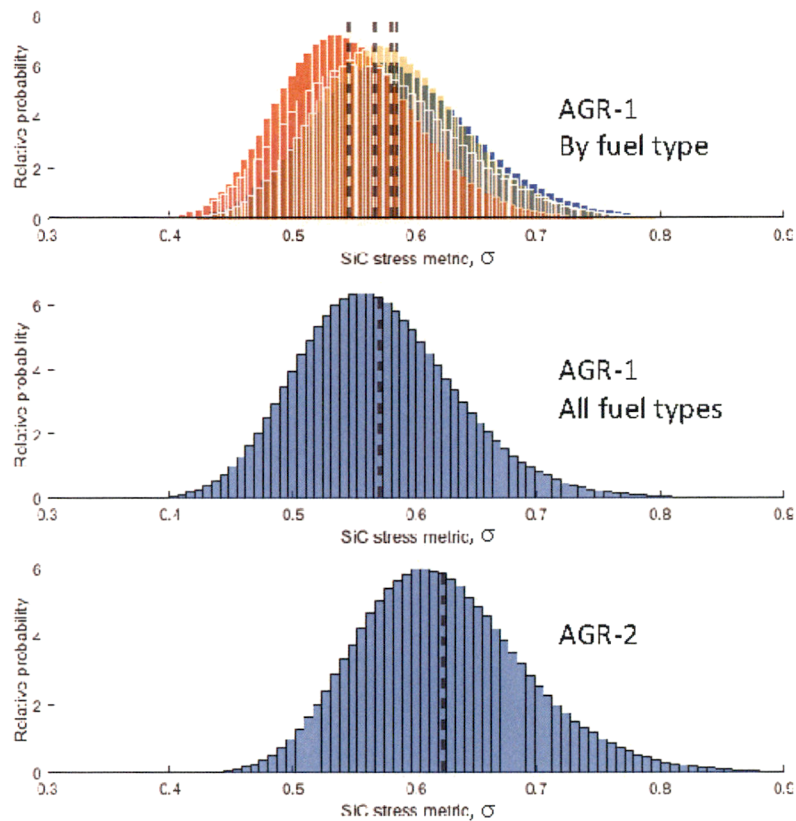| Test	SiC Stress Metric, σ			
	Mean	Distribution quantiles		
		1%	50%	99%
AGR-1	0.570	0.440	0.566	0.742
AGR-2	0.623	0.485	0.618	0.810

Figure 2. Histograms of output from the Monte Carlo simulation illustrating estimated distribution of the stress metric for the compacts with highest burnup, for each fuel type in AGR-1, for all AGR-1 fuel types combined, and for AGR-2. Vertical lines show mean values calculated from the Monte Carlo results. Histograms represent 1 million random deviates for each of the four radius/thickness values of the inner four spheres of the particles, for each fuel type.

The data in Table 3 and Figure 2 demonstrate that (a) there is a significant range in values for the stress metric based on statistical variations in particle geometry, and (b) the peak values (99th percentile) based on this analysis are within the range of values (0.643-0.816) listed in Table 4-2 of the Electric Power Research Institute (EPRI) topical report and representing values for previous and current fuel designs.

Planned changes to EPRI-AR-1(NP):

Material from the above response, including Table 3, will be added to the end of Section 5.3.6 (Key Property Ranges Observed in AGR-1 and AGR-2 TRISO Coated Particles).

2. SiC microstructure

The AGR-1 and AGR-2 fuel specifications did not include quantitative limits on SiC microstructure (e.g., SiC grain size). Instead, a visual standard was included that exhibited a grain size considered to be excessively large. The visual standard comprises the two micrographs in Figure 3 below, with further guidance that the "specification will be met if the average SiC grain size of 3 coated particles is judged to be smaller than the average grain size shown in the visual standards." Thus the AGR program considered the example micrographs to represent an approximate upper bound on the acceptable grain size, with no specified lower bound. By comparison, examples of the actual AGR-1 microstructures are shown in Figure 4, including the AGR-1 Baseline and AGR-1 Variant 3 fuel types, which bound grain size for the AGR-1 and AGR-2 fuels. This range in microstructures was explored intentionally during the AGR-1 campaign to examine and understand any performance differences. Additional quantitative data on AGR-1 and AGR-2 SiC grain size were provided in Table 5-3 of the topical report, and discussed in Reference 58 [Gerczak et al. 2016]
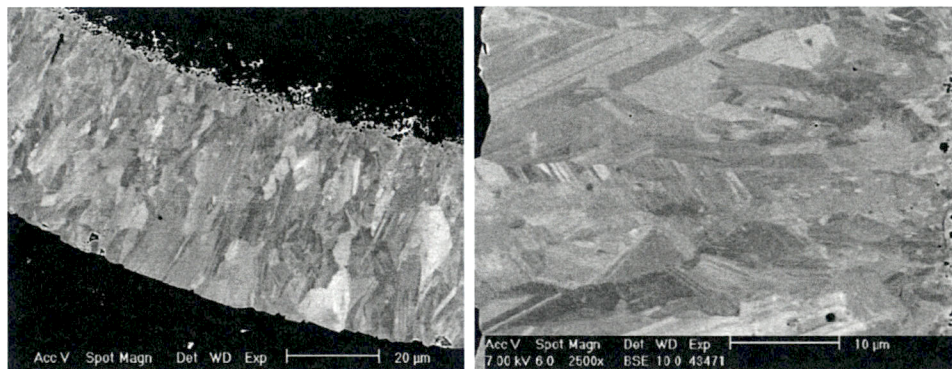

Figure 3. Visual standard for SiC microstructure used in the AGR-1 and AGR-2 fuel specifications.
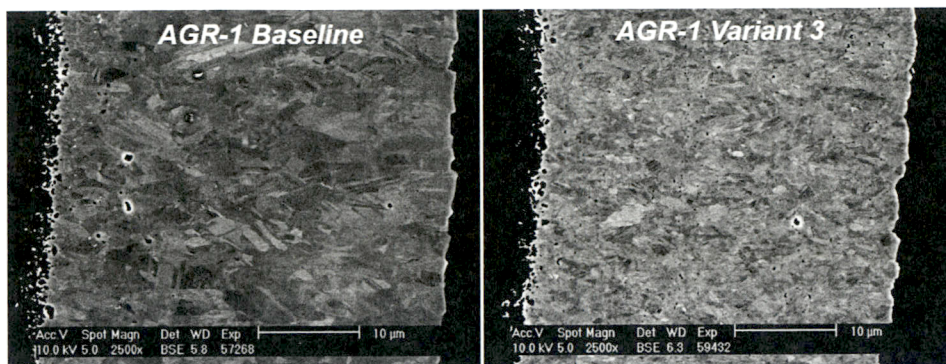
Figure 4. Micrographs of AGR-1 Baseline and Variant 3 SiC, showing microstructure.

Notwithstanding differences in SiC grain size, no major differences in fuel performance among the AGR-1 and AGR-2 SiC fuel types were observed in the data. This means primarily that there were no differences in fission product release in-pile or during heating tests at 1600-1700°C, nor any differences in TRISO or SiC failure fractions. The only observed difference was an increase in fission product release from particles with fine-grained SiC at a temperature of 1800°C for durations longer than 100 hours. This negligible difference in performance indicates that none of the AGR SiC types were approaching a limiting value in terms of grain size.

Planned Changes to EPRI-AR-1(NP):

Material from the above response, including Figure 3, will be added to a new Section 5.3.2.4 (SiC Microstructure). Additional material from above will be added to a new Section 7.5 (Effect of SiC Microstructure).

3. UCO kernel stoichiometry

The AGR-1 fuel specification included a specification for the mean C:U ratio as well as critical limits, as shown in Table 4. The kernel chemistry was measured in aggregate (i.e., on a batch of kernels). Reliable determination of the variation in stoichiometry among individual kernels was infeasible. A supporting study of individual AGR-1 kernels using optical microscopy to evaluate the volume fractions of oxide and carbide phases was performed, indicating that the C:U ratio could range from approximately 0.15 to 0.46 [Ebner 2005]. The data suggests that the critical limits for AGR-1 were not met, but the data analysis method was deemed insufficiently reliable to assess conformance with the specification. Nonetheless, it provided semi-quantitative data indicating that individual kernel stoichiometry could vary considerably from the mean but still result in acceptable performance during irradiation.

Subsequently, the AGR-2 specification included only a mean with tighter tolerance compared to AGR-1, and no critical limits. The measured values for both experiments are provided in Table 4, along with the corresponding percent of carbide phase. Note that calculation of the percent of carbide phase from C:U ratio also requires O:U ratio and assumes that the dioxide (UO_2) is the only oxide phase present.

Table 4. UCO kernel chemistry specifications and measured C:U ratio.

Fuel	Mean C:U (spec)	Critical Limits (spec)	Measured C:U (% UC_x)
AGR-1	0.5 ±0.2	≤1% below 0.2 ≤1% above 0.8	0.325 (~32% UC_x)
AGR-2	0.4 ±0.1	None	0.392 (~29% UC_x)

Thermochemical calculations have been performed previously on the relative stability of the uranium oxide and carbide phases in UCO fuel, as well as the stability of fission product oxides and carbides. Homan et al. (1977) presented the graphic shown in Figure 5, which indicates the range of burnup over which the various phases are stable given a specific starting UO_2/UC_2 content in the kernels at 1800 K. The results indicate that at UC_2 content as low as 10% the UC_2 phase will still persist and limit the formation of CO gas up to ~18% FIMA. Beyond this burnup, the oxide/carbide equilibrium for strontium establishes the oxygen potential, and thereafter the equilibrium in the zirconium system. On the other hand, at UC_2 content as high as 80%, the rare earth fission products are still retained in the kernel as oxides. This demonstrates the wide range of UO_2/UC_2 ratios that maintain effectiveness at (a) limiting CO gas formation and (b) promoting the formation of rare earth oxides over the formation of rare earth carbides in order to increase retention of rare earths in the kernel. Subsequent thermochemical studies have suggested that UC_x content as low as 5.5% (C:U ≈0.1) is sufficient for acceptable performance of low enriched uranium UCO TRISO fuel up to 16% FIMA [McMurray et al. 2017].
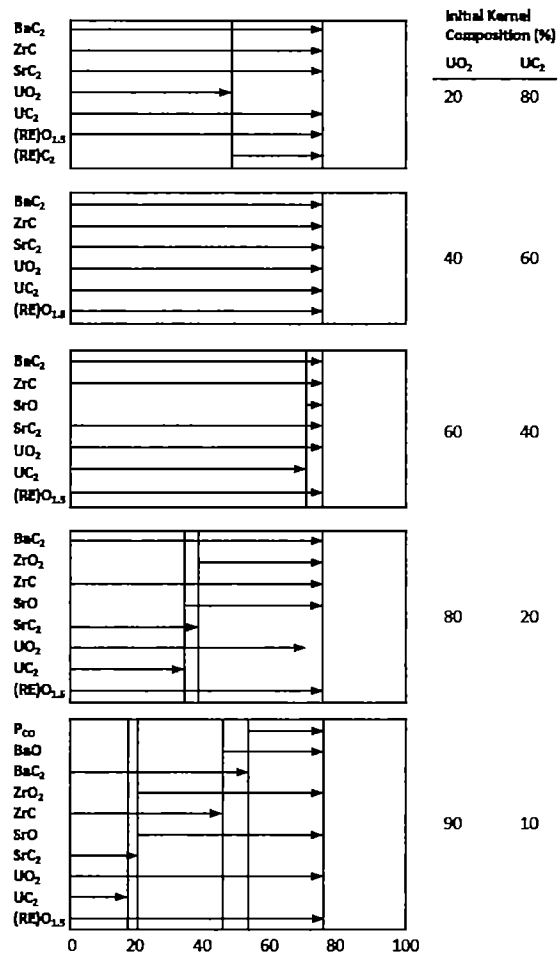
Figure 5. Phases present in UCO kernels as a function of starting UC₂ content and burnup [reproduced from Homan et al. 1977].

Based on the preceding discussion, it can be concluded that the AGR-1 and AGR-2 UCO kernel chemistry—with ~30% UC_x—is well within the envelope needed to suppress CO gas formation and promote rare earth oxides. Furthermore, the AGR-1 kernel chemistry study indicated a significant range in C:U values among individual kernels, with no detrimental effect on fuel performance apparent in the irradiation or post irradiation examination (PIE) results.

Planned Changes to EPRI-AR-1(NP):

Material from the above response, including Figure 5, will be incorporated in the current fourth paragraph of Section 5.3.6 (Key Property Ranges Observed in AGR-1 and AGR-2 TRISO Coated Particles).

4. Uninterrupted coating

Because uninterrupted coating is the de facto standard in modern TRISO fabrication, it is considered a process requirement when applying the results of this topical report.

Planned Changes to EPRI-AR-1(NP):

In Section 8 (Summary/Conclusions), the second paragraph of the supporting discussion under Conclusion 2 will be modified.

References

Homan, F. J., et al., "Stoichiometric Effects on Performance of High-Temperature Gas-Cooled Reactor Fuels from the U-C-O System," Nucl. Tech., 35 (1977), 428-441.

McMurray, J.W., et al., "Determining the Minimum Required Uranium Carbide Content for HTGR UCO Fuel Kernels," Ann. Nucl. Energy, 104 (2017), 237-242.

Ebner, M. A., "Composition Distribution of Fuel Kernels in LEU Composite 69302," Idaho National Laboratory, EDF-5723, April 2005.

<u>RAI 3</u>

The TR states that "fuel particles tested in AGR-1 and AGR-2 exhibited property variations...with remarkably similar excellent irradiation and accident safety performance results. The ranges of those variations in key characteristics of the kernels and coatings are reflected in measured particle layer properties provided in Table 5-5 from AGR-1 and AGR-2." Table 5-5 provides a set of characteristics for both tested fuel and specified ranges for "acceptable" fuel, both for mean values and extremes. In some cases, the specification range is larger than the tested fuel range, sometimes substantially. Based on the provided data, there is a clear basis for use of the measured values in Table 5-5, but the basis for the specified range and especially the Maximum Allowable Fraction Beyond the Critical Limit(s) is not clear. Additionally, the table references the AGR-1 and -2 dataset separately in some cases. Provide a table with a clear requested range for each property for approval to be referenced in the conclusions. Further, provide a basis for useage of the values in this table for ranges beyond the tested ranges, paying particular attention to Maximum Allowable Fraction Beyond the Critical Limit(s), where the allowed particles may be substantially "worse" than those tested.

<u>Response</u>

After extensive evaluation, Idaho National Laboratory (INL) and Electric Power Research Institute staff are providing Table 5 below (which will replace Table 5-5 in the topical report) in response to the request to "provide a table with a clear requested range for each property for approval to be referenced in the conclusions". The data in Table 5 provide the extrema of the 95% confidence limits on the means and the extrema of the 95%/98% tolerance limits on the distributions for the five separate fuel populations irradiated in the AGR-1 and AGR-2 experiments. Details on the definition of the ranges in Table 5, the derivation of the revised values, and the recommended use of the information are provided below.

Two ranges are given for each property in Table 5, one drawn from confidence intervals on the means and one drawn from tolerance intervals for the individual populations. Confidence intervals quantify the sampling variability in sample means. Tolerance intervals describe ranges within which a stated fraction of the population lies. The process of creating these intervals is limited in accuracy by the stated confidence level. Both of these intervals were calculated assuming normality in the batch or composited lot populations. The experiments included five TRISO fuel types: AGR-1 Baseline, its three variants, and AGR-2 UCO particles. Because the UCO TRISO fuel types sometimes had a strong influence on particle properties (for example, AGR-1 Variant 1 fabrication involved a deliberate change in coating conditions that would result in lower IPyC density), and fuel types were not randomly selected from a fixed set of possibilities, the ranges given in Table 5 are not commonly used statistical intervals representing the entire population of fabricated particles. They are instead drawn from collections of such intervals

calculated for each fuel batch or composited lot individually, based on assumptions of randomness and normality within those subgroups.

These values are not intended to define a comprehensive envelope of TRISO fuel that is expected to have acceptable performance, and they are not intended to replace the fuel specification values that will be moved from the current Table 5-5 to the new Appendix C. The data in Table 5 characterize the range of properties for particles that performed well during the AGR-1 and AGR-2 irradiations, but do not define the only ranges or combination of property ranges that would perform well under these irradiation conditions or under service conditions that may be proposed by fuel fabricators and reactor designers. The values are provided to facilitate comparison of other TRISO fuel populations to the fuel tested in the AGR-1 and AGR-2 irradiations. Comparative analysis of another population possessing particle properties that deviate from those in Table 5 will vary in complexity based on the specific properties in question (not all particle properties impact fuel performance in the same manner), the magnitude of the deviations (including which end of the distribution exceeds the limits in Table 5), and the intended irradiation conditions. More detailed data describing AGR-1 and AGR-2 particles are available for comparisons between AGR fuel and other TRISO fuel populations (see the references listed in Table 5-3 of the topical report).

Table 5. Coating layer property ranges for irradiated AGR-1 and AGR-2 UCO particles.

Particle Property	95% Confidence Interval Extrema	95%/98% Tolerance Limit Extrema
Buffer thickness (μm)	96.5 – 105.0	75.2 – 124.7
IPyC thickness (μm)	38.6 – 41.1	32.4 – 47.6
SIC thickness (μm)	34.8 – 36.2	30.6 – 41.2
OPyC thickness (μm)	39.1 – 44.3	33.6 – 51.6
Buffer density (g/cm^3)	1.04 – 1.11[a,b]	NA
IPyC density (g/cm^3)	1.84 - 1.92[b]	1.808 – 1.958[b]
SIC density (g/cm^3)	3.196 – 3.209	3.191 – 3.217
OPyC density (g/cm^3)	1.878 – 1.923	1.850 – 1.949
IPyC anisotropy (BAF$_{True}$)[c]	1.024[d]	1.036[d]
OPyC anisotropy (BAF$_{True}$)[c]	1.018[d]	1.030[d]
Aspect Ratio	1.057[d,e] 1.039[d,f]	1.102[d,e] 1.068[d,f]

a. Range of measured means only. No confidence intervals available.
b. Indirectly measured by analysis of interrupted batches (AGR-1) or comparable batches (AGR-2 buffer density).
c. BAF$_{True}$ = (1+N)/(1-N), where N is the optical diattenuation.
d. Upper bound of 95% confidence interval or 95% confidence - 99% coverage tolerance interval, as appropriate.
e. AGR-1, OPyC layer
f. AGR-2, SiC layer

It should be noted that the ranges given in Table 5 are narrower than the ranges specified in the AGR-1 and AGR-2 fuel specifications (means and 1% critical limits). TRISO particle performance is primarily defined by the probability of in-service coating layer failure. This behavior varies with key fuel properties, and the impact on coating layer fracture differs in magnitude for each property. Within a certain range of values, the impact on fuel performance will be negligible. The AGR fuel specification ranges were determined based on past performance demonstrations and on thermomechanical modeling of fuel performance to determine ideal property values as well as to identify the extremes of property distributions where fuel performance would be expected to begin to degrade appreciably. The AGR fuel specification 1% critical limits are established to be within this range; appreciable increases in fuel failure would only be expected outside of these bounds. Beyond these bounds, the particle failure probability increases, with performance generally becoming worse as the property value gets further from the mean. Thus, a particle in a fuel population could reside outside of the Table 5 ranges, but still be within the AGR specification and be expected to perform well under

the AGR irradiation conditions, based on the amassed knowledge of TRISO fuel performance over the last several decades.

These considerations are all important when comparing a fuel population to the AGR-1 and AGR-2 fuels. As a simple guide, the tolerance limit extrema in Table 5 are considered of greater importance than the mean confidence limits, because the tolerance limits serve to define the fraction of particles with the most extreme property values. The mean value for a fuel population may be outside of the range in Table 5 while the 95%/98% tolerance limits still reside inside of the corresponding limits in Table 5. This would indicate a similar or smaller fraction of particles with properties outside of these bounds, and therefore it would be straightforward to conclude that the fuel performance would be equivalent to the AGR fuel in similar irradiation conditions.

However, if a particle property tolerance limit is outside of the limits given in Table 5, there may be an argument to be made to conclude that the fuel is either substantially the same as AGR-1 and AGR-2, or that the differences would not be expected to significantly elevate the particle failure fractions. The important point is that a tolerance limit outside of the range in Table 5 simply means that a higher fraction of the fuel is above or below the Table 5 value. This does not necessarily result in appreciable degradation in fuel performance.

In addition, if the fuel in question has a sufficiently wide distribution such that some fraction of particles are in the region where fuel performance might be expected to degrade (i.e., below AGR fuel specification critical limits), it would still be necessary to consider the magnitude of the effect (i.e., how much the failure fraction might increase, informed by computational modeling) as well as the actual fraction of fuel with properties in this region. Such considerations formed the basis of the AGR fuel specification 1% critical limits; while the limit value represents a point beyond which fuel performance would likely suffer, it is allowable to have a small fraction (in this case, 1 percent) below that value because of the low impact on cumulative particle failure.

It is also important to note that the specifications for allowable defects and in-service performance (i.e., allowable fuel failure fractions) may be unique to a particular reactor design. The basis for development of the AGR fuel specifications was the historic allowable failure fractions for modular HTGRs (Table 4-1 in the topical report). A reactor design that resulted in a significant change in the specifications for fuel quality or in-service failure fractions would impact this analysis. For example, a reactor design with allowable in-service failure fraction an order of magnitude higher than those listed in Table 4-1 would likely result in a more relaxed fuel quality specification, because a higher percentage of fuel may be allowable beyond the AGR-1 and AGR-2 1% critical limits.

Such detailed statistical analyses for all potential cases are beyond the scope of this report. Ultimately it will be up to an applicant to provide a justification for applying AGR-1 and AGR-2

D-26

particle performance results to a TRISO fuel population that deviates from the AGR-1 and AGR-2 fuel properties.

The intended application of Table 5 is summarized below.

1. An applicant would compare the particle property characteristics of its fuel population to the AGR-1 and AGR-2 tolerance limit extrema in Table 5.
2. If the candidate fuel population 95%/98% tolerance limits (or 95%/99% for a one-sided tolerance limit) characteristics are within the bounds of Table 5, the applicant could assume that the performance of its fuel population would be as good as the AGR-1 and AGR-2 fuel, given similar irradiation conditions.
3. If the characteristics of one or more of the particle properties exceed the tolerance limit extrema in Table 5, the applicant would need to address that property or properties in order to justify the applicability of the AGR-1 and AGR-2 performance results.

The remaining discussion in this response describes the derivation of the data in Table 5. Ranges for the mean were drawn from the collection of two-sided 95% confidence intervals on the mean for each fuel type. Ranges characterizing the tails of the property distributions were drawn, except as noted, from the collection of 95% confidence - 98% coverage tolerance intervals for each fuel type. Because the collections of intervals generally overlap, only the minimum and maximum of those tolerance limits are reported for each property. The approach is illustrated schematically for three particle populations in Figure 6. Note that while each of the type-specific intervals represent an assumed normal distribution, the ranges provided in Table 5 are not equivalent intervals for the entire population of particles. Nonetheless, the ranges given are considered useful bounds owing to the considerable overlap in the individual distributions and the fact that each individual population was well represented in the irradiation experiments.
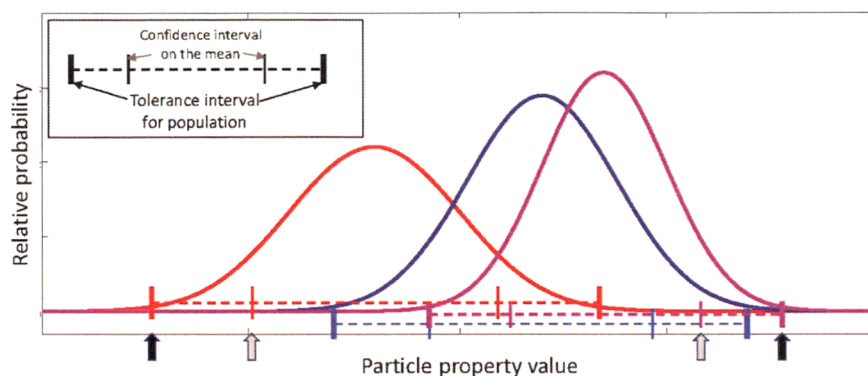
Figure 6. Schematic diagram illustrating the selection of confidence intervals extrema and tolerance intervals extrema from a hypothetical set of populations each characterized by a normal distribution, with confidence intervals and tolerance intervals denoted. The area under each curve represents the relative number of particles per batch/fuel type. Gray arrows identify the extrema of the confidence intervals on the mean for each population. Black arrows identify the extrema of the tolerance intervals.

Analytical data on TRISO particle properties from all of the UCO fuel types irradiated in these two experiments (AGR-1 Baseline, its three variants, and AGR-2 UCO particles) were used to calculate the intervals reported in Table 5. IPyC and OPyC densities were measured on particles from up to four batches within each composited lot. All other particle properties were measured on a single batch or on a composited lot of particles. Particles were randomly sampled at the batch or composited lot level to go through destructive testing from all fabricated particles. When available, the analytical data from each of the destructive analyses were used in interval calculations. Where raw data were not available, reported means, standard deviations and histograms were used to describe the implied normal distributions. Pyrocarbon anisotropies and particle aspect ratios are reported only for the upper bound as the lower bounds are immaterial (tending toward a lower limit of 1). The mean buffer density data for the AGR-1 and AGR-2 particles are inferred from comparable coating runs conducted with the same buffer coating parameter settings. The analytical method for determining buffer density did not provide dispersion information, so only the range of means is reported (not the extreme limits of intervals). IPyC density data for AGR-1 was likewise inferred from coating runs using identical coating parameter settings but terminated after the IPyC layer was deposited. The AGR-2 IPyC density data are based on the actual fuel used for the irradiation.

For all coating layer properties excluding anisotropies, tolerance intervals were calculated individually at the lowest grouping level, e.g., at the batch level, where batches were present, and on the composited lot otherwise. Interval calculations were performed using R 6.1.3 [R Core Team 2019], and the associated tolerance package [Young 2010]. Anisotropy data included

within- and between-particle variability for each lot; both were accounted for in the statistical intervals. Tolerance intervals for anisotropy for each particle type were calculated using the Liao, Lin and Iyer approach [Krishnamoorthy and Mathew 2009] to account for both sources of variation.

Planned Changes to EPRI-AR-1(NP):

The first three paragraphs of Section 5.3.6 (Key Property Ranges Observed in AGR-1 and AGR-2 TRISO Coated Particles) will be rewritten to reflect the material in the above response. Table 5 and Figure 6 will be incorporated in Section 5.3.6. In Section 8 (Summary/Conclusions) a paragraph will be added to the supporting discussions following Conclusion 2 and Conclusion 3. Information from the AGR fuel specifications that is currently in Table 5-5 will be moved to a new Appendix C.

References

Krishnamoorthy, K. and Mathew, T. (2009). Tolerance regions. Published by John Wiley & Sons Inc, Hoboken, New Jersey.

R Core Team (2019). R: A language and environment for statistical computing. R Foundation for Statistical Computing, Vienna, Austria. URL https://www.R-project.org/.

Young, D.S. (2010). tolerance: Functions for Calculating Tolerance Intervals. R package version 0.2.2, URL http://CRAN.R-project.org/package=tolerance.

RAI 4

TR conclusion 3 states "fission product release data and fuel failure fractions, as summarized in this report, can be used for licensing of reactors employing UCO TRISO-coated fuel particles that satisfy the parameter envelope defined by measured particle layer properties in Table 5-5." The phrases "as summarized in this report" and "can be used for licensing of reactors" lack specificity, though the subsequent discussion is relatively clear.

(a) Consider revising to more specifically reference the data presented, and narrow the scope of the request "can be used for licensing of reactors" to something more appropriate for the TR.

(b) Conclusion number 3 further states that the aggregate AGR-1 and AGR-2 fission product release data and fuel failure fractions can be used for licensing of reactors employing UCO TRISO-coated fuel particles that satisfy the parameter envelope detailed in the topical report. The staff notes that while the topical report supports fission gas release rates for most isotopes, it does not cover short-lived isotopes which decayed away before the particles discussed in EPRI-AR-1(NP) could be characterized. Therefore, the data set does not cover all of the fission gas release data necessary for licensing. Provide justification to support the statements in conclusion number 3 or limit the conclusion to the isotopes covered by the topical report.

Response

The phrase "as summarized in this report" refers to the fission product release data reported in Sections 7.1.2, 7.3.1, 7.3.4, 7.3.6 and fuel failure fractions reported in Sections 7.5. The report will be modified to more clearly delineate the data.

The phrase "can be used for licensing of reactors" was not intended to imply that the data are sufficient by themselves for qualification of TRISO fuel for all reactor applications. The statement will be modified to clarify that the data can be used to support regulatory approval of TRISO fuel use.

The extensive fission gas release-rate-to-birth-rate ratio (R/B) data from both irradiations presented and discussed in Sections 6.7 and 6.8 are based entirely on short-lived isotopes of krypton and xenon. These R/B data provide an indication of particle integrity during irradiation which is one of the principal metrics of TRISO fuel performance. On the other hand, the staff correctly points out that no data for short-lived fission products were obtained during PIE and safety testing. While many important elements with reactor safety implications are analyzed in PIE and safety testing because long-lived isotopes persist for years, in some cases no long-lived radioisotopes suitable for straightforward measurement are available. An example is iodine, for which ^{131}I ($t_{1/2}$ = 8.02 days) may be important for off-site dose calculations. In addition, no data for release of short-lived condensable isotopes (e.g., isotopes of iodine) were obtained during

irradiation, where analysis is limited to fission gas release. The report will be modified to emphasize that Conclusion 1 applies only to those data presented in this report.

Planned Changes to EPRI-AR-1(NP):

Section 8 (Summary/Conclusions), Conclusion 3 will be modified. Conforming changes will be made to Conclusion 3 in other parts of the report: Abstract, Executive Summary, Section 1.3 (Key Conclusions for NRC Review and Approval), and Section 7.6 (formerly Section 7.5) (Particle Failure Statistics). A paragraph will be added to the supporting discussion under Conclusion 3 in Section 8.

Enclosure 2

Planned Changes to EPRI-AR-1(NP) Resulting from Requests for Additional Information (RAIs) Dated January 2, 2020

Planned changes resulting from the RAIs are provided below. Additions to report wording are provided in red font and deletions are noted via strikethroughs. Explanatory information is provided in italics.

ABSTRACT

Pursuant to RAI 4, the following change will be made to Conclusion 3.

3. Aggregate AGR-1 and AGR-2 fission product release data and fuel failure fractions, as summarized in this report, can be used ~~for~~ to support licensing of reactors employing UCO TRISO-coated fuel particles that satisfy the parameter envelope defined by measured particle layer properties in Table 5-5 from AGR-1 and AGR-2.

EXECUTIVE SUMMARY

Pursuant to RAI 4, the following change will be made to "Key Findings."

- Aggregate AGR-1 and AGR-2 fission product release data and fuel failure fractions, as summarized in this report, can be used ~~for~~ to support licensing of reactors employing UCO TRISO-coated fuel particles that satisfy the parameter envelope defined by measured particle layer properties in Table 5-5 from AGR-1 and AGR-2.

ACRONYMS

Pursuant to RAI 1, the acronym "MeV" will be added to p. x.

MeV   million electron volts

CONTENTS

Pursuant to RAI 2, SiC microstructure, a new Section 5.3.2.4 will be added. The previous Section 5.3.2.4 will become Section 5.3.2.5.

5.3.2.4 SiC Microstructure
5.3.2.5 Diversity in TRISO Particle Properties

Pursuant to RAI 3, the title of Section 5.3.6 is changed to reflect the removal of specification information.

5.3.6 Key ~~Specifications and~~ Property Ranges Observed in AGR-1 and AGR-2 TRISO Coated Particles

Pursuant to RAI 2, SiC microstructure, a new Section 7.6 will be added. The previous Section 7.5 will become Section 7.6.

7.5 Effect of SiC Microstructure
7.6 Particle Failure Statistics

Pursuant to RAI 3, a new Appendix C will be added to the report to provide information on the AGR fuel specifications.

C Information from the AGR-1 and AGR-2 Fuel Specifications
C.1 TRISO Fuel Particle Properties
C.2 References

LIST OF FIGURES

Pursuant to RAI 2, SiC microstructure, a new Figure 5-2 will be added with the grain size micrographs.

Figure 5-2 Visual standard for SiC microstructure used in the AGR-1 and AGR-2 fuel specifications

Pursuant to RAI 3, a new Figure 5-3 will be added.

Figure 5-3 Schematic diagram illustrating the selection of confidence intervals extrema and tolerance intervals extrema from a hypothetical set of populations each characterized by a normal distribution, with confidence intervals and tolerance intervals denoted

Pursuant to RAI 2, UCO kernel stoichiometry, a new Figure 5-4 will be added.

Figure 5-4 Phases present in UCO kernels as a function of starting UC_2 content and burnup

Pursuant to RAI 1, a new Figure 6-30 will be added.

Figure 6-30 Ranges for key irradiation parameters for AGR-1 and AGR-2 fuel

Existing Figures 6-30 through 6-32 will be renumbered.

Figure 6-31 AGR-1 R/B ratios for ^{85m}Kr, ^{88}Kr, and ^{135}Xe versus time in EFPDs. Figure courtesy of Idaho National Laboratory and used with permission of Battelle Energy Alliance, LLC.

Figure 6-32 AGR-2 R/B ratios for ^{85m}Kr, ^{88}Kr, and ^{138}Xe versus time in EFPDs. Figure courtesy of Idaho National Laboratory and used with permission of Battelle Energy Alliance, LLC.

Figure 6-33 ^{85m}Kr fission gas release for AGR-1 (end of life) and AGR 2 (after the first three irradiation cycles) compared to historic performance in U.S. and German TRISO fuel irradiations. Figure courtesy of Idaho National Laboratory and used with permission of Battelle Energy Alliance, LLC.

LIST OF TABLES

Pursuant to RAI 3, the title of Table 5-5 will be changed.

Table 5-5 ~~Particle layer property 95% confidence values on means and dispersion limits~~ Coating layer property ranges for irradiated AGR-1 and AGR-2 UCO particles

Pursuant to RAI 2, kernel-to-buffer volume ratio, a new Table 5-6 will be added.

Table 5-6 Mean and percentiles of the stress metric calculated from the Monte Carlo simulation

Pursuant to RAI 1, a new Table 6-6 will be added.

Table 6-6 Ranges of values for key irradiation parameters for AGR-1 and AGR-2 fuel

Pursuant to RAI 3, new Tables C-1 and C-2 will be added.

Table C-1 AGR-1 Layer Property and Aspect Ratio Specifications
Table C-2 AGR-2 Layer Property and Aspect Ratio Specifications

Section 1.3

Pursuant to RAI 4, the following change will be made to Conclusion 3.

3. Aggregate AGR-1 and AGR-2 fission product release data and fuel failure fractions, as summarized in this report, can be used ~~for~~ to support licensing of reactors

employing UCO TRISO-coated fuel particles that satisfy the parameter envelope defined by measured particle layer properties in Table 5-5 from AGR-1 and AGR-2.

Section 5.3.2.4

Pursuant to RAI 2, SiC microstructure, a new Section 5.3.2.4 will be added. The previous Section 5.3.2.4 will become Section 5.3.2.5.

5.3.2.4 SiC Microstructure

The AGR-1 and AGR-2 fuel specifications did not include quantitative limits on SiC microstructure (e.g., SiC grain size). Instead, a visual standard was included that demonstrated a grain size considered to be excessively large. The visual standard is comprised of the two micrographs in Figure 5-4 below, with further guidance that the "specification will be met if the average SiC grain size of 3 coated particles is judged to be smaller than the average grain size shown in the visual standards." Thus the AGR program considered the example micrographs to represent an approximate upper bound on the acceptable grain size, with no specified lower bound. The AGR-1 test intentionally explored a range in grain sizes to evaluate the impact on performance. Quantitative data on AGR-1 and AGR-2 SiC grain size were provided in Table 5-3, and discussed in Reference 58 [Gerczak et al. 2016].
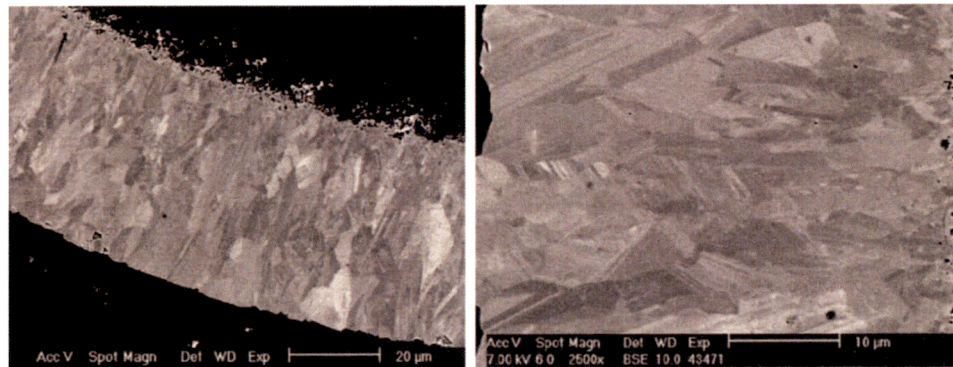

Figure 5-2. Visual standard for SiC microstructure used in the AGR-1 and AGR-2 fuel specifications

5.3.2.5 Diversity in TRISO Particle Properties

Properties of the resulting TRISO particles …

<u>Section 5.3.6</u>

Pursuant to RAI 3, the section will be modified as shown below. It will also be renamed because the specification data will be moved from Table 5-5 to new Appendix C.

5.3.6 Key ~~Specifications and~~ Property Ranges Observed in AGR-1 and AGR-2 TRISO Coated Particles

~~Table 5-5 presents the ranges of means and dispersion critical limits for key TRISO fuel particle coating properties that impact fuel performance, compared to the applicable specifications. The data for all of the fuel types (i.e., all four AGR-1 fuel types and the AGR-2 UCO) are combined into a single range and/or dispersion critical limits in cases where the specifications for AGR-1 and AGR-2 were the same. In cases where the AGR-1 and AGR-2 specifications differed, separate values are given for AGR-1 and AGR-2. Note that when a specification exists for a mean value, this is provided as an acceptable minimum and/or maximum value(s) of the mean with 95% confidence.~~

~~In all cases, the dispersion critical limits are specified that no more than 1% of the particles may be above or below the indicated limits. The reported dispersion data indicate the calculated values above or below which 1% of the population statistically exists. From the range of measured mean and dispersion values for each parameter, the maxima and minima (as applicable) that define or bound the entire range for these five particle populations are highlighted in bold text. The only instance where a specification limit was exceeded is the upper range on the mean for AGR-2 OPyC thickness, which is highlighted in red.~~

~~Table 5-5, therefore, provides a summary of the ranges of key particle coating properties that were tested in the AGR-1 and AGR-2 irradiations. Note that selection of key particle properties for this list is influenced, in part, by extensive thermomechanical modeling of particle performance and sensitivity studies to determine which properties have the greatest impact on particle failure probability, as well as historic TRISO fuel experience.~~

Table 5-5 summarizes the key coating layer properties for the particles used in the AGR-1 and AGR-2 irradiation experiments. Note that selection of key particle properties for this list is influenced, in part, by extensive thermomechanical modeling of particle performance and sensitivity studies to determine which properties have the greatest impact on particle failure probability, as well as historic TRISO fuel experience. The data represent a combination of the values from all of the AGR-1 and AGR-2 fuel types (fuel types include AGR-1 Baseline, its three variants, and AGR-2 UCO particles), except in the case of aspect ratio.

Two ranges of values are given for each property, one drawn from confidence intervals on the means and one drawn from tolerance intervals for the populations. Ranges for the mean were drawn from the collection of two-sided 95% confidence intervals on the mean for each fuel type. Ranges characterizing the tails of the property distributions were drawn, except as noted, from the collection of 95% confidence – 98% coverage tolerance intervals for each fuel type. The approach is illustrated schematically for three particle

populations in Figure 5-3. Note that while each of the type-specific intervals represent assumed normal distribution, the ranges provided in Table 5-5 are not equivalent intervals for the entire population of particles. Nonetheless, the ranges given are considered useful bounds owing to the considerable overlap in the individual distributions and the fact that each individual population was well represented in the irradiation experiments. When comparing a fuel population to the AGR-1 and AGR-2 fuels, the tolerance limit extrema in Table 5-5 are considered of greater importance than the mean confidence limits, because the tolerance limits serve to define the fraction of particles with the most extreme property values. The mean value for a fuel population may be outside of the range in Table 5 while the 95%/98% tolerance limits still reside inside of the corresponding limits in Table 5. This would indicate a similar or smaller fraction of particles with properties outside of these bounds, and therefore it would be straightforward to conclude that the fuel performance would be equivalent to the AGR fuel in similar irradiation conditions.

The values in Table 5-5 are not intended to define a comprehensive envelope of TRISO fuel that is expected to have acceptable performance. The data characterize the range of properties for particles that performed well during the AGR-1 and AGR-2 irradiations, but do not define the only ranges or combination of ranges that would perform well under these irradiation conditions or under service conditions proposed by fuel fabricators and reactor designers. The values are provided to facilitate comparison of other TRISO fuel populations to the fuel tested in the AGR-1 and AGR-2 irradiations. Comparative analysis of another population possessing particle properties that deviate from those in Table 5-5 will vary in complexity based on the specific properties in question (not all particle properties impact fuel performance in the same manner), the magnitude of the deviations (including which end of the distribution exceeds the limits in Table 5-5), and the intended irradiation conditions. More detailed data describing AGR-1 and AGR-2 particles are available for comparisons between AGR fuel and other TRISO fuel populations (see the references listed in Table 5-3). Ultimately it will be up to an applicant to provide a justification for applying AGR-1 and AGR-2 particle performance results to a TRISO fuel population that deviates from the AGR-1 and AGR-2 fuel properties.

Pursuant to RAI 3, the current version of Table 5-5 will be replaced with the version shown below.

Table 5-5
Coating layer property ranges for irradiated AGR-1 and AGR-2 UCO particles

Particle Property	95% Confidence Interval Extrema	95%/98% Tolerance Limit Extrema
Buffer thickness (µm)	96.5 – 105.0	75.2 – 124.7
IPyC thickness (µm)	38.6 – 41.1	32.4 – 47.6
SiC thickness (µm)	34.8 – 36.2	30.6 – 41.2
OPyC thickness (µm)	39.1 – 44.3	33.6 – 51.6
Buffer density (g/cm³)	1.04 – 1.11 [a, b]	NA
IPyC density (g/cm³)	1.84 - 1.92 [b]	1.808 – 1.958 [b]
SiC density (g/cm³)	3.196 – 3.209	3.191 – 3.217
OPyC density (g/cm³)	1.878 – 1.923	1.850 – 1.949
IPyC anisotropy (BAF $_{True}$) [c]	1.024 [d]	1.036 [d]
OPyC anisotropy (BAF $_{True}$) [c]	1.018 [d]	1.030 [d]
Aspect Ratio	1.057 [d, e] 1.039 [d, f]	1.102 [d, e] 1.068 [d, f]

a. Range of measured means only. No confidence intervals available.
b. Indirectly measured by analysis of interrupted batches (AGR-1) or comparable batches (AGR-2 buffer density).
c. BAF $_{True}$ = (1+N)/(1-N), where N is the optical diattenuation.
d. Upper bound of 95% confidence interval or 95% confidence - 99% coverage tolerance interval, as appropriate.
e. AGR-1, OPyC layer
f. AGR-2, SiC layer

It should be noted that the ranges given in Table 5-5 are narrower than the ranges specified in the AGR-1 and AGR-2 fuel specifications (means and 1% critical limits) (see Appendix C for AGR fuel specification information). TRISO particle performance is primarily defined by the probability of in-service coating layer failure. This behavior varies with key fuel properties, and the impact on coating layer fracture differs in magnitude for each property. Within a certain range of values, the impact on fuel performance will be negligible. The AGR fuel specification ranges were determined based on past performance demonstrations and on thermomechanical modeling of fuel performance to determine ideal property values as well as to identify the extremes of property distributions where fuel performance would be expected to begin to degrade appreciably. The AGR fuel specification 1% critical limits are established to be within this range; appreciable increases in fuel failure would only be expected outside of these bounds. Beyond these bounds, the particle failure probability increases, with performance

generally becoming worse as the property value gets further from the mean. Thus, a particle in a fuel population could reside outside of the Table 5-5 ranges, but still be within the AGR fuel specification and be expected to perform well under the AGR irradiation conditions, based on the amassed knowledge of TRISO fuel performance over the last several decades.

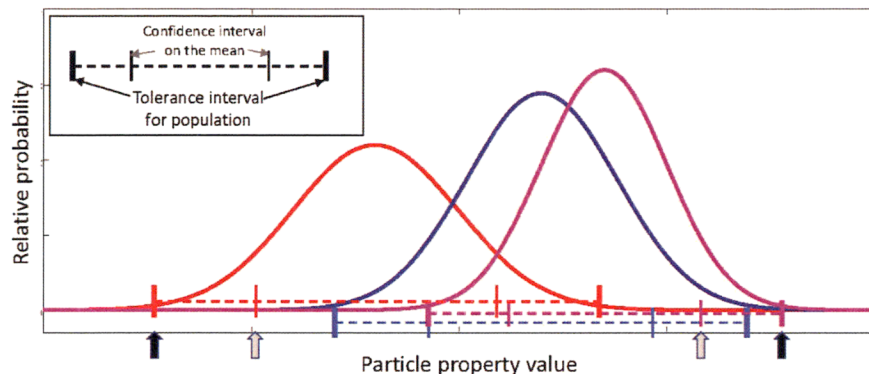*Pursuant to RAI 3, Figure 5-3 will be inserted following Table 5-5.*

Figure 5-3. Schematic diagram illustrating the selection of confidence intervals extrema and tolerance intervals extrema from a hypothetical set of populations each characterized by a normal distribution, with confidence intervals and tolerance intervals denoted. Area under each curve represents the relative number of particles per batch/fuel type. Gray arrows identify the extrema of the confidence intervals on the mean for each population. Black arrows identify the extrema of the tolerance intervals.

Pursuant to RAI 2, UCO kernel stoichiometry, the fourth paragraph of Section 5.3.6 will be modified as follows and relocated to follow Table 5-5 and Figure 5-3. Also, a new Figure 5-4 will be added.

As noted in Section 4.2, because the kernel is thermomechanically decoupled from the coating layers, there is not a *unique* set of kernel specifications that are critical to successful TRISO fuel as long as the scaling discussed in Section 4.2 is considered. Historically, a broad range of fissile and fertile kernels in a variety of chemical forms have been irradiated successfully around the world. ~~In terms of UCO, work by Homan et al. [25] has shown that depending on the burnup desired a broad range of uranium carbide contents in the kernel (between ~10 and ~50%) can produce acceptable fuel performance that balances the reduction in CO that comes with the addition of uranium carbide to the kernel with the potential for increased mobility of lanthanide carbide fission products as more uranium carbide is added. More recent work by McMurray et al. [65] suggests even~~

~~lower carbide contents (as low as 5%) could be acceptable based on a reassessment of the~~
~~uranium oxycarbide system using the latest updates in thermodynamic databases.~~
Thermochemical calculations have been performed previously on the relative stability of the uranium oxide and carbide phases in UCO fuel, as well as the stability of fission product oxides and carbides. Homan et al. [25] presented the graphic shown in Figure 5-4, which indicates the range of burnup over which the various phases are stable given a specific starting UO_2/UC_2 content in the kernels at 1800 K. The results indicate that at UC_2 content as low as 10% the UC_2 phase will still persist and limit the formation of CO gas up to ~18% FIMA. Beyond this burnup, the oxide/carbide equilibrium for strontium establishes the oxygen potential, and thereafter the equilibrium in the zirconium system. On the other hand, at UC_2 content as high as 80%, the rare earth fission products are still retained in the kernel as oxides. This demonstrates the wide range of UO_2/UC_2 ratios that maintain effectiveness at (a) limiting CO gas formation and (b) promoting the formation of rare earth oxides over the formation of rare earth carbides in order to increase retention of rare earths in the kernel. Subsequent thermochemical studies have suggested that UC_x content as low as 5.5% (C:U ≈ 0.1) is sufficient for acceptable performance of low enriched uranium UCO TRISO fuel up to 16% FIMA [65]. The AGR program chose to target about 30% uranium carbide in their kernel fabrication to provide ample carbide phase to meet a burnup of ~20% FIMA while experiencing negligible CO gas formation.
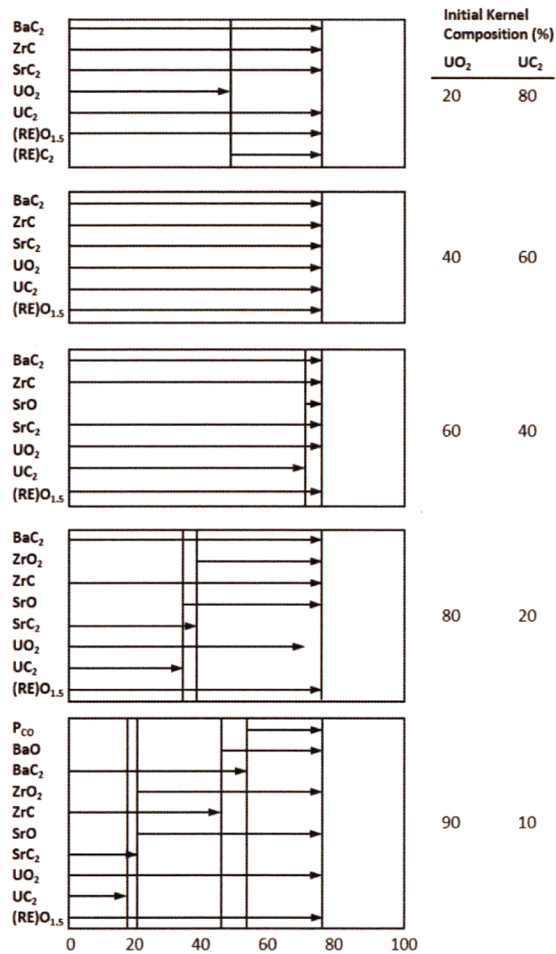
Figure 5-4. Phases present in UCO kernels as a function of starting UC₂ content and burnup [reproduced from Homan et al. 1977]

Pursuant to RAI 2, kernel-to-buffer volume ratio, the following content will be added to Section 5.3.6, following Figure 5-4.

Section 4.2.6 introduced the concept of a SiC stress metric (σ), defined in Eq. 4-1. The stress in the SiC layer is proportional to the volume of kernel (V_k) and buffer (V_b), the inner radius (r_{SiC}) and thickness (t_{SiC}) of the SiC layer, and the intended peak burnup (B). Values for this tensile stress metric for various TRISO particle designs are provided in Table 4-2 based on nominal particle dimensions, showing that historic particle design has sought to maintain a value similar to that of the German reference UO₂ TRISO particle.

In the stress metric, the four fundamental geometric terms are the kernel radius, buffer thickness, IPyC thickness, and SiC thickness. Using the as-fabricated fuel characterization data, bounding values for the stress metric, σ, in Eq. 4-1 were calculated to demonstrate the particle-to-particle variability in the AGR-1 and AGR-2 fuels. The distribution of σ for particles with the greatest burnup achieved in each particle type was calculated using Monte Carlo simulation, based on sample means and standard deviations of kernel diameter and layer thicknesses of each particle type. In simulation, the distribution of the quantity of interest is estimated by generating normal random deviates for each of the uncertain terms involved in its calculation and calculating the resultant stress metric for each set of those values. The 1st, 50th, and 99th percentiles of the simulated stress metric distribution, for compacts with highest burnup for each fuel type, are provided in Table 5-6.

The data in Table 5-6 demonstrate that (a) there is a significant range in values for the stress metric based on statistical variations in particle geometry, and (b) the peak values (99th percentile) based on this analysis are within the range of values (0.643-0.816) listed in Table 4-2 representing values for previous and current fuel designs.

Table 5-6
Mean and percentiles of the stress metric calculated from the Monte Carlo simulation. Minimum, median and max are the 1%, 50%, 99% percentile values of the generated stress metric values.

Test	SiC Stress Metric σ			
	Mean	Distribution quantiles		
		1%	50%	99%
AGR-1	0.570	0.440	0.566	0.742
AGR-2	0.623	0.485	0.618	0.810

Section 6.6

Pursuant to RAI 1, the following new material will be appended to the end of the section.

The key parameters for tristructural isotropic (TRISO) fuel performance are burnup, temperature, fast neutron fluence, and power. The ranges of values have been summarized in the Table 6-6 and Figure 6-30.

The ranges provided are based on volume averaged values for individual compacts, with the exception of time averaged temperature and particle power. Temperature and power are time averaged over the course of the irradiation. Burnup and fast fluence ranges are based on end-of-life values. Two different sets of parameter ranges have been provided: one data set for all AGR-1 capsules and AGR-2 Capsules 5 and 6, and a separate data set for AGR-2 Capsule 2. This approach has been taken because the AGR-2 Capsule 5 and 6 values predominantly fall within the range for the AGR-1 capsules; the exception is the slightly lower minimum burnup for AGR-2 (7.3% FIMA) compared to AGR-1 (11.1% FIMA). AGR-2 Capsule 2 was irradiated at a significantly higher peak temperature relative to the other capsules, so this population of fuel compacts is considered separately.

Power is provided in two different units in the table. The first represents power density over the entire compact (W/cm³) and the second is the power per particle (mW/particle). The AGR-1 and AGR-2 particles had kernels with different diameters (350 μm and 427 μm, respectively) so the power per particle values are given for each of these experiments separately in columns 2 and 3 (see footnotes a and b).

Table 6-6
Ranges of values for key irradiation parameters for AGR-1 and AGR-2 fuel

Property	AGR-1 + AGR-2 Capsules 5 and 6		AGR-2 Capsule 2	
	Max	Min	Max	Min
Burnup (% FIMA)	19.6	7.3	13.2	10.8
Fast fluence (n/m² x 10⁻²⁵; E > 0.18 MeV)	4.30	1.94	3.47	2.88
Time-average temperature (°C)	1210	800	1360	1034
Time-avg compact power density (W/cm³)	90	50	92	74
Time-avg particle power (mW/particle)	66[a]/86[b]	37[a]/48[b]	88	71

a. AGR-1 values
b. AGR-2 Capsules 5 and 6 values

Figure 6-30
Ranges for key irradiation parameters for AGR-1 and AGR-2 fuel

The safety test data presented in the report are for heating in dry helium at temperatures of 1600-1800°C for durations as long as 400 hours. These data generally bound the ranges of conditions typical of past modular high temperature gas reactor designs. Future license applicants will need to justify the applicability of the data to their specific designs.

New Section 7.5

Pursuant to RAI 2, SiC microstructure, a new Section 7.5 will be added as follows. The previous Section 7.5 (Particle Failure Statistics) becomes Section 7.6.

7.5   Effect of SiC Microstructure

Notwithstanding differences in grain size, no major differences in fuel performance among the AGR-1 and AGR-2 SiC fuel types were observed in the data. This means

primarily that there were no differences in fission product release in-pile or during heating tests at 1600-1700°C, nor any differences in TRISO or SiC failure fractions. The only observed difference was an increase in fission product release from particles with fine-grained SiC at a temperature of 1800°C for durations longer than 100 hours. This negligible difference in performance indicates that none of the AGR SiC types were approaching a limiting value in terms of grain size.

Section 7.6

Formerly Section 7.5, this section is renumbered, as shown below.

7.6 Particle Failure Statistics

The statistics for both SiC layer failure and …

In addition, pursuant to RAI 4, the following change will be made to the last paragraph of the Section 7.6.

Aggregate AGR-1 and AGR-2 fission product release data and fuel failure fractions, as summarized in this report, can be used ~~for~~ to support licensing of reactors employing UCO TRISO-coated fuel particles that satisfy the parameter envelope defined by measured particle layer properties in Table 5-5 from AGR-1 and AGR-2.

Section 8

Pursuant to RAI 1, the supporting discussion under Conclusion 1 will be modified as follows.

The AGR program has demonstrated excellent irradiation performance of a statistically large population of UCO TRISO fuel particles under conditions of high burnup and high temperature. Compact-average burnup ranged from 7.3 to 19.6% FIMA, fuel compact time-average temperatures ranged from 800 to 1360°C, fast neutron fluence ranged from 1.94 to 4.3×10^{25} neutrons/m^2 (E > 0.18 MeV), and power density ranged from 50 to 92 W/cm^3. Results for irradiation, PIE, and safety testing from two experiments (AGR-1 and AGR-2), with fuel fabricated using a range of process parameters, show consistently robust performance.

Pursuant to RAI 2, uninterrupted coating, the second paragraph of the supporting discussion under Conclusion 2 will be modified as follows.

In terms of coating characteristics, AGR-1 coated particles were fabricated using a range of coating conditions that produced: (1) different combinations of PyC anisotropy and density, which in some cases were intentionally at the edge of the historic specification range; and (2) different microstructures of the SiC—a larger grain, made with traditional hydrogen and MTS coating gases, and a finer grain, by introducing argon gas as a diluent to improve fluidization during SiC deposition. Based on the in-pile results available at the

time, the AGR program decided the AGR-2 PyC coating would be applied using baseline conditions used in AGR-1 and would use argon dilution during the SiC coating step (similar to Variant 3 in the AGR-1 fuel) for the best fluidization in the 6-in. coater. Coating was carried out using an uninterrupted process for all fuel types, as this was considered important for production of high-quality coatings. Despite these variations in coating conditions, the performance of intact TRISO particles was nominally the same, albeit with slightly higher fission gas release in AGR-2 due to slightly higher uranium contamination of the particle batch fabricated in the larger engineering scale coater.

Pursuant to RAI 3, a paragraph will be added to the end of the supporting discussion under Conclusion 2.

These results demonstrate TRISO-coated particles can be made in a variety of coaters under a range of process conditions with some flexibility in coating parameter space in terms of acceptable values of density and anisotropy of the PyC and the microstructure of the SiC to achieve satisfactory irradiation performance.

The values in Table 5-5 are not intended to define a comprehensive envelope of TRISO fuel that is "acceptable." The data characterize the range of properties for particles that performed well during the AGR-1 and AGR-2 irradiations, but do not define the only ranges or combination of ranges that would perform well under these irradiation conditions or under service conditions proposed by fuel fabricators and reactor designers. Ultimately it will be up to an applicant to provide a justification for applying AGR-1 and AGR-2 particle performance results to a TRISO fuel population that deviates from the AGR-1 and AGR-2 fuel properties.

Pursuant to RAI 4, Conclusion 3 will be modified and a clarifying paragraph will be added to the beginning of the supporting discussion, as shown below.

Conclusion 3:

Aggregate AGR-1 and AGR-2 fission product release data and fuel failure fractions, as summarized in this report, can be used ~~for~~ to support licensing of reactors employing UCO TRISO-coated fuel particles that satisfy the parameter envelope defined by measured particle layer properties in Table 5-5 from AGR-1 and AGR-2.

Conclusions related to fission product release are limited to those isotopes addressed in Section 6.7, 6.8, 7.1, and 7.3. In-pile release measurements involved short-lived fission gases, while release data obtained during post-irradiation analysis consisted entirely of long-lived isotopes. The fuel failure fractions from AGR-1 and AGR-2 are those summarized in Section 7.6.

The fission gas release measured during AGR-1 was extremely low. About 300,000 TRISO fuel particles were irradiated without a single particle failure, making it the best irradiation performance of a large quantity of TRISO fuel ever achieved in the U.S., and substantially exceeding the German levels of burnup. …

Pursuant to RAI 3, a paragraph will be added to the end of the supporting discussion under Conclusion 3.

These results demonstrate the UCO TRISO-coated particles that underwent irradiation and subsequent high-temperature heating as part of the AGR-1 and AGR-2 experiments exhibited excellent performance and meet historic design specifications for allowable particle failures with significant margin. The data support the use of LEU UCO TRISO fuel for future high-temperature reactor designs, with specific kernel geometry and enrichment dependent on reactor design and burnup goals, provided overall particle design remains similar to those demonstrated by the AGR program.

The values in Table 5-5 are not intended to define a comprehensive envelope of TRISO fuel that is "acceptable." The data characterize the range of properties for particles that performed well during the AGR-1 and AGR-2 irradiations, but do not define the only ranges or combination of ranges that would perform well under these irradiation conditions or under service conditions proposed by fuel fabricators and reactor designers. Ultimately it will be up to an applicant to provide a justification for applying AGR-1 and AGR-2 particle performance results to a TRISO fuel population that deviates from the AGR-1 and AGR-2 fuel properties.

Pursuant to RAI 3, Appendix C will be added to the report to present information from the AGR fuel specifications.

C Information from the AGR-1 and AGR-2 Fuel Specifications

C.1   TRISO Fuel Particle Properties

The following tables present the AGR-1 and AGR-2 fuel specifications for TRISO coating layer properties and particle aspect ratios. AGR-1 specifications were extracted from Table 5.2 of EDF-4380, "AGR-1 Fuel Product Specification and Characterization Guidance," Rev. 8 [1] and the AGR-2 specifications were extracted from Table 5 of SPC-923, "AGR-2 Fuel Specification, Rev.3 [2].

Table C-1
AGR-1 Layer Property and Aspect Ratio Specifications

Coated Particle Property	Mean [a]	Critical Region	Fraction in Critical Region
Buffer thickness (μm)	100 ± 15	≤ 55	≤ 0.01
IPyC thickness (μm)	40 ± 4	≤ 30	≤ 0.01
		≥ 56	≤ 0.01
SiC thickness (μm)	35 ± 3	≤ 25	≤ 0.01
OPyC thickness (μm)	40 ± 4	≤ 20	≤ 0.01
Buffer bulk density (g/cm³)	1.03 ± 0.15	not specified	not specified
IPyC density (g/cm³)	1.90 ± 0.05	≤ 1.80	≤ 0.01
		≥ 2.00	≤ 0.01
SiC density (g/cm³)	≥ 3.19	≤ 3.17	≤ 0.01
OPyC density (g/cm³)	1.90 ± 0.05	≤ 1.80	≤ 0.01
		≥ 2.00	≤ 0.01
IPyC anisotropy (BAF$_o$) [b]	≤ 1.035	≥ 1.06	≤ 0.01
OPyC anisotropy (BAF$_o$) [b]	≤ 1.035	≥ 1.06	≤ 0.01
Aspect Ratio (faceting) [c]	not specified	≥ 1.14	≤ 0.01

a. Specified composite mean values and fraction in critical regions determined at the 95% confidence level. The ± values represent an allowable range for the mean value and are not standard deviations of the mean.
b. BAF$_o$ is to be measured on loose TRISO particles before compacting.
c. Aspect ratio is defined as the ratio of maximum to minimum diameters of the OPyC layer.

Table C-2
AGR-2 Layer Property and Aspect Ratio Specifications

Coated Particle Property	Mean [a]	Critical Region	Fraction in Critical Region
Buffer thickness (μm)	100 ± 15	≤ 58	≤ 0.01
IPyC thickness (μm)	40 ± 4	≤ 30	≤ 0.01
		≥ 52	≤ 0.01
SiC thickness (μm)	35 ± 3	≤ 23	≤ 0.01
OPyC thickness (μm)	40 ± 4	≤ 20	≤ 0.01
Buffer bulk density (g/cm³)	1.05 ± 0.10	Not specified	Not specified
IPyC density (g/cm³)	1.90 ± 0.05	≤ 1.80	≤ 0.01
		≥ 2.00	≤ 0.01
SiC density (g/cm³)	≥ 3.19	≤ 3.17	≤ 0.01
OPyC density (g/cm³)	1.90 ± 0.05	≤ 1.80	≤ 0.01
		≥ 2.00	≤ 0.01
IPyC anisotropy (BAF$_o$) [b]	≤ 1.045	≥ 1.06	≤ 0.01
OPyC anisotropy (BAF$_o$) [b]	≤ 1.035	≥ 1.06	≤ 0.01
Aspect Ratio (faceting) [c]	Not specified	≥ 1.14	≤ 0.01

a. Specified composite mean values and fraction in critical regions determined at the 95% confidence level. The ± values represent an allowable range for the mean value and are not standard deviations of the mean.
b. BAF$_o$ is to be measured on loose TRISO particles before compacting.
c. Aspect ratio is defined as the ratio of maximum to minimum diameters of the coated particle as measured for SiC-coated particles after removal of the OPyC layer.

D-48

C.2   References

1. EDF-4380, "AGR-1 Fuel Product Specification and Characterization Guidance," Rev. 8, April 21, 2006.

2. SPC-923, "AGR-2 Fuel Specification, Rev. 3, January 9, 2009.

D.3 RAI 5 Provided Initially by E-mail Dated November 25, 2019

From: Hoellman, Jordan <Jordan.Hoellman2@nrc.gov>
Sent: Monday, November 25, 2019 11:38 AM
To: steve.nesbit@lmnt-consulting.com
Cc: 'Sowder, Andrew' <asowder@epri.com>; cmarciulescu@epri.com
Subject: RE: RE: RE: RE: RE: UCO TRISO Audit Follow-up

Hi Steve,

Our QA folks have reviewed the NGNP QAPD assessment from 2012 and have developed the following clarification question that we'd like to schedule a brief teleconference to discuss.

The staff assessment of "Next Generation Nuclear Plant Quality Assurance Program Description," dated September 12, 2012 (ADAMS Accession No. ML12241A157), found that the QAPD was acceptable for use during the technology development and high level design phase of the NGNP project. As such, the staff is seeking clarification on the scope of the activities performed by Idaho National Laboratory to obtain and submit the data used by EPRI in their topical report titled "Uranium Oxycarbide (UCO) Tristructural Isotropic (TRISO) Coated Particle Fuel Performance: Topical Report EPRI-AR-I(NP)".

Unfortunately, the QA folks are not available at the time of our public meeting on December 9th. We are available next week (week of Dec. 2nd) if you can support.

Please let me know so we can proceed in resolving this aspect of the TR.

Feel free to call if you'd like to discuss.

Thanks,
Jordan

Jordan Hoellman
Project Manager
NRR / DANU / UARP
U S Nuclear Regulatory Commission
office: OWFN 02-C06
phone. (301) 415-5481
email. Jordan.Hoellman2@nrc.gov

D.4 Response to RAI 5 Provided by Letter Dated March 9, 2020

Responses to RAIs for Topical Report EPRI-AR-1(NP)

2020-002_____EPRI Advanced Reactor Strategic Program (EPRI-AR)

March 9, 2020

Document Control Desk
U. S. Nuclear Regulatory Commission
11555 Rockville Pike
Rockville, MD 20852

Docket No. 99902021

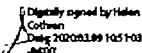Attention: Jordan Hoellman, NRO/DAR/ARPB

Subject: Response to Request for Additional Information (RAI) on Topical Report EPRI-AR-1(NP), "Uranium Oxycarbide (UCO) Tristructural Isotropic (TRISO) Coated Particle Fuel Performance"

Please find enclosed the Electric Power Research Institute (EPRI) response to a U. S. Nuclear Regulatory Commission (NRC) RAI related to its review of Topical Report EPRI-AR-1(NP). EPRI submitted Topical Report EPRI-AR-1(NP) "Uranium Oxycarbide (UCO) Tristructural Isotropic (TRISO) Coated Particle Fuel Performance" to the NRC for review on May 31, 2019. The NRC notified EPRI it had accepted the topical report for review by letter dated August 5, 2019. On October 8 and 9, 2019 the NRC conducted a regulatory audit of the topical report at the Idaho National Laboratory (INL) Offices and documented the results in an audit report dated November 19, 2019. On November 19, the NRC provided draft RAIs on the topical report (ML19336A057). EPRI, INL and the NRC met on December 9, 2019 for technical discussions and EPRI provided responses to the four RAIs by letter dated February 26, 2020. The fifth RAI, related to quality assurance, was discussed during a clarification phone call on January 15, 2020, and EPRI is providing a response to the fifth RAI in the enclosure to this letter. There are no planned changes to the topical report pursuant to the enclosed RAI response.

If you have questions about this submittal, please contact EPRI project manager Cristian Marciulescu by phone at 704-595-2401, or by email at cmarciulescu@epri.com.

Sincerely,

Helen
Cothron

Helen Cothron
EPRI Advanced Nuclear Technology Program Manager

EPRI-AR-2020-001   Responses to RAIs for Topical Report EPRI-AR-1(NP)
2020-002_____EPRI Advanced Reactor Strategic Program (EPRI-AR)

March 9, 2020
Page 2

Enclosure: Responses to EPRI-AR-1(NP) RAI#5

c: A. Cubbage, NRO/DAR/ARPB
    J. Monninger, NRO/DAR
    John Segala, NRO/DAR/ARPB
    A. Sowder, EPRI
    C. Marciulescu, EPRI
    S. Nesbit, LMNT Consulting
    P. Demkowicz, INL
    J. Kinsey, INL

Enclosure

Response to EPRI-AR-1(NP) Request for Additional
Information (RAI) #5 Related to Quality Assurance

<u>RAI #5</u>

The staff assessment of "Next Generation Nuclear Plant Quality Assurance Program Description," dated September 12, 2012 (ADAMS Accession No. ML12241A157), found that the QAPD was acceptable for use during the technology development and high-level design phase of the NGNP project. As such, the staff is seeking clarification on the scope of the activities performed by Idaho National Laboratory to obtain and submit the data used by EPRI in their topical report titled "Uranium Oxycarbide (UCO) Tristructural Isotropic (TRISO) Coated Particle Fuel Performance: Topical Report EPRI-AR-I(NP)".

<u>Response</u>

The basic objectives of the NGNP QAPD, as stated in its Section 2.2, are to "... *assure that NGNP technology development activities result in defensible data and records, and that the NGNP is designed, constructed, and operated in accordance with governing regulations and license requirements.*" In the Nuclear Regulatory Commission's (NRC's) 2012 assessment report, the staff concluded that the quality assurance program described in the QAPD was acceptable for use during technology development and high-level design phases of the project.

The Electric Power Research Institute topical report covers foundational fuel performance testing from the Advanced Gas Reactor (AGR)-1 and AGR-2 tests including the irradiation, safety testing and post-irradiation examination results. These research and development activities are associated with "technology development" activities, and the quality assurance standards reflected in the NGNP QAPD and assessed by the NRC staff were implemented during the performance of those activities. A summary depiction of the key technology development activities performed in conjunction with the overall data collection sequence of fuel fabrication, irradiation, and post irradiation examination (PIE)/safety testing is provided in the following flowcharts (Figures 1-3).

Figure 1.

March 9, 2020

Figure 2

Page 3
Responses to RAI #5 for Topical Report EPRI-AR-1(NP)
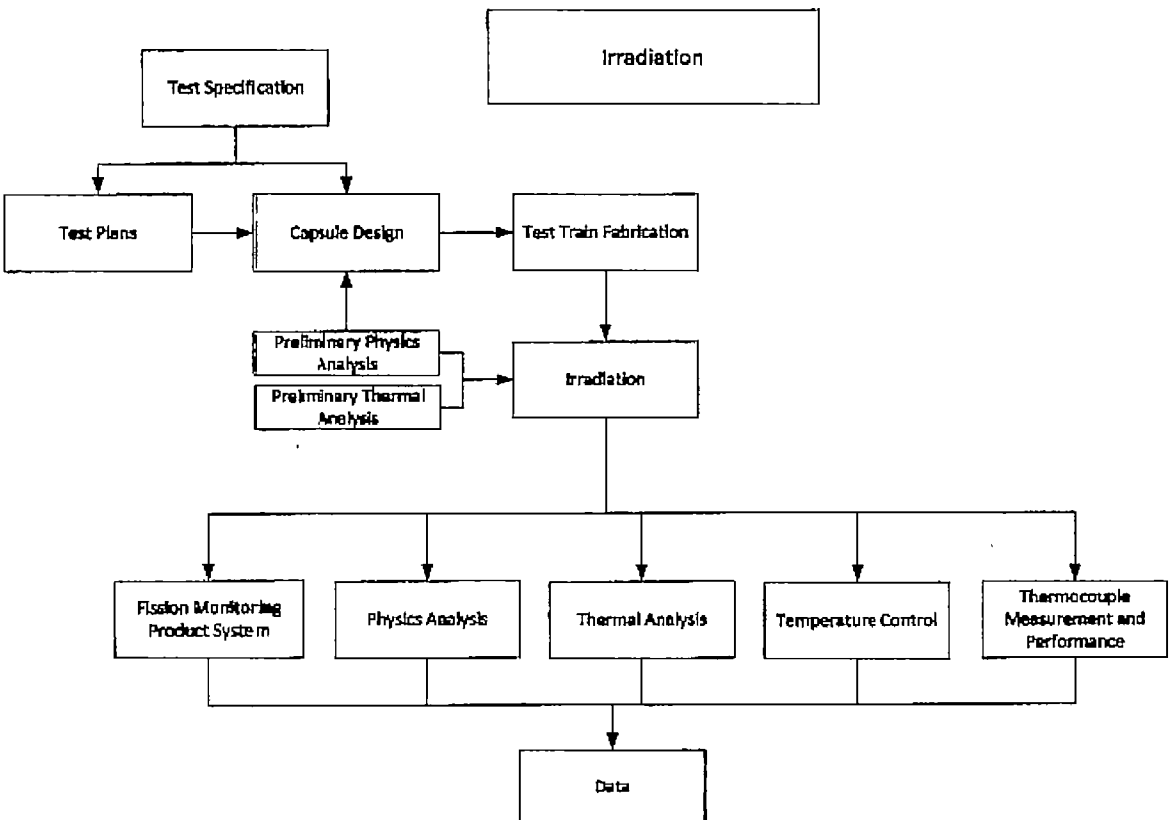
Enclosure

```
                                    ┌─────────────────────┐
                                    │     Irradiation     │
                                    └─────────────────────┘

        ┌──────────────────┐
        │ Test Specification │
        └──────────────────┘
                  │
         ┌────────┴────────┐
         ▼                 ▼
  ┌───────────┐     ┌───────────────┐     ┌─────────────────────┐
  │ Test Plans │───▶│ Capsule Design │───▶│ Test Train Fabrication │
  └───────────┘     └───────────────┘     └─────────────────────┘
                            ▲                        │
                            │                        ▼
              ┌────────────────────────┐     ┌───────────────┐
              │ Preliminary Physics    │     │  Irradiation  │
              │ Analysis               │────▶│               │
              ├────────────────────────┤     └───────────────┘
              │ Preliminary Thermal    │            │
              │ Analysis               │            │
              └────────────────────────┘            │
```

| Fission Monitoring Product System | Physics Analysis | Thermal Analysis | Temperature Control | Thermocouple Measurement and Performance |

Data

Post Irradiation Examination and Safety Testing

```
Technical Program
      Plan
        |
        v
     PIE Plan
        |
        v
Test Train Receipt and
    Inspection
        |
        v
   Test Train            -->    Compact Gamma      -->    Safety Testing
 Disassembly and                 Spectrometry              (dry helium)
   Metrology                          |                        |
        |                 +-----------+-----------+            |
        v                 v                       v            v
Analyze Capsule      Compact Cross            Compact
Components; Fisson    Section Microscopy     Deconsolidation   <--
Product Inventory                           Leach Burn Leach
                                                  |
                                                  v
                                           Particle Gamma
                                             Counting
                                                  |
                                                  v
                                           Particle Analysis
```
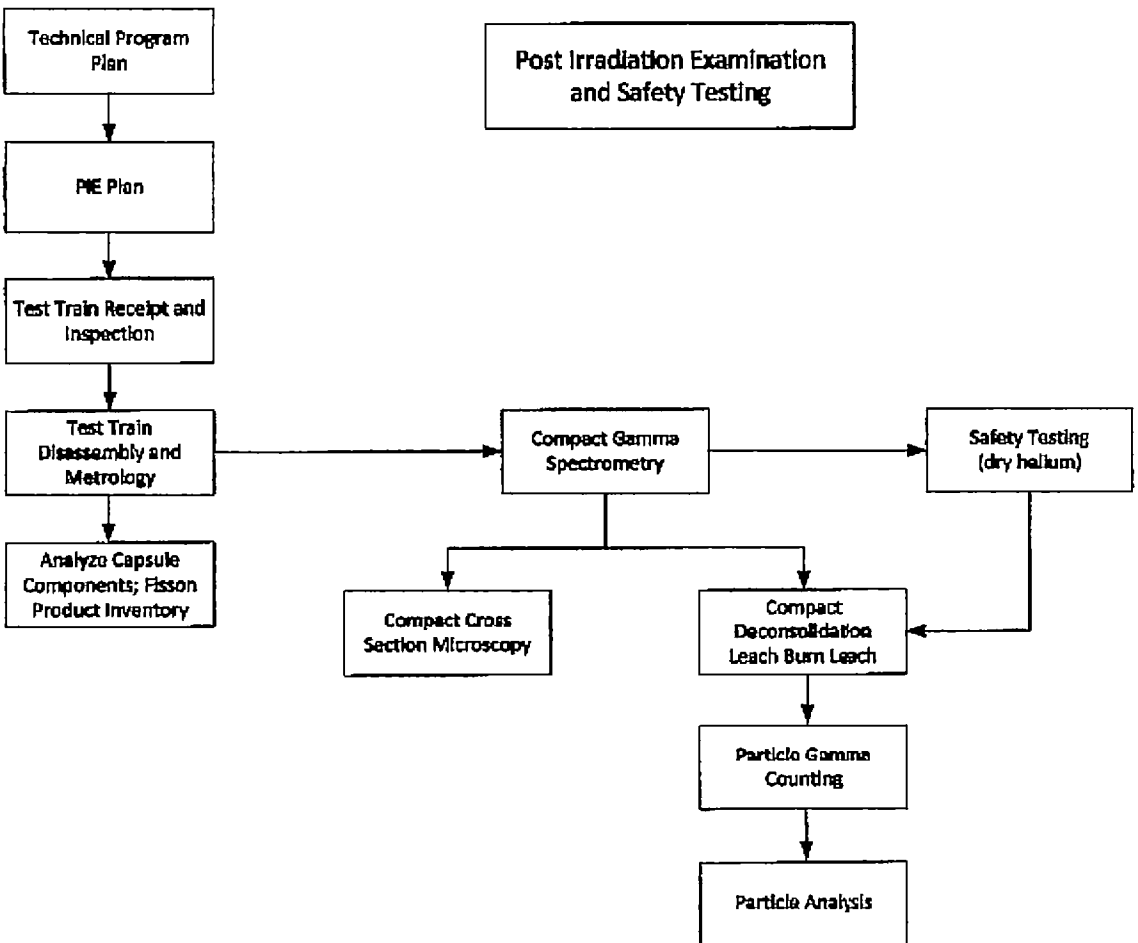
The Electric Power Research Institute, Inc. (EPRI, www.epri.com) conducts research and development relating to the generation, delivery and use of electricity for the benefit of the public. An independent, nonprofit organization, EPRI brings together its scientists and engineers as well as experts from academia and industry to help address challenges in electricity, including reliability, efficiency, affordability, health, safety and the environment. EPRI also provides technology, policy and economic analyses to drive long-range research and development planning, and supports research in emerging technologies. EPRI members represent 90% of the electricity generated and delivered in the United States with international participation extending to nearly 40 countries. EPRI's principal offices and laboratories are located in Palo Alto, Calif.; Charlotte, N.C.; Knoxville, Tenn.; Dallas, Texas; Lenox, Mass.; and Washington, D.C.

Together .Shaping the Future of Electricity

Programs:

Technology Innovation

Nuclear Power

Advanced Nuclear Technology

3002019978